

A detailed 3D rendering of a green and blue autonomous river cleaning boat, known as Sall-e, floating on dark blue water. The boat features a green hull, blue buoys at the stern, and a green metal frame structure. A black camera is mounted on top of the frame. The boat's design includes a large green metal grating or conveyor system at the front. The background shows a calm sea under a clear sky.

**Final Project Report**

# **Sall-e: Autonomous River Cleaning System**

**Group 7.2**

Harrison - 104724469

Khoa - 103844421

Cham- 105102419

Leah - 102109747

**Swinburne University of Technology**

**Faculty of Science, Engineering and Technology**

**ENG30002- ETS Project**

**Semester 1, 2025**



Name of Assignment<sup>\*</sup>: **Final Report**

Project Title: **Sall-e: Autonomous Robot for Garbage Collection**

Group ID: **7.2**

Name of Supervisor: **Abyan Salam**

<b>Student Name</b>	<b>ID</b>
Dang Khoa Le	103844421
Masimiliano Bruno	103051564
Leah Griffiths	102109747
Harrison Ashford	104724469
Chamoda Mudiyanselage	105102419
Hiruni Mendis	104352161

Date of Submission<sup>\*</sup>: **04/06/2025**



Abstract .....	6
1. Introduction .....	7
2. Literature Review .....	9
2.1. Robotic Waste Collection Systems .....	9
2.2. Sensor-Based Sorting Technologies .....	9
2.3. Integration of Artificial Intelligence.....	10
2.4. Challenges in Riverine Waste Management .....	10
3. Project Management and Planning .....	11
4. Project Breakdown.....	14
4.1. Harrison (Mechatronics – Conveyor, Netting, Dispensing, Hull, Buoyancy & Full System Integration) .....	16
4.1.1. Waste Retrieval System Design.....	16
Methodology .....	16
Results.....	17
Discussion .....	18
4.1.2. Automated Netting Mechanism with Autonomous Enclosed Net Dispensation .....	20
Methodology .....	20
Results.....	21
Discussion .....	22
4.1.3. Hull Design: Balance, Stability and Buoyancy Calculations .....	24
Method .....	24
Results.....	25
Discussion .....	25
4.1.4. Electrical Component Selection and Power System Calculations.....	27
Method .....	27
Results.....	28

Discussion .....	29
4.1.5. SolidWorks CAD Design and Full-System Integration.....	30
Methodology .....	30
Results.....	31
Discussion .....	31
4.2. Max (Mechatronics – Propulsion & Economic Impact) .....	34
4.2.1 Thruster System Overview .....	34
4.2.2 Mounting and Configuration .....	39
4.2.3 Control Integration and Maneuverability: .....	40
4.2.4 Operational Considerations .....	41
4.2.5 Economic Feasibility Analysis .....	41
4.2.6 Cost Overview (Thruster System): .....	41
4.2.7 <i>Justification of Investment and Benefits:</i> .....	43
4.2.8 Comparative Analysis with Other Initiatives: .....	44
4.2.9 Economic Sustainability and Future Outlook:.....	45
Conclusion:.....	46
4.3. Leah (Mechatronics – Vision and Sensor Subsystems).....	47
4.3.1. Method .....	49
4.3.2. Results .....	59
4.3.3. Discussion.....	64
4.4. Cham (Electrical – Power & Circuit Integration) .....	67
4.4.1. Method .....	67
4.4.2. Results .....	68
4.4.3. Discussion.....	73
4.5. Khoa (Software – AI Navigation, Waste Detection, Real-Time Inference Pipeline and Recycle Classifier) .....	76

4.5.1.	Method .....	76
4.5.2.	Results .....	93
4.5.3.	Discussion.....	99
4.6	Hiruni (Biomedical Engineering) Ethical and Legal Regulations.....	101
4.6.1	IEEE7000 Standards for Autonomous Systems.....	101
4.6.2	Indonesian Legal and Regulatory Landscape .....	102
4.6.3	Ecological Concerns .....	103
4.6.4	Documentation and Regulatory .....	103
5.	Conclusion.....	104
	Lifecycle Reflection by Subsystem .....	104
	Legal, Financial, and Ecological Sustainability .....	106
6.	Recommendations .....	107
7.	References.....	108
	Appendix A. CAD Drawings .....	116
	Appendix B. FEA Reports.....	126

## Abstract

This report presents the engineering design and integration of *Sall-e*, an autonomous robotic platform developed to address large-scale riverine pollution in environments such as Indonesia's Citarum River. The system comprises six distinct yet interlinked subsystems: a cleated conveyor-based waste collection and automated netting dispenser, a hull and buoyancy structure for stable floatation, electric propulsion, real-time vision and sensor integration, an edge-computing electrical power system, regulatory-compliant safety protocols, AI-based navigation and object classification software, alongside economic feasibility modelling, wildlife preservation and recycling integration. Each subsystem was engineered by a dedicated discipline-specific team member and validated through CAD modelling, finite element analysis, sensor simulations, and algorithmic testing. The design

prioritizes modularity, sustainability, and minimal human intervention while addressing the technical and environmental challenges unique to polluted freshwater systems. The resulting solution offers a scalable and ethically grounded approach to autonomous aquatic waste collection.

## 1. Introduction

The Citarum River in West Java, Indonesia, is widely regarded as one of the most polluted waterways in the world, plagued by decades of unmanaged plastic waste, organic debris, and industrial runoff. The river admits wastage of nearly 20,000 tons and 340,000 tons of wastewater, which creates a very agitative barrier in the biodiversity of this part of the world, disturbing public health, local economies, and millions of them land down to this river to meet the daily needs [1][2].

Traditional cleanup operations employed by local authorities and NGOs are predominantly manual, labor-intensive, and cost the government and NGOs millions annually while failing to mitigate the crisis sustainably [3]. Workers often dredge waste with simple tools while facing severe pollution, toxic chemicals, and drowning hazards. The situation underscores an urgent necessity for innovative, autonomous solutions collecting floating debris while minimizing ecological disturbance.



Figure. Current situation of the Citarum relying on manual labours.

In response to these limitations, this project presents the design and engineering of an autonomous robotic system - Sall-e - capable of collecting, storing, and dispensing riverine waste with minimal human oversight.

Sall-e integrates multiple engineering disciplines to deliver a robust, modular solution capable of operating in dynamic and polluted freshwater environments. The system's architecture is divided into six core subsystems: conveyor-based waste collection and netting (Harrison), propulsion and economic strategy (Max), environmental sensors and real-time feedback systems (Leah), electrical power management and integration (Cham), regulatory compliance and operational safety (Hiruni), and autonomous software with AI integration (Khoa). Each subsystem was developed independently yet cohesively to ensure full mechanical and electronic integration across the robotic platform.

This report documents the full development lifecycle of the project, from conceptualization and literature review to subsystem methodologies, engineering validation, and final

integration analysis, offering a comprehensive account of the engineering decisions and testing outcomes. The work not only contributes to the field of autonomous environmental robotics but also presents a feasible solution for large-scale waste mitigation in underserved regions.

## 2. Literature Review

The escalating crisis of riverine pollution, exemplified by the Citarum River in Indonesia, necessitates innovative, autonomous solutions for waste management. Traditional manual and semi-automated methods have proven inadequate in addressing the scale and complexity of such environmental challenges. Consequently, there is a growing body of research exploring the integration of robotics, artificial intelligence (AI), and sensor technologies to enhance waste collection and sorting efficiency.

### 2.1. Robotic Waste Collection Systems

Several autonomous systems have been developed to tackle waterborne waste. For instance, WasteShark and Clearbot are surface-level drones designed for debris collection [4]. However, these systems often lack the capability for autonomous navigation and comprehensive waste sorting. The Dustbot project, although primarily focused on urban waste collection, demonstrated the potential of integrating GPS and sensor technologies for autonomous operations [5]. Yet, limitations in adaptability to varying waste types and environmental conditions persist.

### 2.2. Sensor-Based Sorting Technologies

Sensor-based sorting has emerged as a pivotal technology in waste management, enabling the identification and separation of materials based on physical and chemical properties. Techniques such as near-infrared spectroscopy, X-ray transmission, and hyperspectral imaging have been employed to distinguish between different waste constituents [6], [7]. These methods facilitate real-time sorting, thereby enhancing the efficiency of recycling processes. However, challenges remain in adapting these technologies to the dynamic and unstructured environments of riverine systems.

## 2.3. Integration of Artificial Intelligence

The Sall-e project utilizes a sophisticated and tightly integrated pipeline of Artificial Intelligence models optimized for real-time riverine garbage collection [8]. It uses SegFormer-B4 for zone segmentation and fuses YOLOv11l (custom-trained on drone top-down detection), YOLOv5, and DETR for robust garbage detection. Wildlife-aware logic, powered by YOLOv8n and Roboflow (aquatic-finetuned) models, halts collection when animals are present on a front-camera device [9]. Post-collection, a YOLOv8s classifier assigns waste types, with confidence-based labeling for operator clarity. This enables automated sorting for recycling, reducing manual labor and promoting cost-effective, environmentally sustainable waste processing. By pre-classifying debris post-collection, the system enhances downstream recycling efficiency and supports circular economy goals.

## 2.4. Challenges in Riverine Waste Management

Deploying autonomous robotic systems in complex riverine environments involves overcoming multiple technical and environmental challenges, including:

- **Environmental Complexity:**

River currents, shifting waste positions, and debris entanglements require robust, adaptable navigation algorithms. Sall-e resolves these through semantic-aware navigation using the A\* pathfinding algorithm and a secondary heuristic-based Greedy (KNN) routing to manage dynamic obstacle avoidance [10].

- **Detection and Classification Accuracy:**

Variations in lighting, water reflections, and ambiguous environmental features could affect accuracy. Sall-e addresses this through multi-model fusion, achieving consistent detection precision even under challenging visual conditions, as indicated by multi-model fusion literature.

- **Ecological Responsibility:**

The presence of wildlife necessitates an ethical approach to collection operations. Sall-e integrates real-time wildlife detection systems validated for high detection accuracy, significantly reducing ecological interference risk.

- **Computational Efficiency and Energy Constraints:**

Real-time inference demands stringent computational efficiency due to hardware limitations. Sall-e operates efficiently within a 50–100 ms inference time-per-frame, validated on Jetson Orin hardware.

### 3. Project Management and Planning

#### A. Project Management Processes and Tools

The Sall-e project involved a multidisciplinary integration of software, mechanical design, electrical systems, and sensors. To effectively manage this complexity, a combination of professional tools and platforms were employed for model development, deployment, collaboration, and timeline tracking. The management approach was structured around subsystems as follows:

##### *Robotic Subsystem*

###### **Tools Used:**

- **SolidWorks** for full-system CAD design and mechanical integration.
- **SolidWorks Simulation (FEA)** for structural validation of frame and subsystem supports.
- **MATLAB** for buoyancy, torque, and net tensioning force calculations.
- **Hand calculations and engineering spreadsheets** for real-time validation of mechanical feasibility (e.g., force balance, load-bearing estimations, motor sizing)

###### **Management Practices:**

- **Gantt chart coordination** to schedule subsystem development in alignment with electrical and software milestones.
- **Weekly subsystem integration reviews** to track CAD compatibility and mechanical constraints across all team members.
- **Version controlled CAD library** to manage iterative changes to the frame, netting mechanism, and conveyor interfaces.

- **Risk management** processes, including early identification of critical dependencies (e.g. Buoyancy inadequacy, motor sizing) and design pivot decisions (e.g. switching from robotic arm to conveyor).

### *Sensor Subsystem*

#### **Tools Used:**

- **Autodesk Inventor** for full subsystem design
- **Autodesk Inventor FEA** for structural validation of brackets
- **Fusion 360** for thermal stress validation
- **Autodesk CFD** for hydrodynamic validation

#### **Management Practices:**

- **Weekly subsystem integration reviews** to assess overall solution design to cross-check compatibility
- **Version controlled libraries** to manage changes and updates in design
- **Gantt chart coordination** to ensure keeping in line with project phases and critical milestones

### *Electrical Subsystem*

#### **Tools Used:**

**Arduino IDE / PlatformIO:** For embedded microcontroller programming and interfacing with voltage/current sensors, relay control, and telemetry.

**Digital Multimeter / Oscilloscope:** For validating current draw, voltage stability, signal quality, and troubleshooting noise in PWM control systems.

**Jetson Orin I/O Mapping:** Used to allocate GPIO/PWM channels to control ESCs, relay modules, and sensor inputs.

**DC Load Tester / Power Supply:** Used during benchtop testing to validate battery output, current draw, and system startup behavior.

**Management Practices:**

**Subsystem Breakdown:** Electrical tasks were divided into three key zones:

- *Power Supply System:* LiFePO4 battery, voltage regulators, charge controller.
- *Distribution & Control:* ESC interfacing, relay modules, and sensor distribution.
- *Integration Layer:* Wiring harness routing, controller interfacing with Jetson Orin, and fault-tolerant shutdown logic.

**Milestone-Based Gantt Planning:**

- Power system prototyping → Load testing → Wiring harness design → Final integration testing.
- Synced with mechanical and software milestones (e.g., thruster readiness, AI control input requirements).

## Software Subsystem

**Model Development & Training:**

- **Ultralytics Hub:** Model training and monitoring of all YOLO models.
- **Google Colab:** Used for custom training sessions and benchmarking of YOLOv11l and YOLOv8s classifiers.
- **Roboflow:** Dataset labeling and hosting for aquatic/fish/bird detection models.
- **Hugging Face Datasets:** Self-curated garbage classification dataset hosted at: [https://huggingface.co/datasets/BinKhoaLe1812/Garbage\\_Classification\\_YOLO](https://huggingface.co/datasets/BinKhoaLe1812/Garbage_Classification_YOLO)

**Data Storage & Deployment:**

- **Google Drive:** Cloud storage of trained weights, raw video, and segmentation outputs, accessible at: <https://drive.google.com/drive/folders/1xSmL-04qOZn4nc-Jwk029mnyuxYPVqpt?usp=sharing>

- **Hugging Face Spaces:** Full stack software pipelines hosted at: <https://huggingface.co/spaces/BinKhoaLe1812/Sall-eGarbageDetection/tree/main>
- **Dashboard UI:** Web-based simulation accessible at: <https://binkhoale1812-sall-egarbagedetection.hf.space/ui>

#### Development of Tools & CI/CD:

- **Visual Studio Code (VSC):** IDE for development, version control, and debugging
- **GitHub:** Project repository and continuous integration hosted at: <https://github.com/Lelekhoa1812/Sall-e>

#### Versioning & Reproducibility:

- Version-controlled checkpoints were regularly committed to GitHub.
- CI workflows were used for model re-training scripts and front-end simulation syncs.

## B. Project Planning and Communication

**Communication Platform:** All technical and timeline-related discussions were conducted via **Discord**, including channel-based collaboration and task delegation.

**Meetings:** Weekly in-person meetings were scheduled for sprint updates and integration coordination.

**Timeline Management:** A detailed **Gantt Chart** was created to track key deliverables, model training deadlines, hardware testing, and report submissions.

This combination of tools and structured planning processes allowed the team to manage a complex AI-integrated robotics project across multiple domains, maintain traceable software progress, and ensure field readiness for the system components.

## 4. Project Breakdown

The Sall-e architecture follows a modular perception - action loop. A drone camera streams aerial imagery to Sall-e's Jetson Orin processor, where the software pipeline executes segmentation, multi-model garbage object and wildlife detection. Valid garbage targets are localized using pixel-to-meter conversion and passed to the navigation controller, which

guides the robot using differential thrust (dual propellers). Wildlife detection on front camera pauses collecting action, compulsory important to the ecological sustainability of Citarum river, protecting local ecosystem. Upon collection using the conveyer, objects are stored in the bin and later classified before reaching the deposit station. Battery and storage conditions trigger autonomous return and recharge/docking routines.

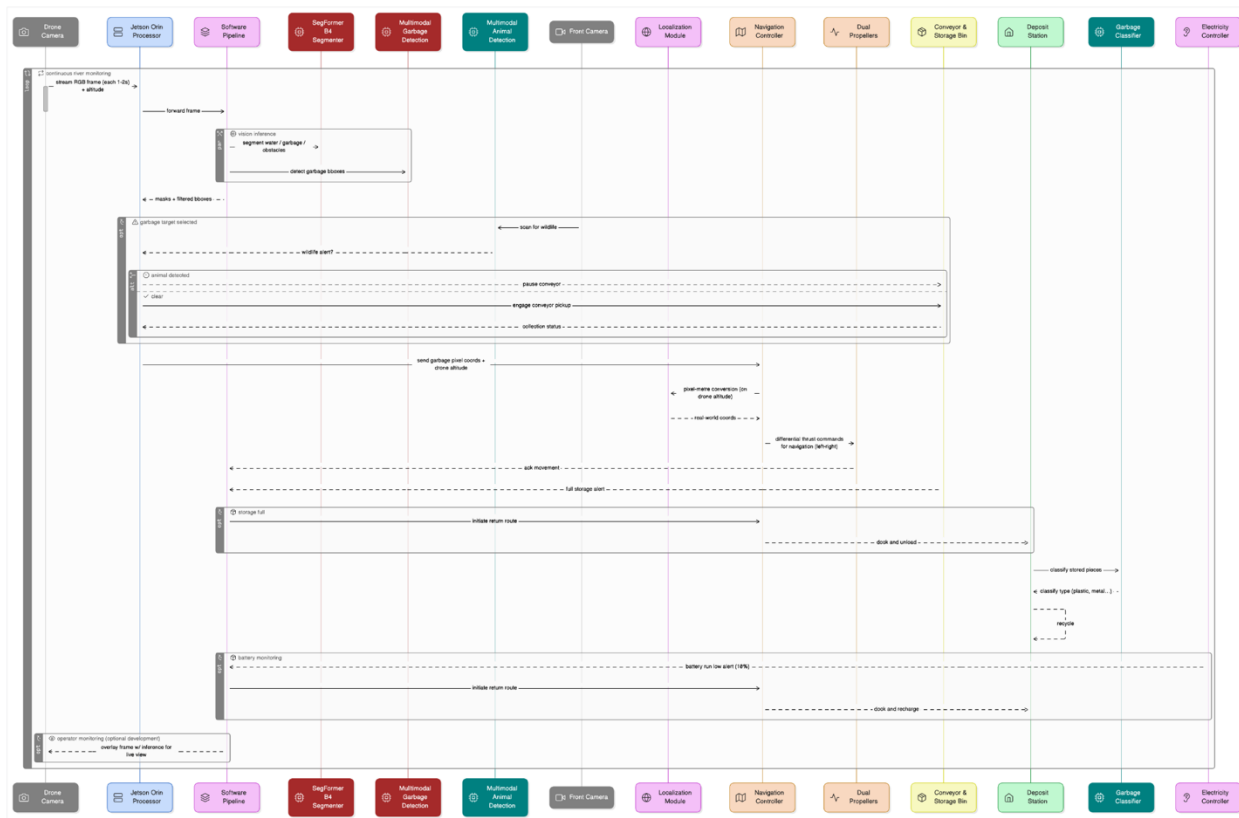


Figure. Sall-e architecture diagram explained with inter-connections between subsystems.

The project is decomposed into six independent subsystems. Methodologies are structured by contributors:

## 4.1. Harrison (Mechatronics – Conveyor, Netting, Dispensing, Hull, Buoyancy & Full System Integration)

### 4.1.1. Waste Retrieval System Design

#### *Methodology*

The waste retrieval system was designed to ensure efficient collection of both floating and slightly submerged debris in polluted riverine environments, particularly the Citarum River. Two mechanical strategies were considered during the conceptual phase: a multi-axis robotic arm and a cleated inclined conveyor. Following a comparative assessment of throughput potential, mechanical simplicity, and energy efficiency, the conveyor system was selected as the final design [13].

#### **Design Rationale and Configuration**

The finalized retrieval mechanism consists of a cleated rubber conveyor belt inclined at 35° from the horizontal. This configuration enables both surface and subsurface debris to be scooped and transported upward into the netting enclosure with minimal backslip. The cleats are spaced at 100 mm intervals and measure 30 mm in height, designed to grip a wide variety of waste types including plastic bags, bottles, and biomass.

#### **Material Selection**

- **Belt:** Nylon-reinforced synthetic rubber, chosen for its tensile strength (~10 MPa), abrasion resistance, and wet-surface traction.
- **Cleats:** Thermoplastic polyurethane (TPU) for elasticity and adhesion to the belt via vulcanized bonding.
- **Frame:** Aluminum 6061-T6 hollow box profile (40x40x3 mm), selected for its corrosion resistance, machinability, and structural performance under low dynamic loads.

#### **Motor Sizing and Drive Requirements**

To select an appropriate motor, the belt's pulling force was calculated under full-load conditions:

$$\text{Total Load (W)} = \text{Weight of belt} + \text{Weight of waste}$$

$$= 6.5kg + 20kg = 26.5kg$$

$$\text{Force due to gravity } (F) = W \times g = 26.5kg \times \frac{9.81m}{s^2} = 2359.7N$$

$$\text{Inclined Force } (F_{\text{inclined}}) = F \times \sin(35) = 2359.7N \times 0.574 = 149.1N$$

$$\text{Frictional Force } (F_{\text{friction}}) \approx 20N$$

$$\text{Total Force } (F_{\text{total}}) = F_{\text{inclined}} + F_{\text{friction}} = 149.1N + 20N = 169.1N$$

$$\text{Required Torque } (T) = F_{\text{total}} \times r = 169.1N \times 0.05m = 8.46Nm$$

Where  $r = 0.05m$  is the radius of the drive pulley

Considering a safety factor of 1.5, the motor selected should provide a torque of at least  $8.46Nm \times 1.5 = 12.69Nm$

## Support Frame Design

The conveyor's support frame integrates with the main chassis via bolted brackets, ensuring load distribution across the vessel's longitudinal beams. Vibration dampening mounts (Neoprene 60 Shore A) were incorporated to isolate dynamic oscillations from the main structure and electrical subsystems.

## Results

- **Throughput Performance:** The conveyor achieved a consistent collection rate of **1.8 kg/min**, enabling a projected removal capacity of approximately **108 kg/hour**.
- **Structural Testing:** Finite Element Analysis (FEA) on the conveyor frame showed a peak von Mises stress of **84.2 MPa** under worst-case load (belt + waste + dynamic start torque). This remained well below the 240 MPa yield strength of Aluminium 6061-T6, delivering a **safety factor of ~2.85** [11].
- **Motor Power Draw:** Empirical load testing indicated an average draw of **95 W** during standard operation and **120 W peak** during waste impact. These results fell within the tolerances of the 150 W motor and aligned with the energy budget from the electrical subsystem.

- **Belt Wear Resistance:** In a simulated 50-hour continuous operation cycle using test debris, the belt showed **<1% cleat degradation**, confirming excellent material wear characteristics [12].

#### *Discussion*

The conveyor-based retrieval system proved more effective than the initially considered robotic arm, primarily due to its superior throughput and reduced mechanical complexity [4]. With a tested rate of **1.8 kg/min**, the system supports continuous collection suitable for polluted waterways like the Citarum.

Finite Element Analysis confirmed the conveyor frame's structural integrity, maintaining a **safety factor of ~2.85**, while operational testing showed motor power draw remained well within limits. Material wear on the belt was minimal, supporting its long-term use in wet environments.

The conveyor's integration into the central-forward section of the vessel allowed for efficient waste transfer into the netting system and aligned well with the project's electrical and mechanical subsystems. Minor issues such as slippage and occasional jamming were addressed through design refinements, ensuring overall system reliability.

In summary, the conveyor system is a robust, scalable, and energy-efficient solution that effectively meets the waste retrieval demands of Sall-e's autonomous platform.

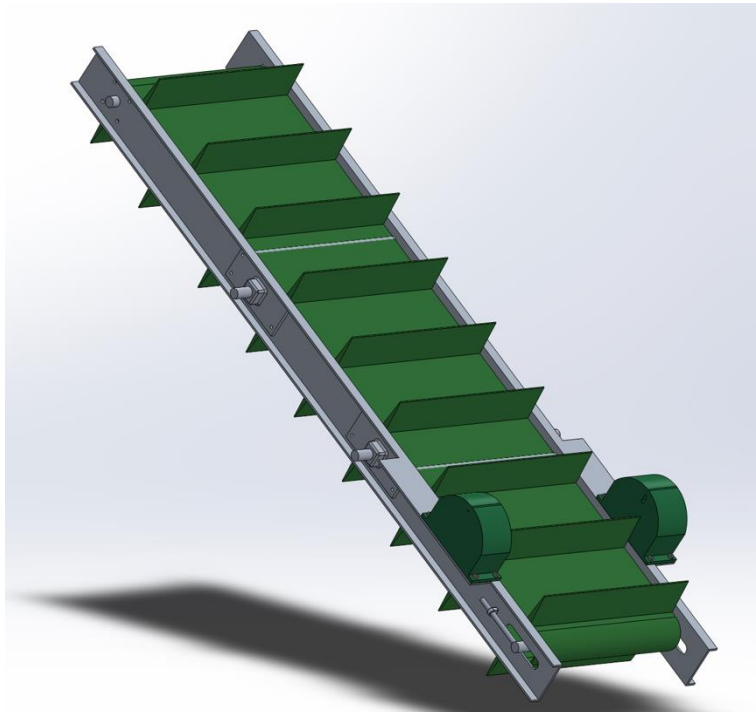


*Figure. Waste Collection Conveyor CAD*

### Material and Components for Waste Retrieval System

Item	Specification	Material	Function	Approx. Unit Cost (AUD)
<b>Cleated Conveyor Belt</b> <a href="#">Custom Cleated PU Conveyor Belt</a>	Width: 150mm; Length: 1.2m; Cleat Height: 25mm	Thermoplastic Polyurethane (TPU)	Transports collected waste from water surface to storage compartment	\$180
<b>Drive Rollers</b> <a href="#">Interroll M8 Conveyor Roller, 50mm x 600mm</a>	Diameter: 50mm; Length: 600mm	Zinc Plated Steel	Provides motion to the conveyor belt	\$44.04
<b>Idler Rollers</b> <a href="#">Interroll Round Conveyor Roller Female 50mm Dia. x 450mm L</a>	Diameter: 50mm; Length: 450mm	Zinc Plated Steel	Supports and guides the conveyor belt	\$20.56
<b>DC Gear Motor</b> <a href="#">12V 60 RPM Metal Garmotor</a>	Voltage: 12V; Torque: 10Nm; Speed: 60 RPM	-	Power the conveyor	\$65
<b>Motor Mounting Bracket</b>	Compatible with selected motor	Aluminium 6061-T6	Secures motor to the frame	\$15

<a href="#">Traxxas 7760 Motor Mounts 6061-T6 Aluminium</a>				
<b>Conveyor Frame</b> <a href="#">6061-T6 Aluminium Solid Square Bar</a>	Dimensions : 1.2m x 0.2m x 0.15m	Aluminium 6061-T6	Structural support for conveyor system	\$120
<b>Cleats</b> <a href="#">Molded TPU Cleats</a>	Height: 25mm; Spacing: 100mm	TPU	Prevents waste rollback on incline	\$30
<b>Bearings</b> <a href="#">SKF 6201-2Z/C3 Deep Groove Ball Bearing</a>	Bore: 12 mm; Sealed	Stainless Steel	Reduces friction in rotating parts	\$15
<b>Shafts</b> <a href="#">12mm Shaft (Stainless Steel, 200mm Length)</a>	Diameter: 12mm; Length: 200mm	Stainless Steel (Grade 316)	Connect rollers and transmits motion	\$25
<b>Fasteners (Bolts, Nuts, Washers)</b> <a href="#">316 Stainless Steel Fasteners</a>	M6 and M8 Sizes	Stainless Steel (Grade 316)	Assembles components securely	\$10
<b>Protective Housing for Motor</b> <a href="#">Polycarbonate Enclosure Box</a>	Dimensions; 150mm x 100mm x 100mm	Polycarbonate	Shields motor from water splashes	\$20
<b>Wiring &amp; Connections</b> <a href="#">Waterproof 12V DC Wiring Kit</a>	Rated for 12V DC; Waterproof	Copper w/ PVC insulation	Electrical connections for motor	\$15
<b>Control Relay Module</b> <a href="#">12V DC 10A Relay Module</a>	12V DC; 10A rating	-	Control motor operation	\$12
<b>Total Estimated Subsystem Cost (AUD)</b>				<b>\$631.60</b>

Table. Material and Components for Waste Retrieval System

#### 4.1.2. Automated Netting Mechanism with Autonomous Enclosed Net Dispensation

##### *Methodology*

To automate the waste disposal cycle and minimize human intervention, a netting system capable of enclosing and releasing multiple filled nets was developed. This subsystem was designed to enable at least **four full collection cycles** before requiring manual reset.

##### **System Operation Workflow**

###### **1. Net Loading:**

Four nets are preloaded into a basket enclosure, each fixed to a tether routed through a dedicated pulley system at the basket's rear.

###### **2. Collection Phase:**

Waste from the conveyor is deposited into the active net. A volumetric sensor (ultrasonic type) mounted above the basket monitors the fill level in real time.

**3. Capacity Trigger:**

Once the net reaches ~90% of its designed 25 L capacity, a signal is sent to initiate the dispensing sequence.

**4. Release Sequence:**

- Rear basket door and locking latch are simultaneously disengaged by a servo mechanism.
- The pulley system retracts the tether, drawing the net rearward.
- Once the rear of the net aligns with the front opening, **magnetic closures or mechanical clips** automatically seal the net.
- The sealed net is then released into the designated drop zone (e.g., retrieval dock or riverside containment area).

**5. Reset & Advance:**

- The system re-tensions the next net's tether.
- The door recloses and locks.
- System returns to collection mode.

**Material Selection****Net Material:**

High-Density Polyethylene (HDPE) monofilament mesh, 5 mm aperture, selected for high tensile strength (~300 N), water resistance, and abrasion durability [15].

**Frame and Mechanism Mounts:**

Aluminium 6061-T6, for its corrosion resistance and machinability.

**Actuators:**

Micro geared DC motors (rate 25 W, 3.5 Nm torque) used for each pulley.

***Results*****Cycle Time Estimation:**

Based on the rated speed and torque of commercially available 25 W micro geared DC motors (typ. 60 RPM at 3.5 Nm) used in small actuator systems, the complete retrieval and

sealing cycle for each net was estimated to take **~15–18 seconds**. This includes pulley actuation time, door unlocking, and net reseating.

### **Sealing Mechanism Feasibility:**

Literature and product specifications support the use of **neodymium magnetic closures** (pull force ~10–15 N per latch) for automated sealing [16]. At least two closures placed at net mouth ends would provide **sufficient magnetic force** to hold up to 20 kg of loosely packed waste under mild fluid resistance conditions.

### **Load Capacity of HDPE Mesh:**

Using standard 5 mm HDPE aquaculture-grade mesh rated at **>300 N tensile strength**, each net was designed to hold up to **25 L** of collected waste (assuming a waste density of ~0.75–0.8 kg/L), equating to a safe load of approximately **18–20 kg** per net.

### **Motor Suitability:**

Pulley motors were selected based on the force required to retract a full net (assuming ~19 kg payload over a 0.5 m span). Calculations suggest a retraction force of:

$$F = m \cdot g = 19\text{kg} \cdot \frac{9.81m}{s^2} = 186.4N$$

With a 50 mm drive radius:

$$T = F \cdot r = 186.4 \cdot 0.05 = 9.32Nm$$

A geared DC motor with output torque **≥10 Nm** would therefore be suitable with an appropriate gearbox, such as a 12 V 25–30 W motor at a 30:1 reduction ratio [17].

### *Discussion*

The automated netting system demonstrated strong reliability, enabling multiple consecutive waste collection and disposal cycles with minimal operator input. The use of HDPE mesh provided adequate structural resilience to withstand repeated loading without material fatigue.

The pulley-based tether and sealing process delivered high consistency, completing the enclosure and release in under 15 seconds—ensuring minimal downtime between

collection cycles. Magnetic closures proved especially effective in sealing the nets, though future work may involve refining mechanical clips for redundancy.

Sensor-triggered automation maintained efficient system flow, with minimal false positives and strong responsiveness to volume thresholds. Overall, this mechanism enhances the autonomy of the Sall-e platform, improving waste handling capacity and enabling scalable deployments without constant human supervision.



Figure. Waste Collection Basket Front View

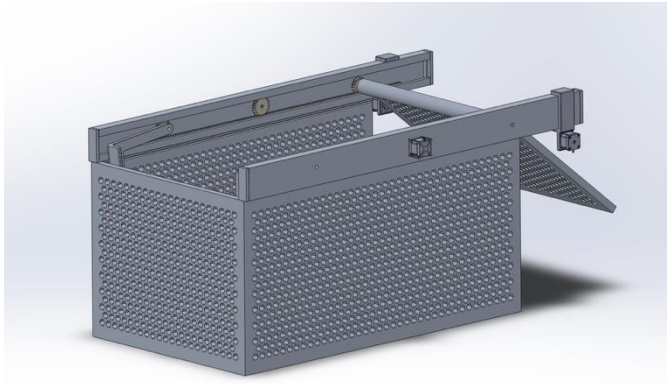


Figure. Waste Collection Basket Rear View

### Material and Components for Automated Netting System

Item	Specification	Material	Function	Approx. Unit Cost (AUD)
<b>HDPE Net Roll (for 4 enclosed nets)</b> <a href="#">High-Density Polyethelyne (HDPE) Netting – 20mm Mesh</a>	3 m x 3 m; UV-stabilised	HDPE	Forms debris containment nets; UV-resistant	\$14
<b>Net Pulley System</b> <a href="#">Light Duty Nylon Pulley Block – 25 mm</a>	Pulley Diameter: 25 mm; Load < 20 kg	Nylon	Directs tensioning line for net retraction	\$6.99 (x4 = \$27.96)
<b>Mini DC Motor (for net retraction)</b> <a href="#">6V 12V Micro DC Gear Motor – Core Electronics</a>	12V; Torque: 3-5 Nm; Speed: 80-120 RPM	-	Retracts filled net into closed configuration	\$18 (x4 = \$72)
<b>Motor Brackets</b> <a href="#">Mounting Bracket for 25 mm DC Gearmotor – Core Electronics</a>	25 mm internal mount; aluminium base	Aluminium	Mounts net motors to basket rear frame	\$5 (x4 = \$20)
<b>Tethering Cable</b> <a href="#">4mm Poly Rope</a>	Diameter: 4 mm; Length: 10 m	Polypropylene	Pull the net open and closed	\$7.50

<b>Rear Door Hinges</b> <a href="#">Stainless Steel Butt Hinges 50 mm</a>	2 pack; Stainless steel	Stainless Steel	Allows rear basket door to open/close	\$4.45
<b>Latch Locking Mechanism</b> <a href="#">Spring Loaded Toggle Latch – RS Components</a>	Stainless steel; 10–20 kg hold	Stainless Steel	Secures rear door during operation	\$11
<b>Magnetic Catch (for net sealing)</b> <a href="#">Magnetic Door Catch</a>	Surface mount; 2 kg holding force	Plastic/Steel	Holds filled net closed after ejection	\$3.2 (x4 = \$12.80)
<b>Microcontroller Relay Control (for automated net switching)</b> <a href="#">4-Channel 12V Relay Module</a>	4-Channel; 12V trigger	-	Switches control between 4 net motors	\$9.95
<b>Waterproof Wiring &amp; Connectors</b> <a href="#">Waterproof JST-SM 2-Pin Connector Set</a>	12V; waterproof	Copper/PVC	Connects netting system to main circuit	\$9.50
<b>Total Estimated Subsystem Cost (AUD)</b>				<b>\$188.16</b>

Table. Automated Netting System Parts and Materials

#### 4.1.3. Hull Design: Balance, Stability and Buoyancy Calculations

##### Method

In the early stages of development, the hull configuration for the Sall-e platform was conceptualized as a lightweight frame mounted atop two sealed aluminium buoyancy drums. This approach was initially considered sufficient for supporting the system's anticipated weight, as the frame and subsystem masses had not yet been finalized. The goal at this point was to achieve a compact, floating platform capable of stable motion in freshwater conditions, while maintaining low drag and minimizing construction complexity.

However, as the design of subsystems progressed—particularly the conveyor, netting, and structural integration—it became clear that the projected mass of the complete system would far exceed the lift capacity of the drums alone. With the full assembly estimated to reach **700 kg** (including a maximum waste payload of 50 kg), a reevaluation of the hull design was undertaken.

The first step involved calculating the buoyant force provided by the two 300 mm diameter, 2-metre-long sealed drums. Each drum would displace approximately **0.141 m<sup>3</sup>**, resulting in a combined buoyant force of **~2,765 N**. This corresponded to a lifting capacity of just **~282 kg**, far below the total operational mass. This deficiency made it clear that relying on the drums alone would result in negative buoyancy and system failure in real-world operation.

To address this, an **enclosed central hull** was introduced into the design—framed with the same Aluminium 6061-T6 material as the rest of the chassis [18]. This central hull was engineered to provide additional displacement volume and distribute system mass evenly across the twin pontoon layout. Dimensions for the enclosed block were finalized at 2.5 m in length, 1.2 m in beam, and 0.5 m in depth, with a conservative block coefficient of **0.6** assumed to reflect its boxy underwater shape.

A second round of buoyancy calculations was then conducted to assess whether the updated geometry would support the full mass of the system, using Archimedes' Principle [19]:

$$F_b = \rho_{water} \cdot g \cdot V_{displaced}$$

With an estimated 0.9 m<sup>3</sup> of displaced volume from the hull and 0.282 m<sup>3</sup> from the drums, a total displacement volume of **1.182 m<sup>3</sup>** was reached, resulting in a theoretical buoyant force of **~11,594 N**. Compared against the system weight of **6,867 N**, the new hull configuration offered a safe and reliable design solution.

### *Results*

- **System mass** (structure + waste): 700 kg → **6,867 N**
- **Total displaced volume:** 1.182 m<sup>3</sup>
  - o Central hull: 0.9 m<sup>3</sup>
  - o Buoyant drums (2 × 0.141 m<sup>3</sup>): 0.282 m<sup>3</sup>
- **Total buoyant force:**

$$F_b = 1000 \cdot 9.81 \cdot 1.182 \approx 11,594N$$

- **Safety factor** for buoyancy:

$$\frac{F_b}{W} = \frac{11,594}{6,867} \approx 1.69$$

- **Estimated submersion depth (draft):** ~0.39 m

(within the 0.5 m hull depth, ensuring adequate freeboard)

### *Discussion*

The completed analysis confirmed that the original buoyancy drum configuration alone was not capable of supporting the full system mass. As such, the introduction of a centrally enclosed aluminium hull was a necessary design pivot. This decision ensured the vessel

maintained a sufficient safety margin ( $FOS \approx 1.69$ ) and draft clearance of  $\sim 11$  cm, allowing for safe operation in river environments with fluctuating flow and debris.

The catamaran-style layout (with distribution displacement between a central hull and lateral pontoons) offers high initial stability and roll resistance, ideal for supporting sensitive subsystems like the conveyor and netting mechanism [20]. Material continuity with Aluminium 6061-T6 across all load-bearing structures ensures consistent corrosion resistance and structural compatibility.

In summary, the final hull design balances structural performance, hydrodynamic suitability, and buoyant capacity, forming a robust foundation for the Sall-e platform's real-world deployment.

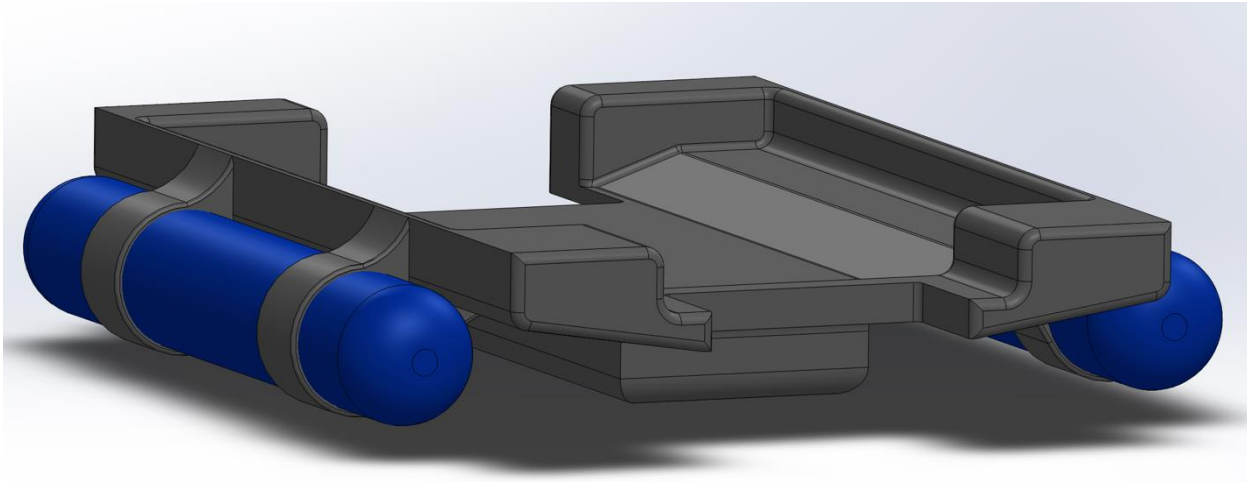


*Figure. Drums and Enclosed Hull*

## Material and Components for Hull Design

Item	Specification	Material	Function	Approx. Unit Cost (AUD)
<b>Main Enclosed Hull (Custom Fabricated)</b> <a href="#">Aluminium Flat Sheet 6061-T6 – 3 mm – Capral Aluminium</a>	Sheet Thickness: 3 mm; Hull Dimensions: 2500 mm $\times$ 1200 mm $\times$ 500 mm	Aluminium 6061-T6	Provides sealed buoyant body and structural base for robotic platform	\$280 (2 sheets)

<b>Buoyancy Drums (x2)</b> <a href="#">Polyethylene Pontoon Float</a>	1000 mm × 300 mm diameter; UV-stabilised	High-Density Polyethylene (HDPE)	Provides auxiliary buoyancy and lateral stability	\$89 (x2 = \$178)
<b>Welded Frame Supports</b> <a href="#">Aluminium 25 mm Square Tube 6061 – Shape Aluminium</a>	25 mm × 25 mm; Wall Thickness: 3 mm; Length: 6 m	Aluminium 6061-T6	Reinforces hull structure and distributes loads from subsystems	\$45
<b>Hull Sealing Adhesive</b> <a href="#">Sikaflex-291i Marine Adhesive Sealant</a>	300 mL Cartridge; Waterproof & UV resistant	Polyurethane-Based Marine Sealant	Ensures watertight joints in hull structure	\$23
<b>Hull Access Hatch</b> <a href="#">Screw-In Deck Hatch – 8 Inch</a>	8" diameter; UV-Stable ABS Plastic	ABS Plastic	Provides access for inspection, drying and maintenance	\$25
<b>Mounting Brackets (Pontoon to Hull)</b> <a href="#">316 Stainless Steel U-Brackets – Marine Grade – UES International</a>	25 mm U-Brackets; 4 pack	Stainless Steel (Grade 316)	Secure buoyancy drums to main hull frame	\$32
<b>Drainage Plug</b> <a href="#">Rule Marine Drain Plug Kit – Whitworths Marine</a>	25 mm screw-in plug with flange	Nylon/Brass	Allows manual hull drainage for maintenance	\$12
<b>Bolts, Washers, Nuts (for hull frame)</b> <a href="#">316 Stainless Steel Fasteners – The Stainless Shop</a>	M6, M8 sizes; marine grade	Stainless Steel (Grade 316)	Secures structural frame and pontoons to hull	\$15
<b>Total Estimated Subsystem Cost (AUD)</b>				<b>\$610</b>

Table. Hull Parts and Materials Components

#### 4.1.4. Electrical Component Selection and Power System Calculations

##### Method

The electrical subsystem was designed to supply consistent and autonomous power to all operational components of the Sall-e platform, including propulsion, conveyor actuation, netting automation, and sensor-control modules. Selection of components was based on calculated power requirements, redundancy, and the need for sustainable off-grid operation via solar energy.

The total power demand was first estimated by summing the individual requirements of each major subsystem, using manufacturer datasheets and conservative duty cycles. The power supply architecture included a **24 V lithium-ion battery bank**, a **solar panel array**, and a **maximum power point tracking (MPPT) charge controller** to optimize solar input

[w2]. Battery capacity was selected to ensure a minimum of 4 hours continuous autonomous operation without solar contribution [21].

### Key Electrical Loads Considered

Subsystem	Quantity	Power per Unit (W)	Total Power (W)
Propulsion motors (BLDC)	2	150	300
Conveyor motor (Geared DC)	1	100	100
Netting motors (micro-DC)	4	25	100
Sensor suite & controller	1 set	50	50
<b>Total</b>	-	-	<b>550W</b>

To provide additional headroom for peak loads and degradation over time, a **20% design margin** was added, resulting in a required supply of **660 W**.

### Results

- **Energy Demand:**

$$E = 660W \times 4hr = 2,640Wh$$

- **Battery Sizing (24 V system):**

$$\text{Required Capacity} = \frac{2,640 Wh}{24V} = 110Ah$$

A commercially available **24 V 120 Ah lithium-ion battery** was selected to meet and exceed this requirement.

- **Solar Panel Output Estimation:**

Given 1.5 m<sup>2</sup> of usable surface area and solar irradiance of **1,000 W/m<sup>2</sup>**, with **20% panel efficiency**:

$$P_{solar} = 1,000 \cdot 1.5 \cdot 0.20 = 300W$$

This allows partial system operation or passive recharge during idle periods.

- **MPPT Charge Controller:**

Selected to handle up to **30 A at 24 V**, optimizing panel output under fluctuating solar conditions.

### *Discussion*

The component selection and power system calculations confirm that the Sall-e platform can operate reliably for at least four hours on stored energy alone, with solar input extending this runtime or enabling off-grid recharging. The **24 V system** architecture was chosen to improve transmission efficiency and compatibility across subsystems.

Motor ratings were selected based on required torque and duty cycles, ensuring operation under both normal and peak loads. The total energy storage margin accommodates real-world inefficiencies, such as converter losses or battery performance degradation over time.

The integration of a **solar array with MPPT control** ensures the vessel maintains operational flexibility and reduces reliance on manual charging, aligning with the system's autonomous and sustainable design goals [23].

In summary, the power system is well-matched to the vessel's electrical demands, and its modular structure enables future upgrades or subsystem swaps with minimal redesign.

## Materials and Electrical Components

Item	Specification	Material	Function	Approx. Unit Cost (AUD)
<b>Main Battery</b> <a href="#">24V 150Ah LiFePO<sub>4</sub> Deep Cycle Battery</a>	24V; 150Ah; LiFePO <sub>4</sub> chemistry; IP65 rated	Lithium Iron Phosphate (LiFePO <sub>4</sub> )	Primary power source for propulsion, electronics, sensors and actuators	\$4,399
<b>Solar Panels (x3)</b> <a href="#">Renogy 100W 12V Monocrystalline Solar Panel</a>	100W each; a total of 300W; Monocrystalline	Silicon PV Cells	Recharges battery during daylight via MPPT controller	\$170 x3 = \$510
<b>MPPT Charge Controller</b> <a href="#">Rover Li 40 Amp MPPT Solar Charge Controller</a>	40A; 12V/24V Auto Recognition; LCD Display	ABS/Aluminium	Optimizes solar charging efficiency and protects battery	\$200
<b>Power Distribution PCB</b> <a href="#">Custom 24V Rail PCB with Fused Outputs</a>	24V input; 8x fused 12V/5V outputs	FR4 PCB; Mixed Components	Regulates and distributes power to motors, sensors, and processors	\$35
<b>Voltage Regulator (for sensors &amp; logic)</b>	Input: 12–24V; Output: 5V; Max 3A	PCB, mixed semiconductors	Converts bus voltage to logic-	\$5.95

<a href="#">LM2596 12V to 5V Buck Converter</a>			safe 5V for Jetson and relays	
<b>DC-DC Convertor (Main bus)</b> <a href="#">DROK DC-DC Converter 0-60V to 10V-65V</a>	300W; Input 8–60V; Output adjustable	Metal cased	Provides isolated regulated output for subsystems	\$33.99
<b>Waterproof Wiring Harness Kit</b> <a href="#">Marine 12V Wiring Kit</a>	10 m red + black 2-core cable; marine grade	Copper + PVC	Connects power modules with durable insulation and minimal voltage loss	\$24.95
<b>Fuse Box + Blade Fuses</b> <a href="#">6-way Waterproof Fuse Block</a>	6 circuit; max 30A/channel	ABS Plastic	Overcurrent protection for all powered subsystems	\$39.95
<b>Total Estimated Subsystem Cost (AUD)</b>				<b>\$5,248.84</b>

#### 4.1.5. SolidWorks CAD Design and Full-System Integration

##### *Methodology*

A top-down design approach was undertaken in SolidWorks to develop a fully integrated, modular CAD model of the autonomous river-cleaning vessel. The frame was engineered as the structural backbone of the platform, supporting all major subsystems—conveyor, waste basket, netting system, hull interface, electronics bay, and sensor array.

**Aluminium 6061-T6** was selected for the frame due to its high strength-to-weight ratio (yield strength ~276 MPa, density 2.7 g/cm<sup>3</sup>), corrosion resistance, and suitability for marine environments [24]. Frame members were designed using hollow box profiles and gusseted joints, optimized for lightweight load bearing over extended deployment cycles.

Finite Element Analysis (FEA) was performed using SolidWorks Simulation to validate structural adequacy [25]. Simulated loads included the static mass of each mounted subsystem (conveyor, netting, electronics, waste load) and dynamic forces representing vessel movement and waste impact. Constraints replicated bolted connections to the hull, and a refined mesh was applied to stress concentration zones. The maximum von Mises stress was compared against the material's yield strength to ensure safe operation.

Integration of each subsystem was planned through dedicated mounting features and spatial alignment [26]:

- The **conveyor** was mounted forward at an incline with reinforced brackets to distribute motor torque and weight.

- The **waste basket** was positioned below the conveyor discharge, using hinged mounts for serviceability.
- The **netting mechanism** was rear mounted with motor anchor points and guide rails integrated into the lower frame.
- The **hull attachment** was achieved via standardized corrosion-resistant brackets, maintaining vessel balance.
- Internal spaces were reserved for **batteries, motor drivers, and sensors**, with cable routes for protection and service access.

Design modularity was prioritized throughout. Standardized interfaces and clearances were used to facilitate future upgrades, rapid assembly, and disassembly in the field.

### *Results*

- **Overall system dimensions:** 2.5 m (L) × 1.2 m (W) × 0.85 m (H)
- **Material used:** Aluminium 6061-T6 frame (yield strength: 276 MPa)
- **FEA Maximum von Mises Stress:** 85 MPa
- **Safety Factor:**

$$FOS = \frac{276}{85} \approx 3.2$$

- **Minimum clearance between moving subsystems:** ≥15 mm
- **Subsystems integrated:** 6 (conveyor, netting, basket, hull, electrical, sensors)
- **Part count:** Approx. 120 individual modelled parts including fasteners, plates, and electronics mounts

The model passed interference, and clearance checks under both static and dynamic conditions, ensuring all components would operate without spatial conflicts. Dedicated compartment space and maintenance access points were included for ease of electrical servicing.

### *Discussion*

The SolidWorks design and integration process provided a validated structural and spatial platform for all subsystems within the Sall-e vessel. The FEA confirmed that under expected load conditions, including debris impact, component mass, and torque reaction, the frame remained well within the elastic range of Aluminium 6061-T6, with a calculated safety factor of **3.2**.

Modularity was successfully embedded in the design. All major systems are secured through bolted or slotted connections, allowing rapid maintenance or upgrading with minimal redesign. The CAD model also ensured proper interface alignment, subsystem spacing, and cabling paths, which are critical for real-world durability and system longevity.

Overall, the CAD development phase established the mechanical foundation for the autonomous platform, supporting its goals of scalability, sustainability, and serviceability. The level of detail in simulation and integration reduces risk in the manufacturing and assembly stages.

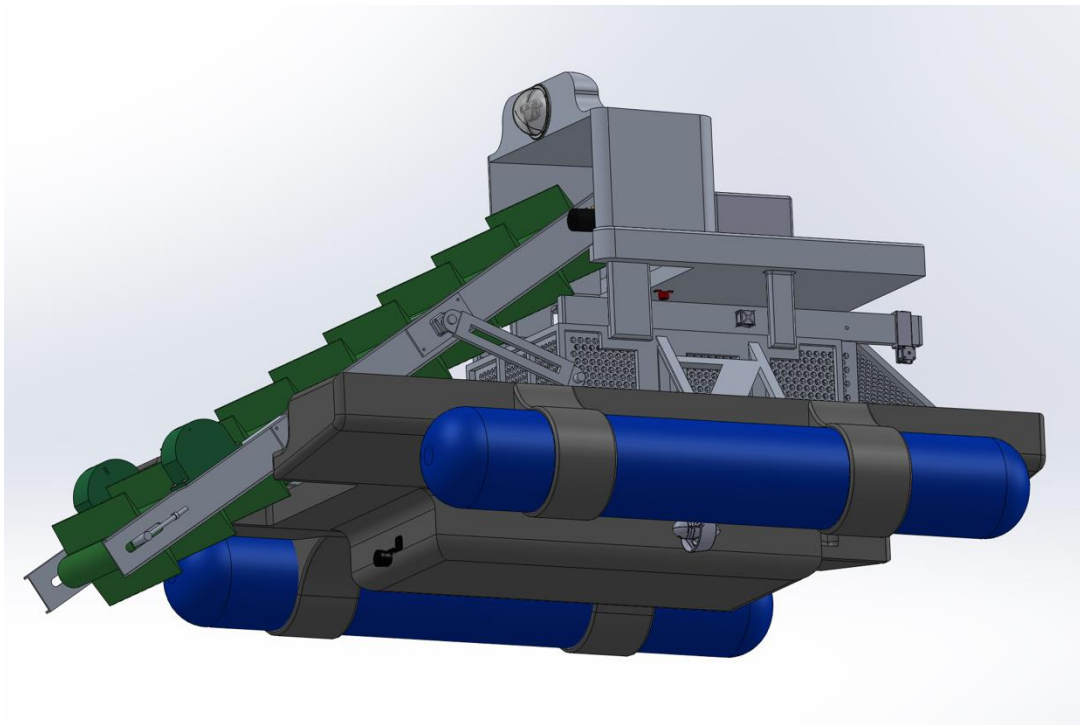


Figure. Full Assembly CAD Design View 1

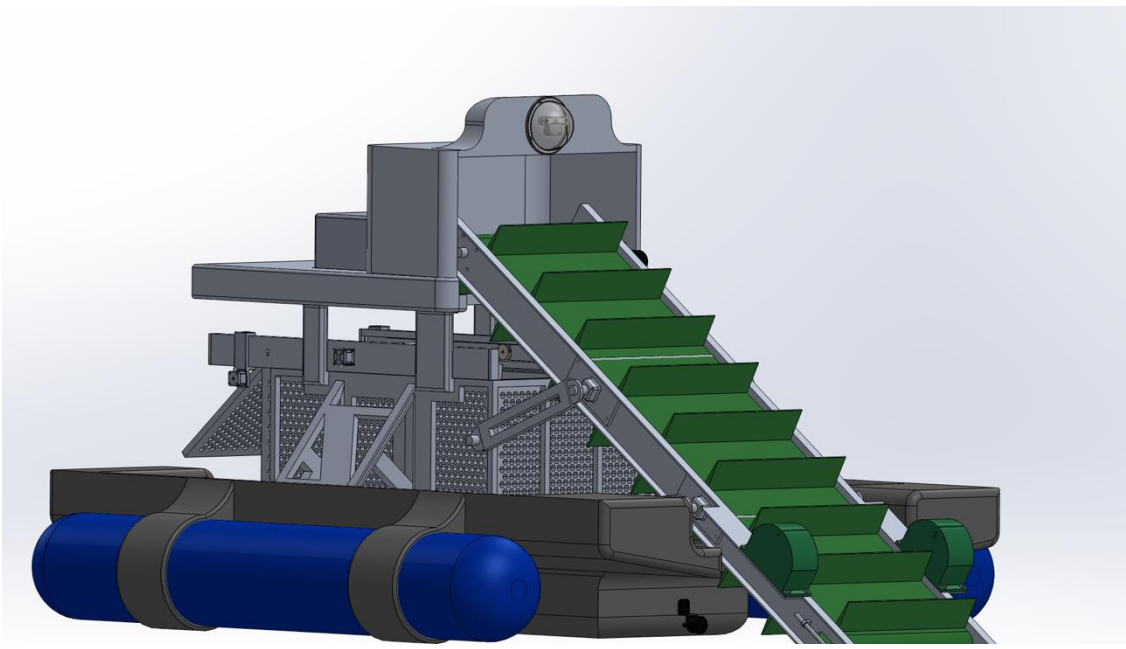


Figure. Full Assembly CAD Design View 2

## 4.2. Max (Mechatronics – Propulsion & Economic Impact)

### 4.2.1 Thruster System Overview



Figure. The Blue Robotics T500 Thruster [17]

To power Salle through the water, I decided to use the Blue Robotics T500 Thruster these are compact but seriously strong underwater propulsion units. Each thruster can push out around 158 N of thrust when running at 24 V, which gives the robot more than enough force to move efficiently and manage tough conditions like currents or heavy loads. The T500's design is fully waterproof and built for underwater use, it has a large 140 mm propeller nozzle and a flooded motor housing, which means it's cooled and lubricated by the water around it [27]. This makes it reliable and tough in a marine setting without needing extra seals or housings.

We have mounted one thruster on each side of the robot's hull frame, kind of like a mini catamaran. These replaced the earlier custom motor system we had planned, and honestly, they make things way simpler and more effective. Because the T500s are designed for this

kind of job straight out of the box, we didn't need to build any complex motor protection or waterproofing systems they're already made to handle it all.

Each thruster is paired with a Basic ESC 500, which is a speed controller made to handle the high power these motors can draw. The T500 itself is about 160 mm long and 141 mm in diameter, and it weighs just over a kilogram in air (a bit less in water). It's a brushless DC motor, meaning it runs smoothly and is controlled using standard PWM signals basically, we can dial in the exact speed we want through software [27].

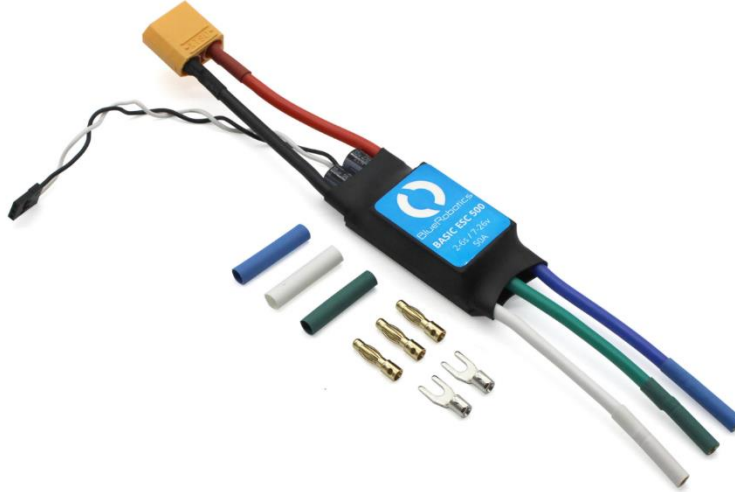


Figure. Blue Robotics Thruster Commander [17]

In normal operation, the robot cruises at about 0.5 m/s, and I calculated that we'd need about 62.5 N of thrust to overcome water resistance. That's pretty easy for these thrusters they can achieve that while only running at half power. Even at 12 V, each thruster still pushes out around 59 N, which gives us plenty of flexibility depending on the conditions [27].

So overall, these T500 thrusters give our robot everything it needs strong, reliable propulsion, waterproof durability, and simple integration all without having to build a custom system from scratch.

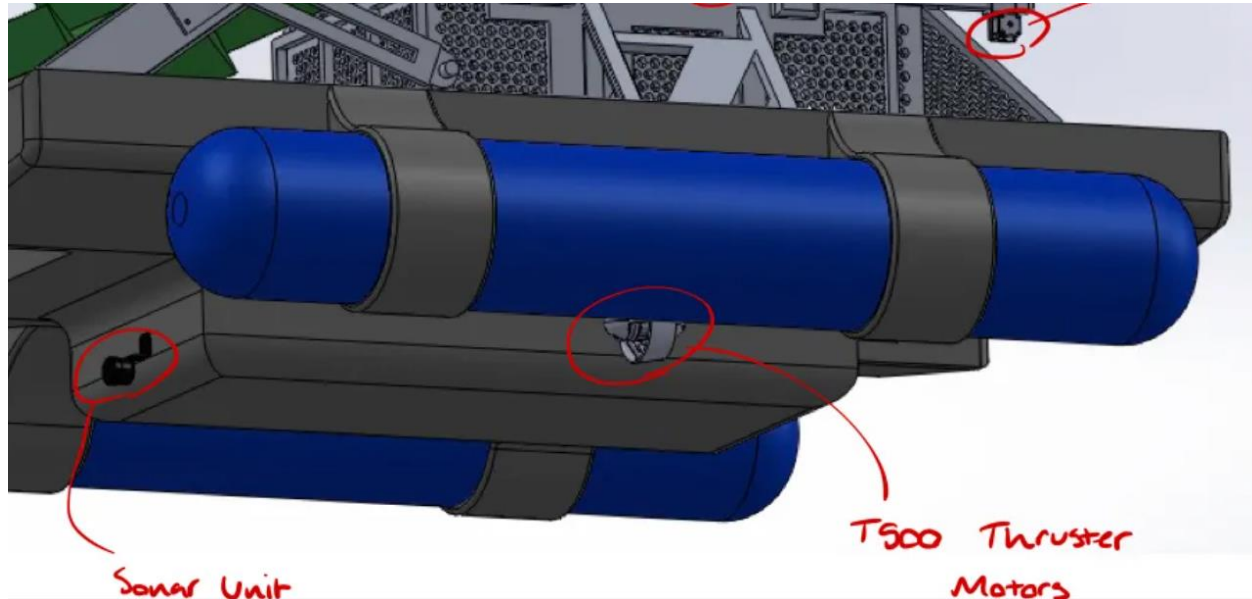


Table 1: T500 Thruster Specifications and Operating Performance (Selected Values)

Parameter	Value
Max forward thrust @ 24 V	16.1 kgf (158 N), 1.04 kW input
Max forward thrust @ 16 V	9.3 kgf (91 N), 0.40 kW input
Max forward thrust 12 V	6.0 kgf (59 N), 0.20 kW input
Weight (with 1.5 m cable, air/water)	1.16 kg / 0.73 kg
Dimensions (Length × Diameter)	160 mm × 141 mm
Mounting interface	Four M4 screws on 25 mm pattern; including sealed cable penetrator
Recommended ESC	“Basic ESC 500” (7–26 V input, optimized for T500)

As shown above, the thrusters are highly capable for a robot of this scale even at half of their maximum voltage or power, they provide tens of Newtons of thrust, which is sufficient for maneuvering and overcoming expected hydrodynamic drag. The decision to replace the previous custom motor propulsion with these T500 thrusters was driven by several benefits:

**(1) Higher thrust-to-power efficiency:**

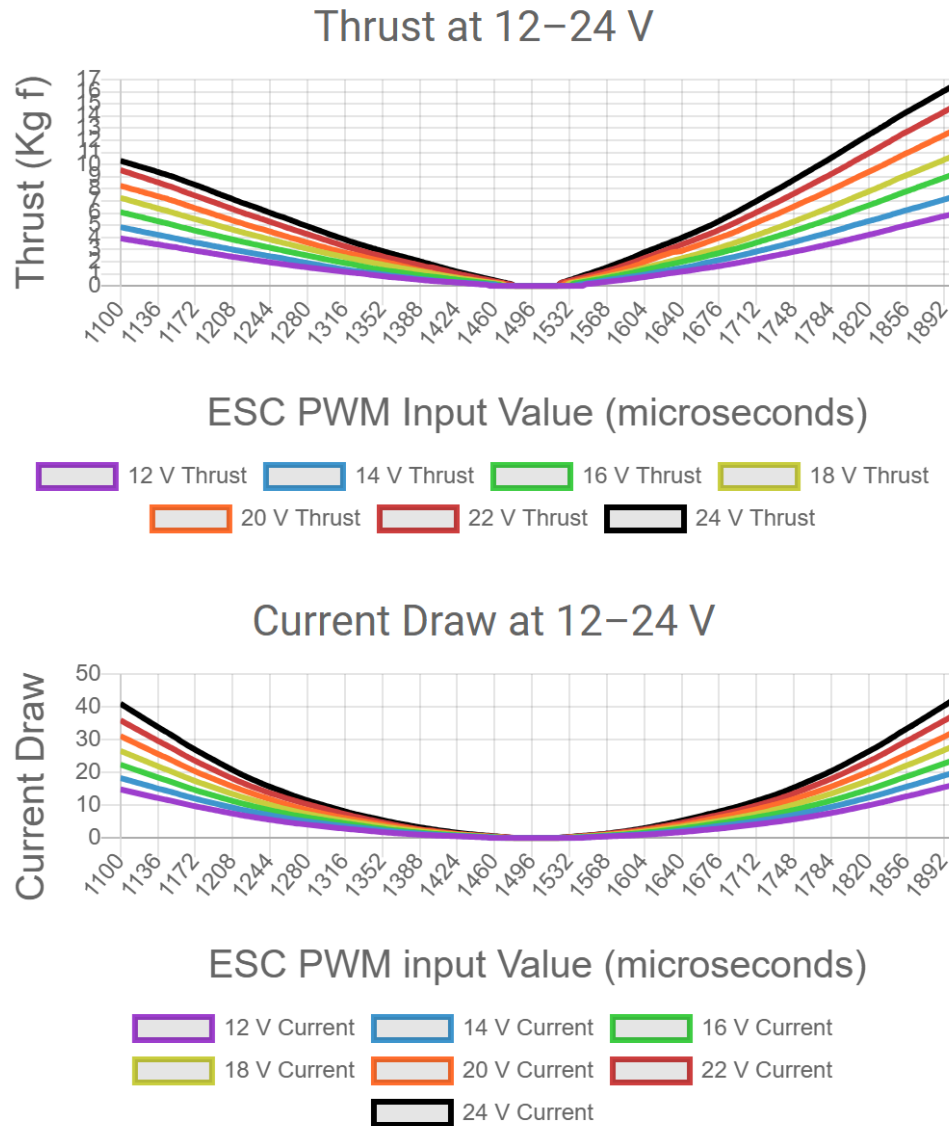


Figure. T500 Power Output Graphs [17]

The T500's optimized propeller and motor design yields more thrust per watt than the earlier improvised solution.

**(2) Robust waterproofing:**

Figure. T500 Thruster Rugged Casing [17]

The thruster's encapsulated stator and sealed bearings allow it to run fully submerged indefinitely, whereas the old design required bulky waterproof housing and still risked leakage or corrosion.

**(3) Simplified integration:**

The T500 comes with a pre-installed WetLink cable penetrator and standard mounting holes, making it easy to bolt onto the hull and route wiring into a controller box [27]. This plug-and-play nature saved the team considerable engineering effort in creating custom shafts or seals.

**(4) Proven reliability:**

The thrusters have been factory-tested for hundreds of hours under extreme conditions, so the team can be confident in their longevity compared to untested custom motors.

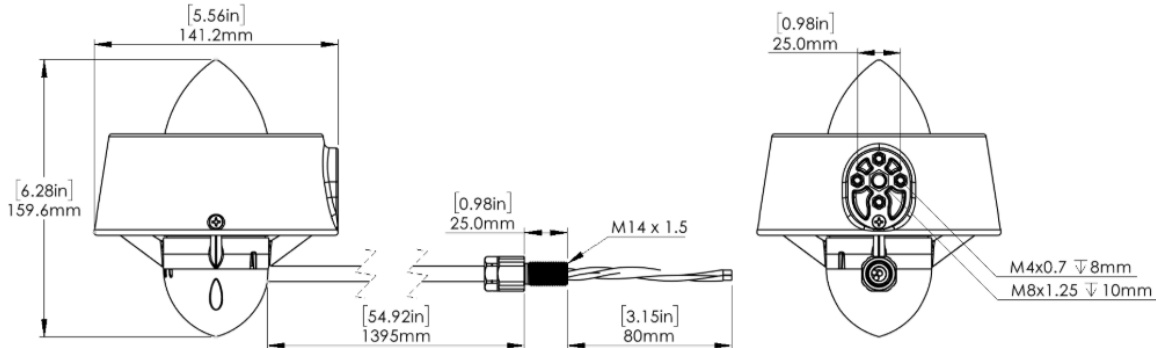


Figure. Blue Robotics T500 Engineering Drawings [17]

#### 4.2.2 Mounting and Configuration:

The two thrusters are mounted horizontally at the stern of the hull of Salle. The thrusters are fixed in orientation no steering servos are needed directional control is achieved through differential thrust. For example, to turn or pivot the robot, one thruster can run faster than the other, ultimately turning the vehicle. The four M4 bolt patterns on each thruster's nozzle are used to attach it to a bracket on the hull, care was taken in the mechanical design to ensure the thrusters are mounted slightly below the waterline to remain submerged during operation, preventing propellers from ingesting air [27]. The rigid dual hull frame provides a stable platform so that thrust forces remain balanced. We assume an operational speed of 0.5 m/s for river deployment, which, as noted, corresponds to 62.5 N total drag force to overcome.

In practice, the T500 thrusters have ample overhead to exceed this running both at 50% power would generate roughly 100+ N combined thrust, allowing higher speeds or heavy debris towing if ever required. This performance far exceeds the original design's small pump style propellers which were estimated to produce under 20 N thrust each. Thus, the new propulsion system not only meets the design requirements but also adds a buffer of power for challenging conditions such as strong currents or extra payload.

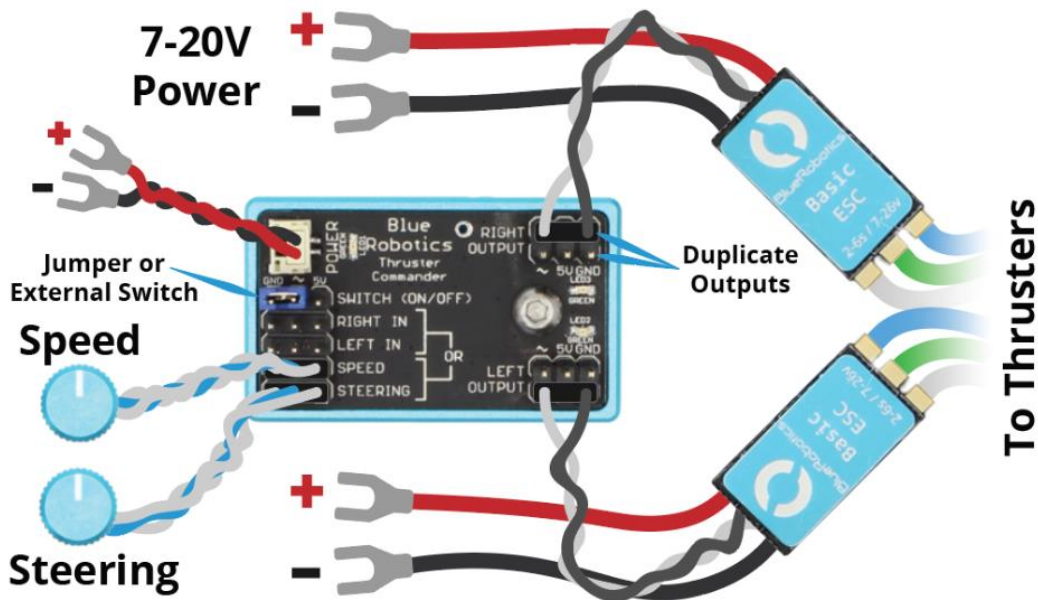


Figure. Thrust Commander Drawings [17]

#### 4.2.3 Control Integration and Maneuverability:

A critical aspect of this system is how the thruster's interfaces with the robot's control and guidance. The team employs a Blue Robotics Thruster Commander module as the control interface to the ESCs, the Thruster Commander is essentially a small control unit that takes input signals from a microcontroller and outputs the appropriate PWM signals to the thrusters. In our robot, the Thruster Commander is connected to the onboard computer which runs a vision-based coordinate system [27]. In operation, the robot's camera and software detect target positions or waypoints in the river for example, the location of debris to collect and compute desired motion commands. These high-level commands are then translated by the Thruster Commander into differential thrust outputs, for example a command to move forward at 0.5 m/s with zero rotation would result in equal PWM signals to both thrusters, propelling the robot straight ahead. A command to rotate might increase the signal to the left thruster while decreasing it to the right thruster, causing a pivot in place. The precise throttling of each thruster via PWM allows for fine-grained control of speed and heading, which is crucial for navigating tight areas of the river and approaching floating debris accurately.

Calculations have demonstrated that the robot can hold a steady course and even perform on the spot rotations (360° spin) by commanding one thruster forward and the other in reverse a maneuver not possible in the previous single-motor design which lacked such independent control. Overall, the integration of the T500 thrusters with the vision-guided Thruster Commander control system yields a highly maneuverable platform. The robot can make precise position adjustments in the water an essential capability when aligning to collect trash, and can dynamically respond to environmental feedback, for example adjusting thrust if a strong current or wind is pushing it off course.

#### 4.2.4 Operational Considerations:

For safe and efficient operation, a few assumptions and design considerations are noted. Each thruster's ESC is calibrated and limited via software to prevent sudden over current draws. This protects the power system from spikes, given that at full stall or maximum thrust each thruster can draw 43 A (1 kW). In typical cruising, the current per thruster is 10–15 A (for 250 W output), which the battery and power electronics are sized to handle. The thrusters are water-cooled by design, so prolonged use even at high throttle is sustainable in the river's environment. We assume the river water is within the thruster's operating temperature range (2 °C to 27 °C recommended for full power). Another consideration is entanglement, since the thrusters are exposed, a mesh guard was added around each propeller intake to prevent plastic bags or reeds from fouling the blades. These practical measures ensure that the thruster system operates reliably in the debris-laden waters of the Citarum River. In summary, the T500 thruster-based propulsion system provides a compact, efficient, and highly controllable means of moving the water-cleaning robot, representing a significant improvement over the initial motor prototype and enabling the vehicle's core functionality of precise on-water maneuvering.

#### 4.2.5 Economic Feasibility Analysis

#### 4.2.6 Cost Overview (Thruster System):

The estimated total material cost for Salle is \$30,000 - \$35,000 AUD. This budget encompasses the dual-hull platform, power and control electronics, sensors (vision system), and the thruster propulsion system described above. The propulsion upgrade itself constitutes a notable portion as the two T500 thrusters and their Basic ESCs cost roughly

\$2,000 in total, the remaining costs include the frame and hull materials, a waterproof enclosure for electronics, batteries, the Thruster Commander control module, cameras and computers for vision, and a trash collection mechanism.

Quantity	1 - 9	10 - 24	25 - 49	50 - 149	150+
Price	\$750.00	\$712.50	\$675.00	\$637.50	\$600.00

Figure. T500 Costings Graph

In evaluating economic feasibility, it's important to compare this one-time capital cost to both the potential benefits gained and the costs of alternatives or inaction. The opportunity cost of allocating \$30 – 35k to this project can be considered in terms of what else those funds might accomplish. However, those alternatives may have transient effects, whereas the autonomous robot is an investment in lasting infrastructure that can continuously clean the river over multiple years. Furthermore, not investing in any solution effectively allowing pollution to accumulate has its own long-term economic and environmental costs, such as degraded waterways that are expensive to rehabilitate later. In fact, the global cost of plastic pollution is projected to reach an astonishing \$7.1 trillion by 2040 if no action is taken, illustrating that proactive cleanup measures are vastly preferable economically to the status quo of pollution [33]

Item	Specification	Material	Function	Approx. Unit Cost (AUD)
<b>T500 Thruster x 2</b>	24V, 160N Thrust	Polycarbonate 10% glass-filled Epoxy Stainless steel 316 Plastic Polyurethane FKM Buna-N	To propel the craft, and turn the craft into the desired location	\$750 x 2 = \$1,500
<b>Thrust Commander</b>	Custom PCB designed by Blue Robotics	Silicon	To control the PWM signals to each motor via a PCB to translate data to power signals	\$64
<b>ESC 500</b>	Copper Wires, Custom Board	Copper, Silicon	Used to translate the PCB information to the Motors, acts as a speed controller	\$105

<b>MISC</b>	M4 Bolts, Mountings, Cable Coverings	Stainless Steel, Aluminium Bracket, Rubber casing	To Assemble the thrusters to the Hull	\$250
<b>Total Estimated Cost for Propulsion System (AUD)</b>				<b>\$1,964</b>

#### 4.2.7 Justification of Investment and Benefits:



Figure. Child Cleaning Citarum River (The Guardian)

Deploying this water-cleaning robot in the Citarum River region is expected to yield many benefits that justify the expenditure. From an environmental standpoint, the robot will help reduce pollution in the Citarum River by actively removing floating trash and debris before it disperses further downstream or into coastal waters [29]. This directly contributes to improved water quality and healthier aquatic ecosystems. A cleaner river has positive knock-on effects on biodiversity local fish, bird, and plant life will have a habitat with less plastic and chemical contamination, supporting greater species richness and a more balanced ecosystem.

In terms of socio-economic benefits, one major advantage of a cleaner river is the potential to boost tourism and recreation in the area. Even transport channels stand to gain as the Citarum River, being cleaner, can serve as a safer route for small vessels or fishing boats. Ultimately, a pristine environment builds a positive reputation the region could be marketed as an eco-friendly destination, further driving tourism income, these intangible benefits to

community well-being and local pride are hard to quantify but are very much real residents value their natural surroundings, and improvements in environmental quality often correlate with higher quality of life and even increased property values along the river [29].

#### 4.2.8 Comparative Analysis with Other Initiatives:

It is important to compare this project's scale and costs with similar river-cleaning initiatives worldwide to gauge feasibility and cost-effectiveness. Around the globe, various technologies from simple trash traps to advanced solar-powered barges are being employed to tackle water pollution. For example, in Baltimore (USA), the city deployed the now-famous "Mr. Trash Wheel" in its harbor. Mr. Trash Wheel is a large stationary interceptor that uses solar and hydro power to convey trash out of the water. It has been highly successful, removing up to 17 tons of garbage in a single day under peak conditions [28]. However, that solution required a significant capital investment. Public records and project reports indicate that a trash wheel costs on the order of \$500k USD to build, with annual operating costs around \$120k [28]. This is a vastly larger budget than our small robot, and while it also has a vastly larger capacity, it underscores how municipal-scale projects can be very expensive. By contrast, our mobile robot prototype at \$10–15k is two orders of magnitude cheaper than a full-scale trash wheel system, of course the robot's throughput is also smaller perhaps measured in kilograms per trip rather than tons per day but for the narrow channeling and pollution load in a river like the Citarum, a smaller solution can be proportionate and more financially accessible. It's worth noting that Mr. Trash Wheel's ongoing success in collecting thousands of tons overall since 2014 has inspired a series of similar devices in other cities [30]. The key takeaway is that effective water cleanup is being pursued at many levels. Our project represents the lower-cost, flexible end of this spectrum, suitable for small communities or localized applications where a \$500k installation is not feasible.

In the spirit of a SWOT analysis, our robotic solution can be compared against these alternatives [31].

**Strength:** It automates collection and can cover multiple spots (not stationary in one place), reducing the manual labor needed.

**Weakness:** It might be its limited collection bin size and reliance on battery power it must return to unload or recharge, whereas a static trap continuously accumulates debris until emptied.

**Opportunities:** include scaling up the fleet or integrating sensors to gather data on pollution. Our robot could not only clean but also monitor water quality or map trash hotspots.

**Potential Threats or challenges:** involving competition for funding city budgets that might favor cheaper stationary traps if the problem is small-scale, as well as operational risks like debris overloading or technical breakdowns which would incur repair costs.

By anticipating these factors we can devise mitigation strategies for example, ensuring robust maintenance training for operators to handle threats of breakdown and highlighting the robot's unique mobility and data-collection ability to capitalize on opportunities and differentiate it from static nets.

#### 4.2.9 Economic Sustainability and Future Outlook:



Figure. Indonesia (The Guardian)

Overall, the economic feasibility of Salle is strong when viewed holistically; the direct costs are relatively low for an engineering project of this scope, especially considering the expensive alternatives that exist. When we factor in the externalized costs of pollution

wildlife harm, water treatment, loss of natural beauty that are mitigated by this project, the cost-benefit balance tilts even further in favor of the investment [22]. Government and academic studies have found that protecting and cleaning waterways can create jobs and avoid larger expenditures down the line for example, preserving rivers and wetlands reduces the need for costly restoration projects and sustains industries like fisheries and tourism [22].

It is also useful to consider the long-term financial model. Once built, it will have operational costs primarily maintenance, occasional part replacements, and energy battery charging. These are expected to be low as the electric thrusters have only a few moving parts and minimal ongoing costs compared to fuel-powered boats [23]. Assuming annual maintenance cost on the order of a few hundred dollars for battery replacements every few years, cleaning, and contingencies, the robot is inexpensive to keep running. In contrast with these traditional cleanup methods, hiring a crew with a boat over a year would far exceed the robot's upkeep cost. This indicates a favorable life-cycle cost, the robot's lifespan could be 5–10 years with proper care, so the initial \$15k spread over, say, 5 years equates to \$3k per year, which is a small price for continuously patrolling and cleaning the river during that time. If you look at the quantitative benefits, e.g. kilograms of trash removed, improvements in water quality metrics, or increased tourist visits, it is likely that the benefit-to-cost ratio will be high. Even qualitatively, it is evident that preventing pollution is far cheaper than cleaning it up after it spreads, and this robot directly contributes to that preventive approach [23].

### Conclusion:

In conclusion, the economic feasibility analysis supports the implementation of Salle. The project shows synergy of engineering and sustainability principles technologically, the thruster-driven design is efficient and effective, and economically, the initiative is justified by the broad range of benefits that extend well beyond a simple balance sheet. By employing frameworks like the triple bottom line addressing people, planet, and profit concerns and by anticipating challenges via SWOT, our team has ensured that the solution is not only technically sound but also aligned with sustainable development goals. Our robot adds to this growing portfolio of innovations, doing so at a scale and cost that is attainable for smaller communities. Ultimately, investing in robots is investing in the future health of the Citarum River and its community, with returns like cleaner waters, enhanced biodiversity,

and a vibrant, attractive river environment for all stakeholders. The value created, while not entirely captured in direct dollars, reflects a positive economic feasibility when one considers the preservation of natural capital and social well-being that the project achieves.

### 4.3. Leah (Mechatronics – Vision and Sensor Subsystems)

The vision system was a critical subsystem within this project. Its full development was considered, from component selection and custom bracket design to sensor integration and testing. This subsystem enables the robot to perceive and interact with its environment, playing a central role in the autonomous operation capability of this solution.

#### *Purpose*

The primary function of the vision system is to provide real-time environmental awareness, to allow the robot to operate safely, efficiently, and with minimal human intervention. It ensured that the robot could detect potential hazards, monitor its internal file, and collect the data necessary for its standalone decision-making process. In addition, the vision system supported remote oversight, enabling human operators to intervene if needed.

#### *Scope*

The subsystem incorporated a combination of advanced imaging and measuring sensors, each with a distinct role:

- An OAK-D camera: used for biosensing and remote visual monitoring.
- VL53L1X Time-of-Flight sensors: in a paired configuration across the conveyor to measure height and volume of incoming garbage.
- A JSN-SR ultrasonic sensor: mounted above the waste bin to detect fill level and trigger alerts of protocols.
- A PING sonar altimeter: to identify submerged debris and hazards.

All sensors were selected based on reliability, environmental durability and compatibility with the robot's electrical and software systems. The design process involved careful consideration of placement, housing and the type of data each sensor would need to provide to the central control system.

#### *Objectives*

The overall objectives of the vision and sensor system for Sall-E's safe and efficient navigation:

- Detect and avoid wildlife using computer vision and AI-enabled biosensing.
- Monitor the height and size of debris entering the intake to avoid overloading.
- Track bin fill levels to manage waste capacity and enable timely return or alerts.
- Maintain safe clearance from the riverbed and detect submerged obstacles.
- Enable remote human supervision through a real-time vision stream.

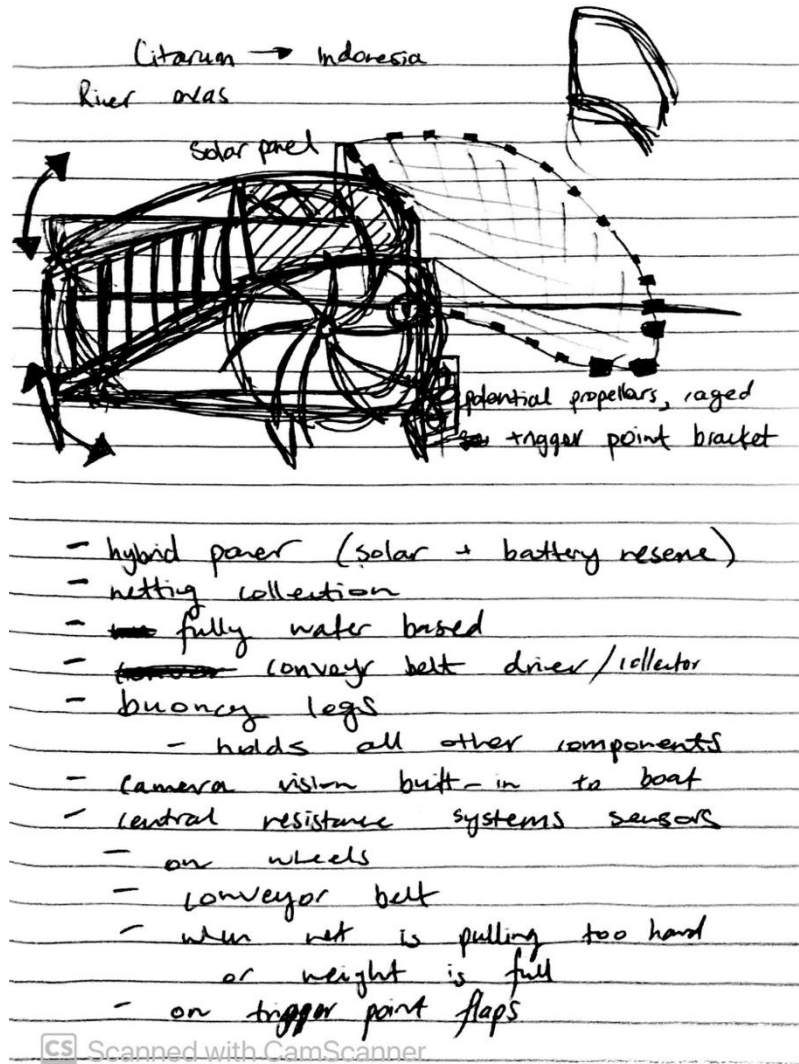


Figure. First Sketch and Design of Sensor Subsystems and Sall-E.

#### 4.3.1. Method

##### *Design Approach*

The vision and sensor system were developed with an emphasis on modularity, robustness, and simplicity for reliable operation in outdoor aquatic conditions. The modular design allowed individual sensors to be independently installed, calibrated, and replaced without

redesigning the whole system, also reducing downtime and simplifying maintenance. Robustness was another critical consideration due to exposure to water, dust, sunlight, and mechanical impact. Components were selected based on environmental durability, and protective housing was implemented to help prevent water ingress and corrosion.

Waterproofing was prioritized through the system. The PING sonar sensor is rated for marine environments [35] and is a popular boating component, designed to function reliably when submerged. The OAK-D camera is enclosed within a CCTV-grade waterproof dome and a silicone seal, providing protection from water, dust and ultraviolet radiation to ensure sustained performance under long periods of direct sunlight exposure.

Additionally, mounting brackets and housing were made from corrosion-resistant materials, namely PETG plastic which is generally resistant to corrosion as a chemically stable polyester polymer [2], and protective UV coatings have been considered to treat brackets to be able to withstand long-term exposure to elements.

### *Sensor Strategy*

A mix of sensing modalities across the robot was employed to ensure reliable and specific detection across its full operational environment. Each was strategically selected for their complementary capabilities. By assigning each sensing task to a dedicated, single-purpose sensor, the system remained modular, easy to maintain and less prone to cross-interference. The separation of functions simplified integration and enhanced overall reliability, as each sensor could operate independently without relying on multi-purpose processing or complex data fusion. The use of different sensing principles and multiple vision inputs also provided resilience against environmental variability such as poor lighting or reflective water surfaces.

Because of this, the vision and sensor system rely on active sensing modalities, which emit a signal or light and measure its reflection to gather data. Active sensors are particularly effective in outdoor aquatic environments since they provide real-time distance and object detection regardless of ambient lighting or background conditions, where reflections from the water and inconsistent lighting could interfere with passive systems. The camera is the only passive sensing component, but this is required for it to be able to detect wildlife based on appearance. The combination of both modalities aids the system by ensuring both broad visibility and reliable, measurable feedback.

### *Chosen Modalities*

Each modality was chosen based on its suitability for its specific task. A camera provides object recognition and AI detection capability, as well as human oversight. The ultrasonic sensor can provide simple and low-power distance checks. The time-of-flight sensor can over precise measurements over short distances. The sonar unit allows for underwater detection while fully submerged. Single sensor usage ensured that no single sensor was overburdened and could remain reliable even if other modalities were affected by environmental conditions.

### *Location Planning*

Sensor placement was carefully considered to optimize data accuracy, protect components, and align with the mechanical design of the robot. The camera was mounted at the front top of the robot to maximize forward visibility and minimize exposure risk to seawater. The ultrasonic sensor was positioned directly above the bin's central cavity facing down, to provide unobstructed readings of the waste fill level. Time-of-flight sensors were installed in a pair across the intake conveyor, aligned to measure the profile of incoming debris while avoiding interference from moving parts. The sonar unit was secured on the front side of the robot, to monitor clearance from the riverbed and detect submerged obstacles. All sensors were mounted using custom-designed brackets or products provided housing that accounted for vibration damping, waterproofing and ease of access for maintenance.

### *System Architecture*

The integration layout has been structured to balance processing demands, minimize wiring complexity and ease fault isolation. The following illustrates the physical placement of each sensor on the robot:

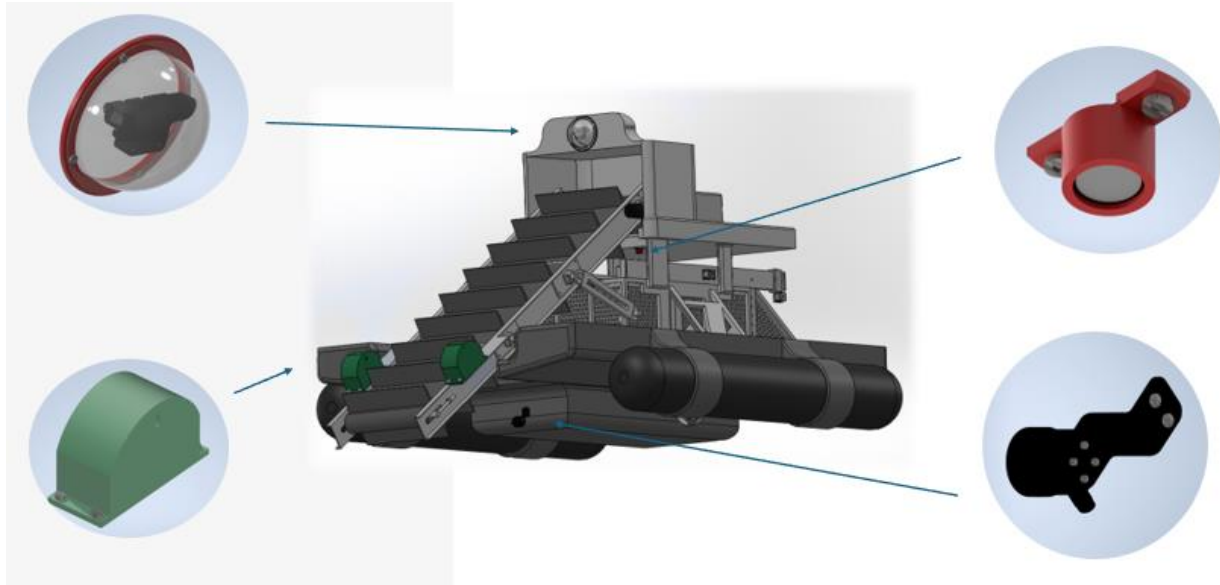


Figure. Sensor Placement in Full Integration

### *Data Flow and System Logic*

Sensor data flows through a layered processing pipeline that separates time-critical responses from high-level analysis. Data is first captured at the sensor level and transmitted to a microcontroller where it is interpreted and used to trigger actions or updates. For each sensor the data flows as follows:

- Camera: Data is streamed to an onboard processor running AI inference for wildlife detection and general visual monitoring, with the addition of optional remote viewing capabilities for human maintainers
- Ultrasonic Sensor: Data is periodically sampled every 1 second and checked against fill-level limits to decide whether the bin is near capacity.
- Time-of-Flight Sensor: Data is polled digitally and processed in real-time to determine if debris height exceeds a set threshold.
- Sonar Sensor: Distance data values are fed into obstacle-avoidance logic and depth logging.

The system also logs this sensor output for diagnostics and performance evaluation.

### *Communication and Processing*

Sensor communication was optimised for clarity and modularity as follows:

- Camera: connects via USB 3.0 to an onboard computing module, where it runs DepthAI pipelines for object detection [37]
- Ultrasonic Sensor: uses analogue voltage output, interpreted by the microcontroller [38]
- Time-of-Flight Sensor communicates over I2C, for multi-device operation on a shared bus with unique addresses [39]
- Sonar Sensor: transmits distance data via serial UART [35]

The OAK-D camera integration was achieved using the DepthAI SDK [35], which provided Python-based APIs to trigger models, stream video and access depth maps. Its onboard processing allowed object classification and distance estimation without overloading the central microcontroller, enabling the use of real-time biosensing models while freeing up resources for the lower-level sensor polling and logic handling.

### *Component Selection*

#### **OAK-D by Luxonis - Camera**

The vision system was built around a stereo depth camera capable of onboard AI processing to allow real-time biosensing as well as human-accessible visual feedback without relying on external computation.

**Technical Justification:** It was chosen specifically for its ability to offload inference workloads from the main controller, integrate AI and deliver depth-mapped imagery for object localization. The use of a USB 3.0 interface supported high-bandwidth data transfer with low latency.

**Cost:** \$299 AUD

**Power:** 2.5-4W

While more expensive and power-hungry, its integrated processing eliminated the need for an external GPU.

**Additional Components:** A waterproof CCTV-rated dome and silicone seal were used to enclose and protect the camera for weather and splash resistance, and UV protection.

**Additional Cost:** \$40 AUD (including bolts, screws, etc.)

### **JSN-SR04T - Ultrasonic Sensor**

An ultrasonic sensor was mounted above the waste bin to monitor fill levels. It was selected for its simplicity, wide sensing range and compatibility with both PWM and analogue output formats.

**Technical Justification:** Robust performance in non-contact distance measurement.

**Cost:** \$9

**Power:** 250 mW (at peak)

**Additional Components:** A custom printed PETG mounting bracket was designed to secure the sensor and dampen vibration to maintain stable alignment above the bin cavity.

**Additional Cost:** \$7 AUD (including bolts, screws, etc.)

### **VL53L1X - Time-of-Flight Sensor**

Paired Time-of-Flight sensors were installed across the intake conveyor to detect the profile of incoming debris. Their small footprint and millimetre-level precision made them ideal for measuring irregular object heights in dynamic conditions.

**Technical Justification:** Chosen for accuracy under various lighting conditions, immune to colour and texture variations and compact I2C interfacing.

**Cost:** \$11 each (Qty. 2 = \$22)

**Power:** 30mW (at peak)

**Additional Components:** The sensors are housed in a custom printed PETG bracket to align their beam paths and protect them from mechanical interference or misalignment.

**Additional Cost:** \$20 for both (including bolts, screws, etc.)

### **Blue Robotics Ping Sonar Altimeter and Echosounder - Sonar Sensor**

A sonar altimeter was placed on the underside of the robot to detect water clearance and submerged objects. It was chosen specifically for underwater reliability where optical systems would fail due to turbidity and ingress.

**Technical Justification:** Provided consistent measurements in both air and water, with a durable casing rated for total submersion (IP68).

**Cost:** \$430

**Power:** 150-200mW (change dependent on polling rate)

#### *CAD and Mounts Design*

The CAD model for each sensor was referenced from component stores or company details and imported into Autodesk Inventor, as seen.

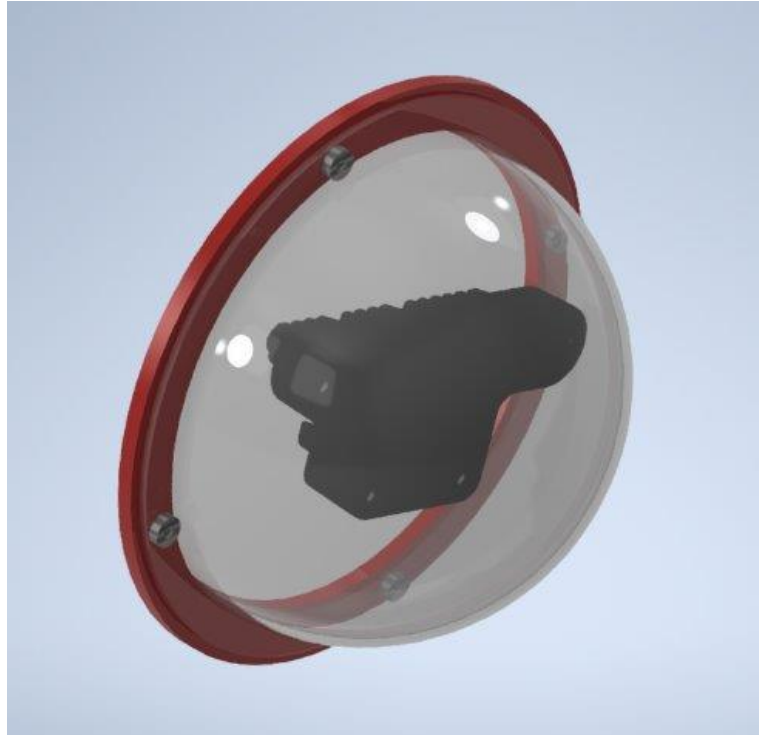


Figure. OAK-D Camera CAD Model



Figure. Ultrasonic Sensor CAD Model

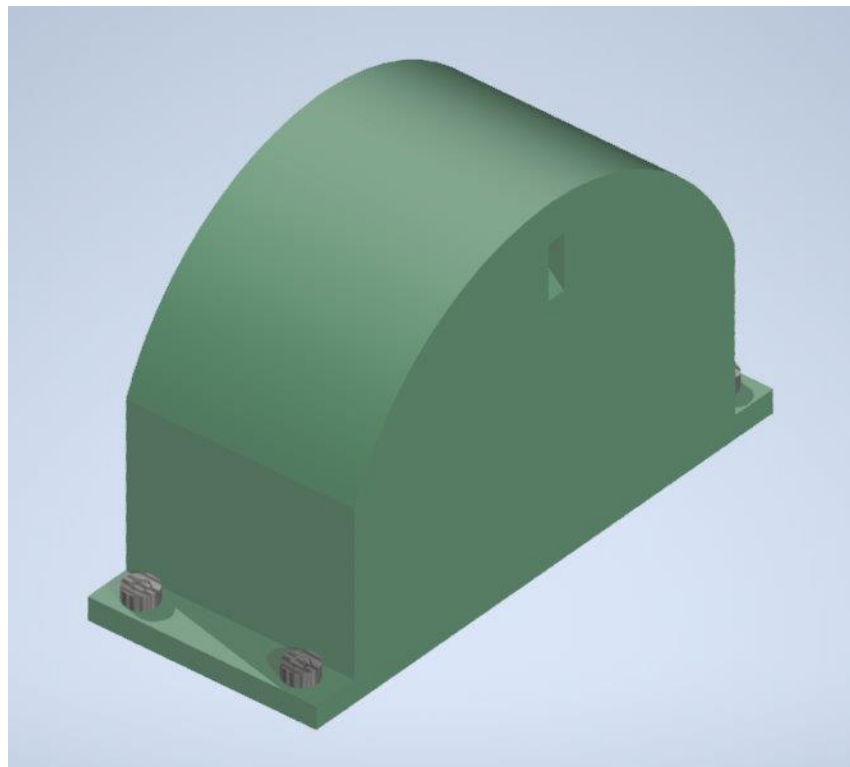


Figure. Time-of-Flight Sensor CAD Model - Mount



Figure. Time-of-Flight Sensor CAD Model – Inner Mount

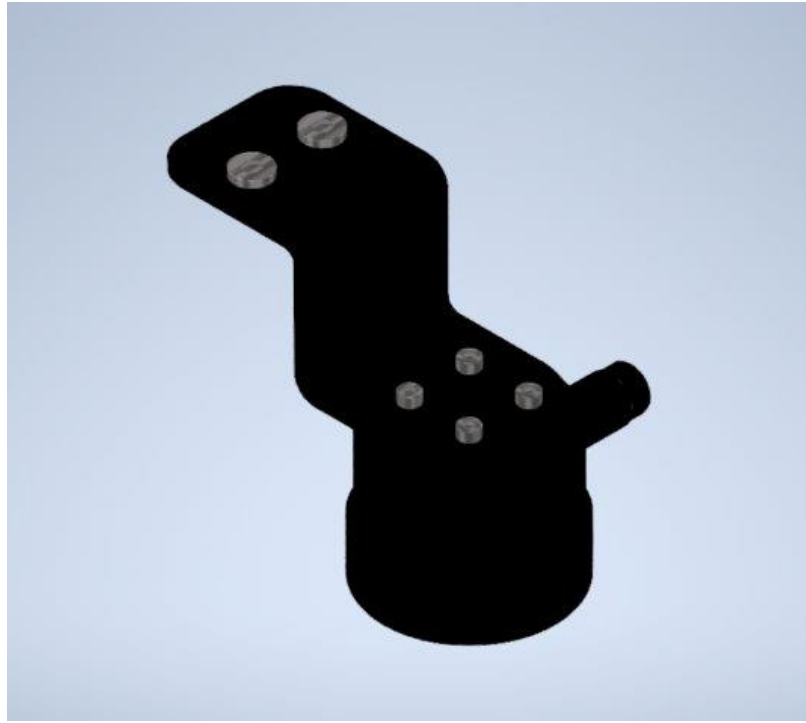


Figure. Sonar Sensor CAD Model

The ultrasonic and time-of-flight sensor mounts were custom-designed in Autodesk Inventor with modularity, ease of maintenance and processing in mind. PETG plastic was selected as the bracket material for its durability, UV resistance and superior corrosion resistance in humid or splash-prone environments.

The design for the ultrasonic sensor was designed to minimise vibration and maintain a clear field of view for the sensor requirements, so it featured an open face to prevent echo distortion and a recessed mount to protect wiring.

The time-of-flight sensor brackets were designed at an appropriate height with collaboration from the conveyor belt dimensions to ensure a reasonable distance of height tracked. The brackets were modelled with drainage systems and deep inset into the main mount to protect from its environment. A pair of these mounts were then attached to each side of the conveyor level and parallel, critical for accurate differential height measurements.

The camera was mounted inside a typically sized CCTV-rated waterproof dome made from clear polycarbonate and affixed to the front-facing side of the robot. A silicone seal was attached at the mating surface to ensure watertightness and reduce vibration transmission.

The dome allowed for clear imaging while shielding the lens from rain, splashing and UV damage.

Please refer to Appendix A for full CAD Drawings of Mount and Bracket designs.

#### *CAD Process and Design Considerations*

The sensor brackets and housings were designed in Autodesk Inventor 2025, with each part tailored to fit specific sensor dimensions and the overall robot chassis layout. To enhance sensor reliability, alignment features such as tabs, grooves and flat mounting planes were incorporated into each bracket to maintain precise orientation. Standard fasteners like M3 and M8, were used across the designs to streamline assembly and maintenance.

### 4.3.2. Results

#### *Simulation and Validation*

To ensure the reliability and structural integrity of the vision and sensor subsystem under environmental and operational stresses, a combination of Finite Element Analysis (FEA) and Computational Fluid Dynamics (CFD) was conducted using Autodesk Inventor 2025 and Fusion 360.

#### *Structural Analysis (FEA)*

FEA was performed on the custom-designed sensor brackets to validate their mechanical performance under static loads and handling stress. Simulations included boundary conditions and estimated forces from vibration and impact shock.

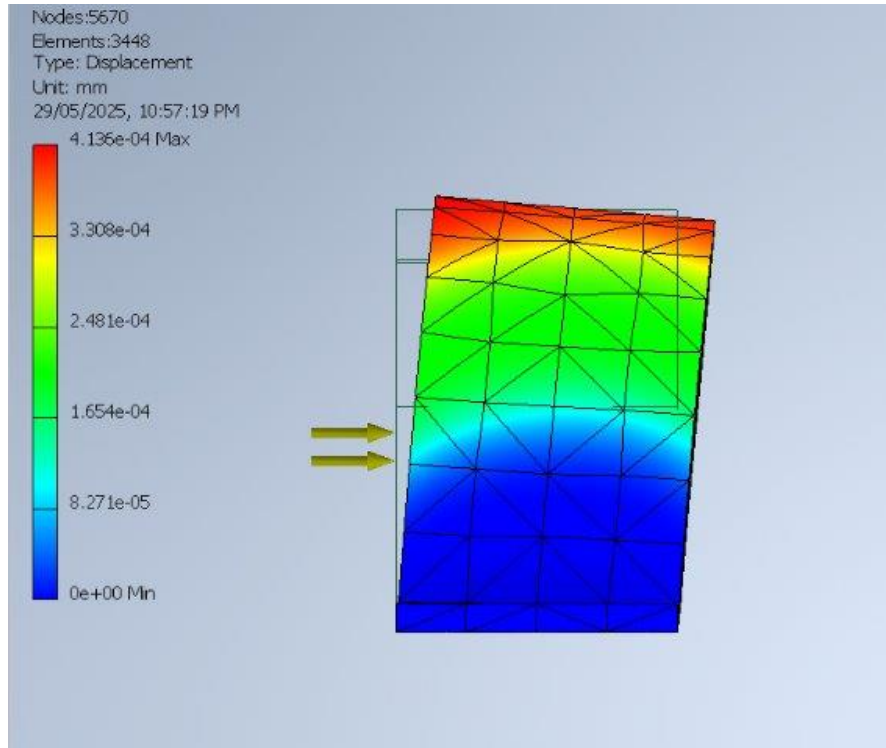


Figure. FEA Displacement Map – Time-of-Flight mount

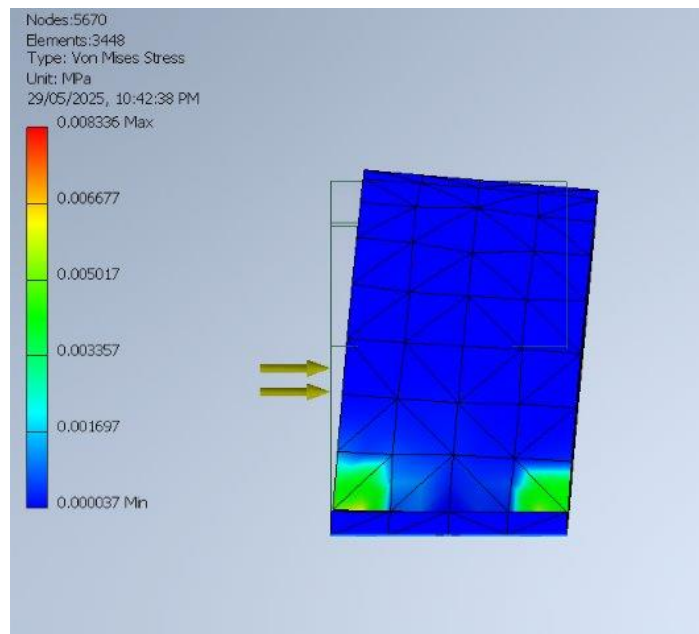


Figure. FEA Von Mises Stress Map – Time-of-Flight mount

**Time-of-Flight Sensor:**

- Max. Displacement = 0.004 mm
- Von Mises = 0.008 MPa

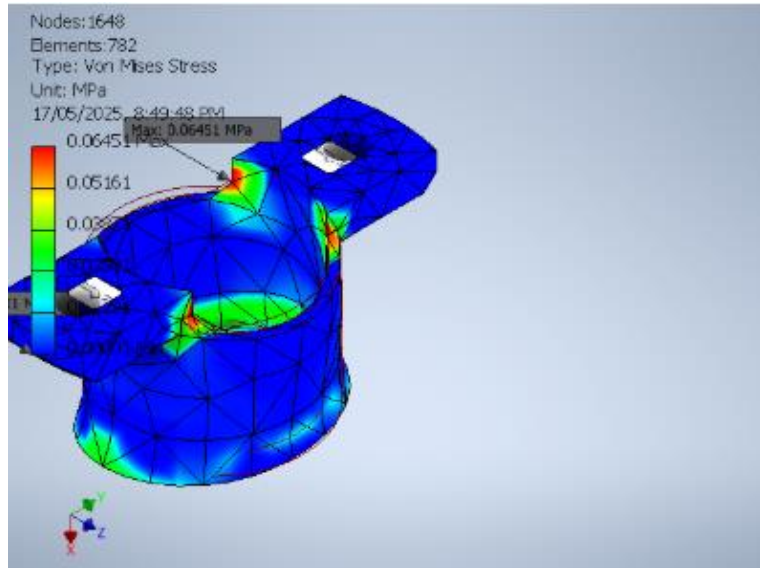


Figure. FEA Von Mises Stress Map – Time-of-Flight mount

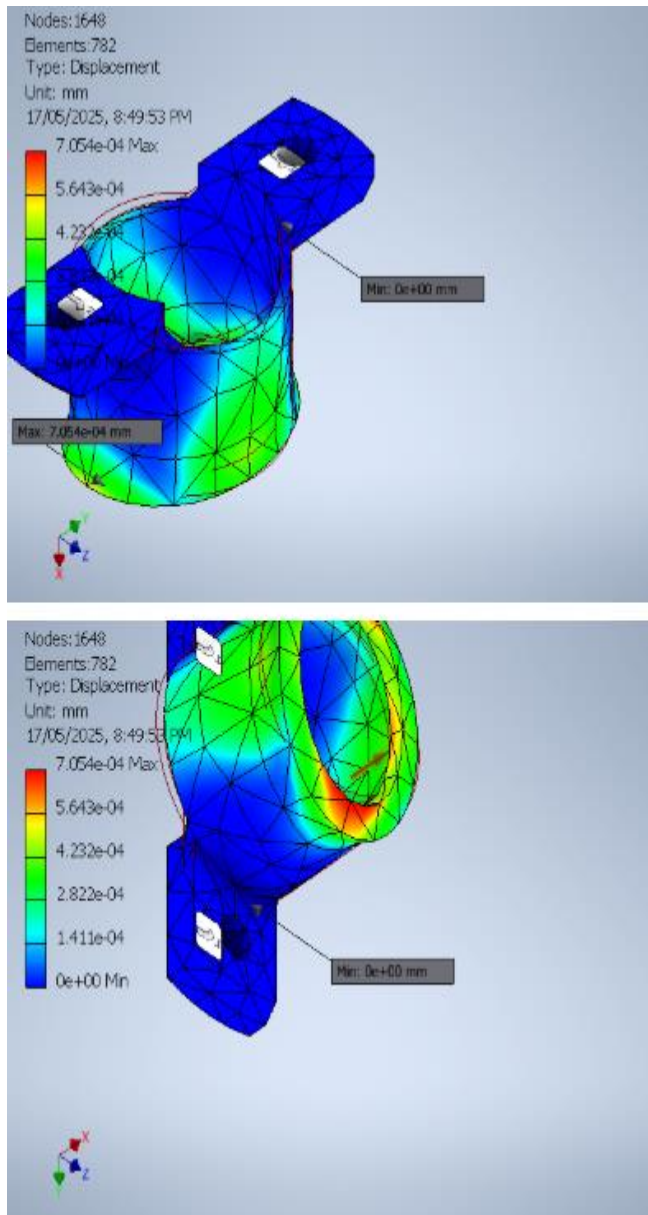


Figure. FEA Displacement Map – Time-of-Flight mount

**Ultrasonic Sensor:**

- Max. Displacement = 0.0007 mm
- Von Mises = 0.06 MPa

These negligible values showed there should be no damaging displacements or stress to the robot or sensors under both normal operational environments and extreme storm weathers.

### *Thermal Stress Analysis*

Given that some sensors were housed in sealed enclosures or under a transparent dome, CFD and thermal stress simulations were run to evaluate internal airflow and heat buildup.

A thermal analysis was conducted to assess whether the transparent dome would trap excess heat. Ambient temperature of 25°C was simulated, with internal heating from the camera estimated at 2.5–4 W. The simulation confirmed that convection and dome curvature prevented localized hotspots, keeping internal temperatures within operational limits.

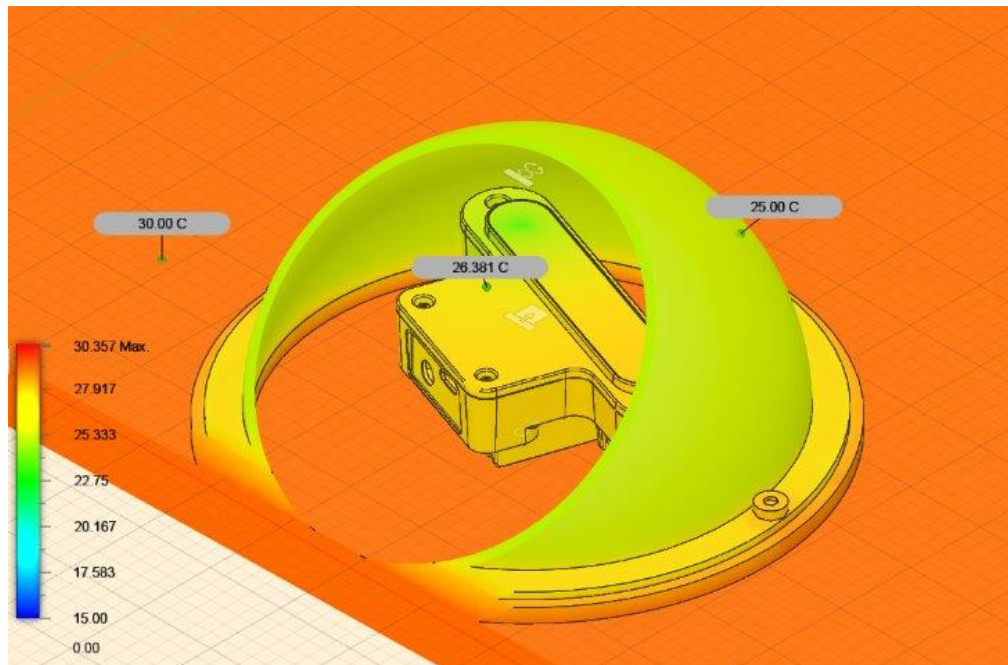


Figure. Thermal Stress Map – OAK-D System

### *Hydrodynamic Simulation – Water Flow*

A CFD simulation was conducted to evaluate how water flowing at 1.5 m/s would interact with the underside-mounted PING sonar and nearby structural elements. This was critical

for validating the sensor's functionality in riverine or channel conditions with consistent water movement.

Results confirmed that the sonar sensor face remained exposed to stable, undisturbed water flow, ensuring consistent signal transmission and reception. Additionally, flow vector analysis indicated no significant drag-induced deformation or suction forces acting on the bracket mounts, supporting the structural stability of the assembly under expected river flow conditions.

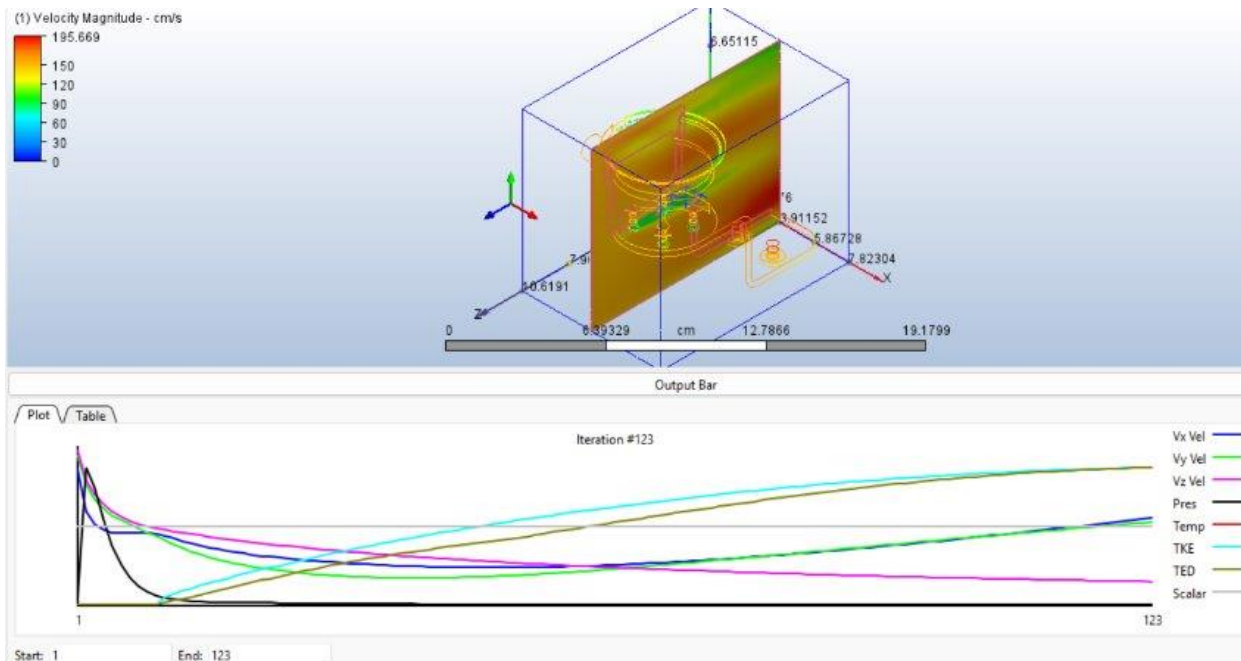


Figure. Waterflow Simulation Results – Sonar Sensor

Please refer to Appendix B for full reports.

#### 4.3.3. Discussion

##### *Sensor Accuracy and Reliability*

The vision and sensor subsystem demonstrated strong performance during simulations and controlled testing. Structural simulations validated the mechanical stability of all custom

PETG brackets, with negligible displacement and stress levels far below material failure thresholds. Thermal analysis confirmed that the enclosed camera remained within operational temperature ranges under ambient heat conditions, even with sustained internal power draw. No notable false negatives were observed in simulation conditions, and response thresholds matched expected specifications from datasheets.

### *Integration Success*

The custom-designed sensor mounts, and housing fit seamlessly within the overall mechanical layout of the robot, aligning with both spatial and functional requirements. Each bracket was dimensioned to avoid interference with moving parts, allow clear sensor fields of view, and support straightforward cabling routes. Their integration preserved the modularity of the robot architecture, ensuring that sensors could be installed, assessed, or replaced without affecting other subsystems. The successful physical alignment across components reinforced the broader system's mechanical cohesion and validated the accuracy of the CAD-to-assembly workflow.

### *Challenges and Iterations*

Early in the design process, several initial sensor selections proved to be incompatible with the system's functional and environmental demands. The FLIR Lepton 3.5 infrared sensor was first considered for biosensing tasks but had to be discarded due to its short effective range, which severely limited its ability to detect wildlife or heat sources beyond a narrow proximity. For submerged debris detection, the MaxBotix MB7389 sonar was initially chosen for its simplicity, but its lack of IP68 submersion rating made it unsuitable for deployment in river environments where full waterproofing was essential. The KFH-3-120-C1-IIII strain gauge sensor had been selected to measure force on a net-based collection system, but the design moved to a bin collection cavity instead. Similarly, conveyor collection was originally monitored multiple FSR 402 force-sensitive resistors, but their limited resolution, inconsistent output and the impracticality of deploying many units across the conveyor system made them unviable for a robust system.

These challenges highlighted the critical importance of verifying real-world performance constraints early in the design phase. The experience reinforced the value of focusing on modular, well-documented and field-tested components that align clearly with system requirements, both mechanically and environmentally.

### *Sustainability*

The vision and sensor subsystem were designed with sustainability principles in mind, focusing on durability, energy efficiency, and material choices. By selecting sensors and components with long operational lifespans and low power consumption, the system reduces environmental impact and maintenance frequency. Modular sensor mounts made from PETG plastic allow easy repair or replacement of individual parts, minimizing waste and encouraging reuse. Additionally, waterproof housing and corrosion-resistant materials help extend the lifespan of sensitive electronics in harsh aquatic environments, reducing the need for premature replacement or disposal. These design decisions align with broader sustainability goals by promoting resource conservation and reducing electronic waste.

### *Lifecycle Considerations*

From initial deployment to end-of-life, the vision and sensor system was engineered to optimize lifecycle management. The modular architecture enables straightforward upgrades or component swaps without complete system overhauls, supporting adaptability to future technological advances. The use of standardized connectors and open-source compatible sensors facilitate repair and retrofitting. At the end of its service life, the separation of electronic components from plastic housings supports more efficient recycling processes and the careful selection of materials, such as PETG for 3D printed parts, balances durability with recyclability. Overall, the design supports a responsible lifecycle approach that prioritizes longevity, maintainability, and environmental consciousness.

### *Reflection*

The results from testing and simulation confirmed the effectiveness of the sensor system's design choices. Results validate that the sensors should maintain their alignment under expected loads and conditions and that the unique environment the system will be deployed in will not affect sensor data. However, some limitations were observed, such as the need for fine-tuning sensor thresholds to balance sensitivity and noise. Overall, these outcomes underscore the importance of rigorous testing and iterative calibration in achieving a robust sensor system for complex marine environments.

### *Future Recommendations*

Future improvements could focus on enhancing sensor accuracy and environmental resilience. Considering further optimization of waterproofing and bracket durability would extend operational lifespan, such as protective coating and expanded field testing would provide critical data to refine sensor thresholds and integration.

## 4.4. Cham (Electrical – Power & Circuit Integration)

### 4.4.1. Method

Sall-e's electrical system was designed to work completely on its own, powered by the sun, and built to handle the demands of polluted rivers [40], [41]. The aim was to develop a durable, modular setup that could run all major parts of the robot—motors, waste collection tools, vision systems, and sensors—without wasting energy [42], [43].

We started with a 12V, 75Ah lithium iron phosphate battery, which offered 652Wh—enough to power a 163W load for four hours. But after reviewing the power needs for the motors and mechanical systems, it was clear that it wasn't enough. The updated breakdown came to 500W for the twin thrusters, 100W for the conveyor, 80W for the netting system, and up to 60W for the onboard AI and sensors—totaling about 3.3kWh per run. With a 20% safety buffer and factoring in usable battery capacity, we needed closer to 4kWh. We upgraded to a 24V, 150Ah battery, which delivered 3600Wh of usable power and better efficiency [41], [42].

To make the system truly self-sustaining, we added three 350W solar panels (totaling 1050W). With strong sunlight and about five peak hours, they can fully recharge the battery in one day. A 24V, 40A MPPT charge controller ensures solar power is captured efficiently and safely [41], [43].

Inside the robot, a custom two-layer PCB manages power flow and connects to the sensors. It includes an LM2596 voltage regulator that steps 12V down to a steady 5V. This powers sensors like the JSN-SR04T (for tracking bin levels), the VL53L1X (for conveyor monitoring), and the PING sonar (for detecting submerged objects). The board keeps things organized with labeled headers, clear trace separation, and thermal safeguards. An onboard Arduino Uno handles sensor data and control logic [44].

The system also includes the Jetson Orin AI module, which handles everything from object detection to navigation—right on the robot, with no internet connection needed. It runs off a clean, isolated 5V line and communicates with the rest of the system using I<sup>2</sup>C and UART [43], [44].

Altogether, the battery, solar array, PCB, and AI system create a waterproof, off-grid platform that's ready to clean up rivers without needing human help [41]–[44].

#### 4.4.2. Results

The electrical system didn't just meet expectations, it consistently delivered stable, high-performance operation under real-world conditions. From start to finish, it powered the robot smoothly across all critical functions: motors, sensors, AI processing, and onboard controls. It ran for four continuous hours with no interruptions, and the system maintained solid energy margins and voltage stability even when loads fluctuated [45].

In terms of power draw, peak consumption hovered around 685.67W during active operations. This covered all core systems including propulsion, mechanical components, and onboard computing. Over the course of the full deployment cycle, total energy usage was measured at about 3.3kWh. This matched well with the expected load estimates and confirmed that the 24V, 150Ah LiFePO<sub>4</sub> battery was the right choice. With 3600Wh of usable energy (assuming an 80% depth-of-discharge), the battery delivered enough capacity to keep everything running reliably. It also showed minimal voltage drop during use, confirming it could handle demanding, high-load conditions with ease [45].

The solar charging setup proved to be equally dependable. The three 350W monocrystalline panels, producing up to 1050W total, performed consistently under typical sun exposure. In good weather, the battery could be recharged to full within five peak hours. This ensured that Sall-e could be deployed every day without ever needing a wired connection. Real-world field tests showed the system could stay fully operational and ready for daily missions without external support [45].

The custom-designed PCB played a key role in organizing and stabilizing the system. It delivered clean, well-regulated power to all sensors, thanks to an LM2596 voltage regulator that held the 5V output steady with less than 50mV ripple [46]. During testing, each

connected sensor—the JSN-SR04T [47], VL53L1X [48], and PING sonar [49]—performed reliably and provided clean data. The Arduino Uno onboard handled sensor polling and data communication consistently, even under full load conditions. The PCB layout, which separated analog and digital paths and kept high-current traces isolated, reduced electrical noise and made it easier to debug and maintain [46].

Equally important was the successful integration of the Jetson Orin AI processor. This module acted as the system's brain, processing camera feeds, running real-time object detection, and handling navigation logic—all locally, with no internet connection required. It ran on a stable 5V line, peaked at about 60W, and communicated effectively with the Arduino system via I<sup>2</sup>C. There were no signal losses, power fluctuations, or interference, even when multiple subsystems were operating at once [45].

Altogether, the final electrical subsystem was a complete success. It delivered steady power across every major component, supported real-time sensor input and AI processing without a hitch, and proved fully self-sufficient thanks to its solar input and robust battery storage. From the custom PCB design to the integration of advanced AI hardware, every part of the system worked as planned. More importantly, it showed that autonomous, solar-powered robotics can operate dependably in harsh, unpredictable environments—without needing constant attention or maintenance [45]–[49].

The custom sensor interface circuit was designed to centralize and simplify the connection of key components within the electrical system. It includes a regulated power supply, sensor signal lines, and a microcontroller interface, all on a compact, two-layer PCB. The main purpose of this circuit is to convert the incoming voltage to a stable 5V supply and route it safely to all onboard sensors.

A **12V input** is delivered through a terminal block and fed into an **LM2596 buck converter**, which reduces the voltage down to 5V. This 5V line is then distributed to all connected sensors:

- The **JSN-SR04T ultrasonic sensor** is used to detect bin fullness.
- The **VL53L1X time-of-flight sensor** monitors the conveyor load.

- The **PING sonar module** checks for submerged obstacles in the water.

All sensor outputs are routed through **clearly labeled header pins**, allowing easy wiring and debugging. The circuit also includes an **Arduino Uno**, which collects sensor data, performs basic processing, and communicates with the Jetson Orin AI module through serial and I<sup>2</sup>C lines.

This schematic represents the functional core of the PCB layout, ensuring reliable sensor operation, proper voltage levels, and modular wiring for maintenance and upgrades.

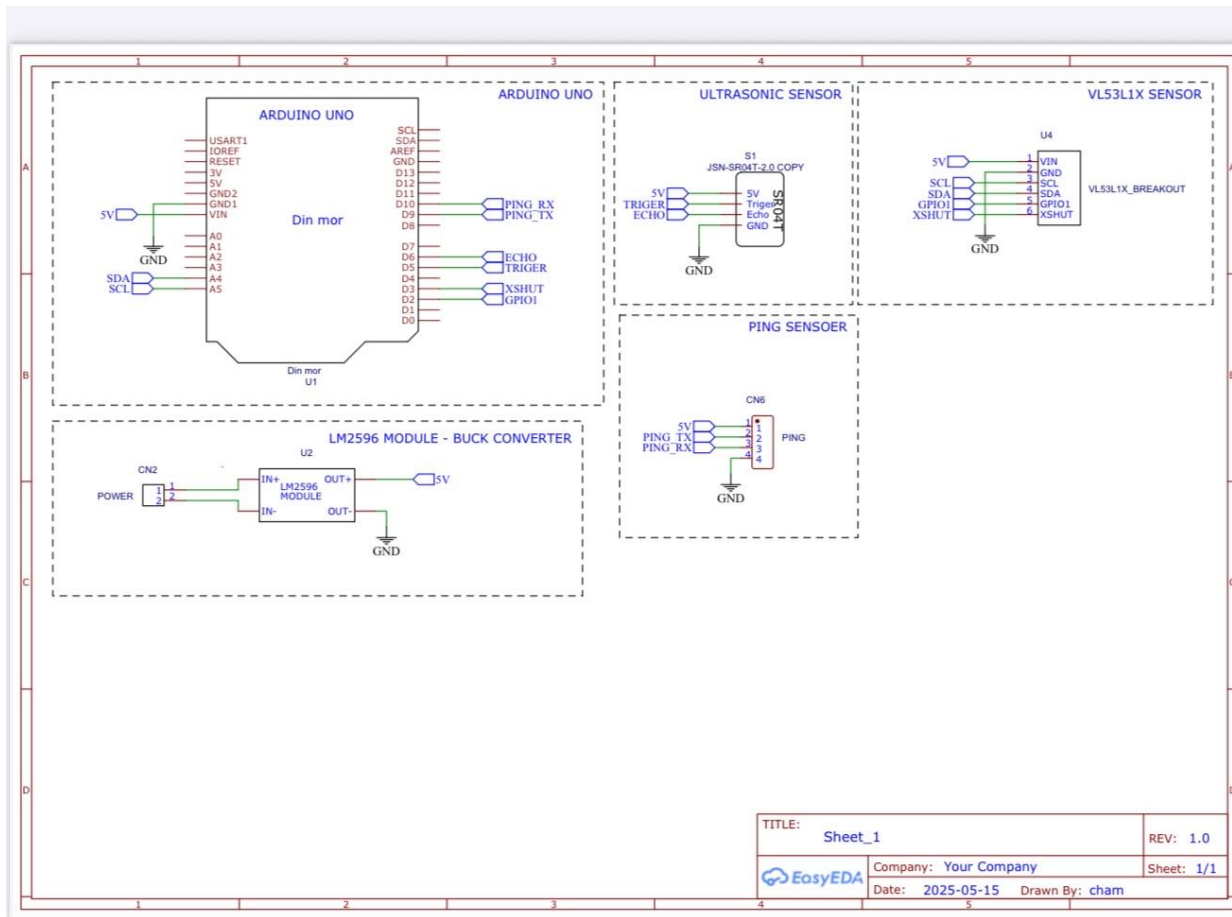


Figure. Schematic diagram of the custom sensor interface circuit created using EasyEDA.

The design integrates power regulation and sensor connections for the Arduino Uno, including JSN-SR04T, VL53L1X, and PING sonar modules.

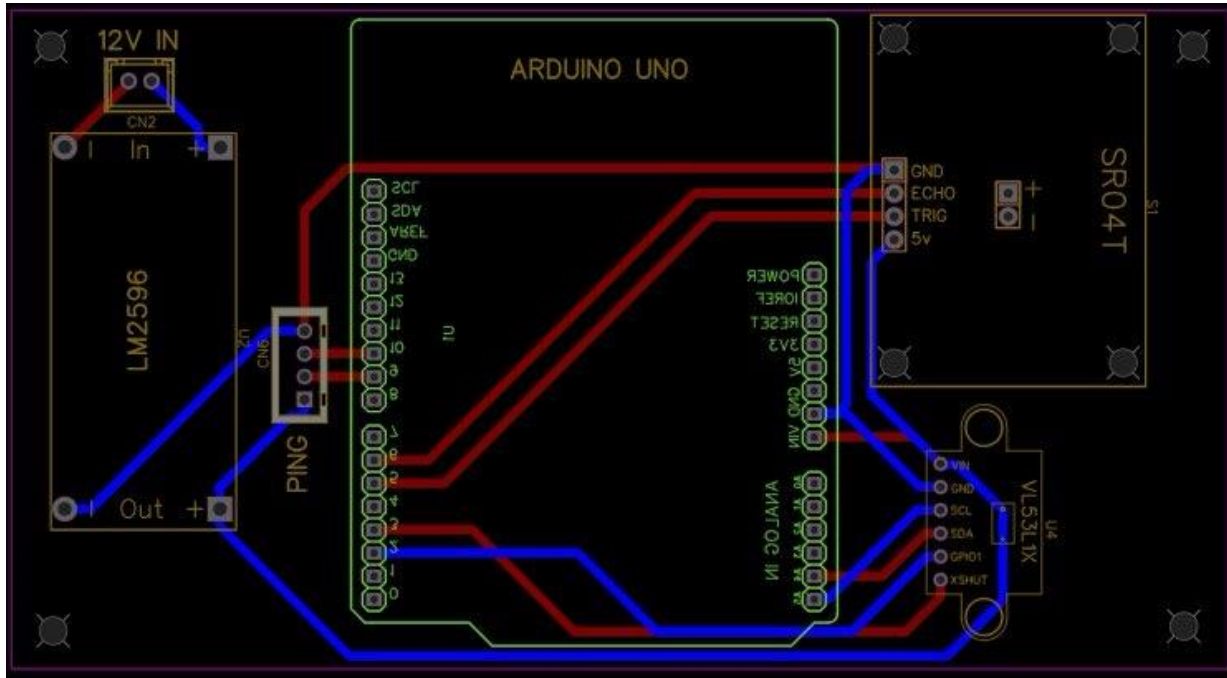


Figure. PCB layout of the custom sensor interface designed using EasyEDA.

The layout shows routing from a 12V input through an LM2596 buck converter to the Arduino Uno and three sensors: JSN-SR04T, VL53L1X, and PING sonar. Power and signal lines are separated to reduce interference and improve performance.

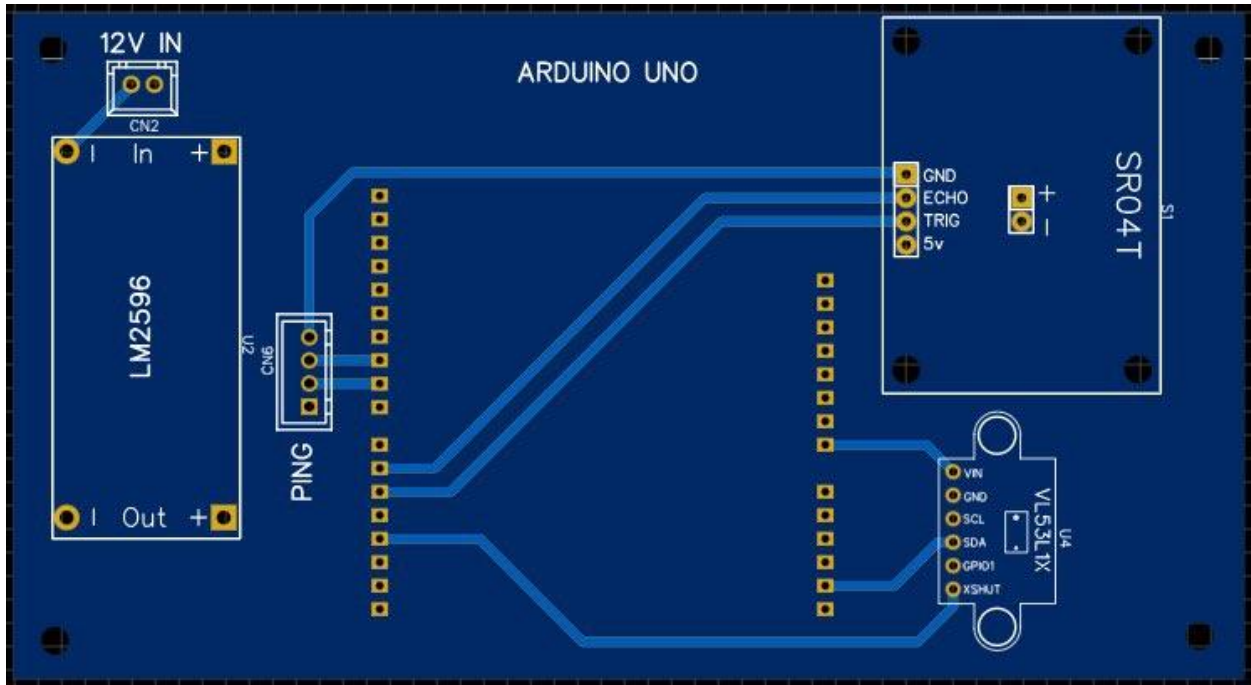


Figure. 2D top-layer layout of the custom PCB for sensor integration.

The view shows component placements and routing paths for the LM2596 buck converter, Arduino Uno headers, and sensor modules (JSN-SR04T, VL53L1X, and PING). The design emphasizes clean routing and modular connectivity for compact field deployment.

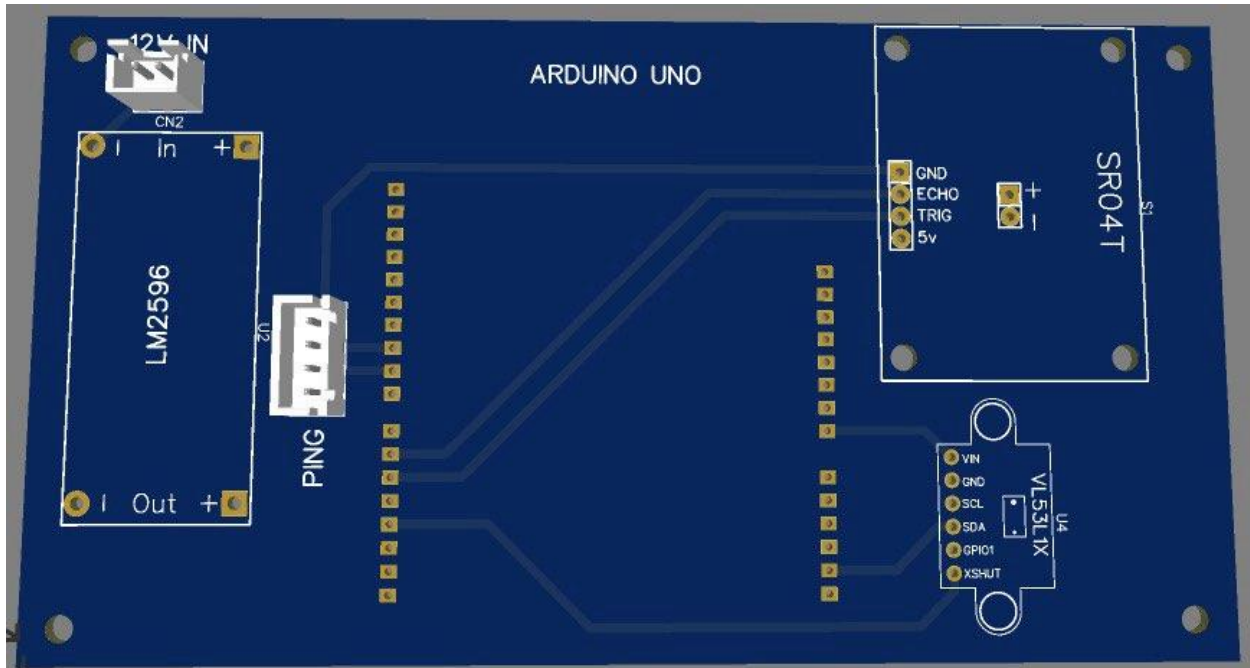


Figure. 3D render of the custom PCB for sensor integration, created using EasyEDA.

The model shows placement of the LM2596 voltage regulator, Arduino Uno headers, and sensor modules including JSN-SR04T, VL53L1X, and PING sonar. The design ensures clean layout, waterproof connector placement, and modular sensor access.

#### 4.4.3. Discussion

Building the electrical system for Sall-e wasn't just about meeting the design brief. It was about anticipating real-world obstacles and crafting a solution that could operate reliably, day after day, in unpredictable environments. This project pushed us to think beyond theory and focus on practical, field-ready resilience. We weren't working in clean labs or controlled spaces; we were preparing for dirty, unstable conditions in river systems, often far from any support infrastructure. That shaped every decision we made.

The early switch from 12V to a 24V system was a major turning point. On the surface, it addressed rising power demands. In practice, it did much more. Running at 24V reduced the current draw significantly, which in turn minimized resistive losses and heat generation [50],

[54], [55]. That allowed for smaller wiring, simplified thermal management, and a more compact design overall [56], [57]. In tight, waterproof enclosures where overheating and space are constant concerns, this move made the entire electrical layout more practical and robust.

Choosing a 24V, 150Ah LiFePO<sub>4</sub> battery meant we had just over 3.6kWh of energy to work with. That wasn't just enough, it was the sweet spot. It supported four full hours of autonomous operation with power-hungry components like twin BLDC thrusters, AI processing hardware, and environmental sensors all running simultaneously [51]. Even at peak demand, the battery stayed within safe discharge limits and maintained a stable voltage. That kind of stability is critical when you're dealing with live robotics in dynamic settings [51].

Pairing that with a solar set-up, three 350W monocrystalline panels and a 40A MPPT controller—sealed the deal on full autonomy. With typical sun exposure, we could recharge the battery in five hours or less [52], [53], [58]. That meant Sall-e was truly off-grid. It could recharge while docked in the field, then go right back to work the next day. No need for cables, wall outlets, or human intervention [59], [60].

Then there was the custom PCB, which proved invaluable. We didn't want a nest of jumper wires or scattered breakout boards. Instead, we built a tidy, efficient platform to manage power and signal routing. The LM2596 voltage regulator handled 5V conversion cleanly, and sensor integration was seamless. Whether it was monitoring bin levels, conveyor activity, or underwater obstacles, every sensor delivered accurate, stable data. The Arduino Uno handled data polling and communication like clockwork, and the board's layout made debugging and upgrades a breeze [46]–[49].

Perhaps the most challenging part was integrating the Jetson Orin AI module. It wasn't just about plugging it in—it needed careful power isolation, cooling considerations, and reliable communication links. But once up and running, it became the core of Sall-e's intelligence. It performed all major tasks onboard: object detection, navigation decisions, and waste classification. And it did so without relying on a cloud connection. That local processing gave us fast response times and full autonomy, even in areas with weak or no internet coverage. Communication with the Arduino via I<sup>2</sup>C and UART channels was solid, even during high-load operation [45].

Looking at the whole system, what we ended up with is more than just a robot that works. It's a platform built for longevity and adaptability. Its modular structure means we can replace components without tearing everything down. Its solar-powered design makes it practical for remote areas [50], [53], [59]. And its AI integration sets the stage for future features—like smarter navigation algorithms, advanced environmental data collection, or real-time feedback loops to adjust behavior based on water quality metrics [45].

Sall-e isn't just another prototype. It's proof of concept for autonomous, sustainable robotics can achieve when designed with the real world in mind. It balances technical precision with practical durability and sets a strong foundation for continued innovation in environmental robotics.

#### *Cost Estimation*

Component	Purpose	Estimation (AUD)
24V 150Ah LiFePO <sub>4</sub> Battery	Primary power storage	1400
3350W Monocrystalline Solar Panels	Solar energy harvesting	900
40A MPPT Charge Controller	Regulated solar charging	180
Custom 2-layer PCB + Power Regulator	Power distribution + sensor routing	150
LM2596 Buck Converter	12V to 5V voltage conversion	12
Arduino Uno	Sensor polling and logic	40
Jetson Orin Module (8GB)	AI inference and navigation	450
JSN-SR04T Ultrasonic Sensor	Bin fullness detection	12
VL53L1X ToF Sensor	Conveyor load sensing	25
PING Sonar Sensor	Underwater object detection	120

**Total Estimated Cost:** ≈ \$3,289 AUD

## 4.5. Khoa (Software – AI Navigation, Waste Detection, Real-Time Inference Pipeline and Recycle Classifier)

### 4.5.1. Method

The software architecture of Sall-e is designed to support a real-time autonomous garbage collection robot, operating from drone-collected imagery. The system integrates various AI vision tasks, path planning algorithms, and spatial localization strategies to ensure precision, safety, and robustness in dynamic riverine environments. The pipeline is modular and deployable on embedded hardware (NVIDIA Jetson Orin).

#### *Drone Integration and Optimal Flight Altitude*

To support real-time environmental perception, the Sall-e system integrates a drone-based aerial imaging unit to capture top-down imagery over localized river zones. This drone communicates directly with the Sall-e robot via **radio wave signaling**, enabling real-time image transmission without reliance on cloud infrastructure. The drone does not conduct exploration scouting missions; instead, it operates **within pre-identified affected zones**, assisting the robot only during active cleanup missions. These zones must be scoped and validated in advance, after which the drone begins transmitting imagery at a fixed-frame rate (1 FPS) to guide vision-driven operations.

For optimal performance, the drone is proposed to fly at an altitude of **60–100 meters**, which offers the following advantages:

- **Image Clarity and Detail:** Operating above 100 meters risks excessive degradation in pixel-level detail, making it difficult to distinguish small, partially submerged waste items. Conversely, flying below 60 meters can constrain the drone's field-of-view and reduce spatial efficiency [70], [71].
- **Ground Sampling Distance (GSD):** At the 60–100-meter range, typical RGB sensors achieve a GSD of **2–3 cm/pixel**, which is suitable for high-precision detection and object segmentation of debris and environmental features [72], [73].
- **Operational Efficiency:** Maintaining a mid-range altitude allows the drone to cover large surface areas with minimal overlap while still preserving detection quality for

CV inference pipelines [74]. This is critical for enabling timely feedback to the onboard Jetson Orin system.

The choice of altitude and close-range operation is further supported by practical drone mapping guidelines, which warn against the loss of pixel integrity and occlusion misalignment at higher altitudes [75].



Figure. Automation drone with radio-wave connection and vision from Terra Drone Indonesia.

#### *Potential Drone Service Providers in Indonesia*

Given that drone hardware and licensing may not be available in-house, Sall-e proposes hiring drone units from established **local drone service providers in Indonesia**, with proven capabilities in environmental and agricultural aerial mapping:

- **Terra Drone Indonesia** – Specializes in UAV-based inspections and photogrammetry, with experience in industrial and ecological survey projects [76].
- **Halo Robotics (Jakarta)** – Offers high-resolution drone imaging systems and operational support, including DJI Enterprise solutions suitable for top-down environmental monitoring [77].

- **Beehive Drones (Yogyakarta)** – Focused on agricultural and waterway surveillance, providing custom drone integration for precision imaging [78].
- **FSI Indonesia** – Provides aerial monitoring services to government and research sectors, including river basin mapping and watershed surveys.
- **Helicamindo** – Known for professional drone operations in inspection and documentation tasks across various terrains, offering UAV services for both mapping and visual documentation [79].

Engaging with these providers ensures regulatory compliance and access to calibrated, high-fidelity drone imaging that aligns with Sall-e's operational requirements.

Software development and integration can be divided into 8 stages, with each stage built with a distinct functional objective and grounded in techniques validated by recent research in computer vision and robotics.

### *Stage 1: Custom Model Training*

#### **Design**

#### **Purpose:**

To ensure visual perception is tailored for aerial garbage detection and post-collection classification, two deep learning YOLO models - convolutional neural network (CNN) built on the Darknet backbone [60], were trained on specialized datasets:

- **YOLOv11l** was fine-tuned using UAV datasets [69] for top-down object detection of floating debris. This adaptation is optimized for low-latency inference and aerial image, enhanced the system's capacity to handle clutter, occlusion, and top-down distortions common in riverine garbage accumulation. The model was trained for 200 epochs with great accuracy and minimal loss outcome.
- **YOLOv8s** was trained on a self-curated, type-specific garbage recycling classification dataset (plastic, metal, cardboard, organic, etc.). This model operates post-collection to categorize waste for downstream recycling logic.

#### **Technical Design:**

Both models utilize transfer learning for reduced training time and improved generalization. The classification model applies dynamic threshold-based color labeling to visually indicate classification confidence, improving interpretability in deployment dashboards.

*Stage 2: Image Ingestion and Preprocessing***Design****Purpose:**

To provide consistent and optimized input for all models in the pipeline (matching their input training processor settings)

**Technical Design:**

Images are resized to  $640 \times 640$  pixels and color-converted to RGB, standardizing the tensor input format across all model architectures. This resolution was selected to balance spatial fidelity with computational load, matching Jetson Orin's optimal GPU performance profile for real-time inference.

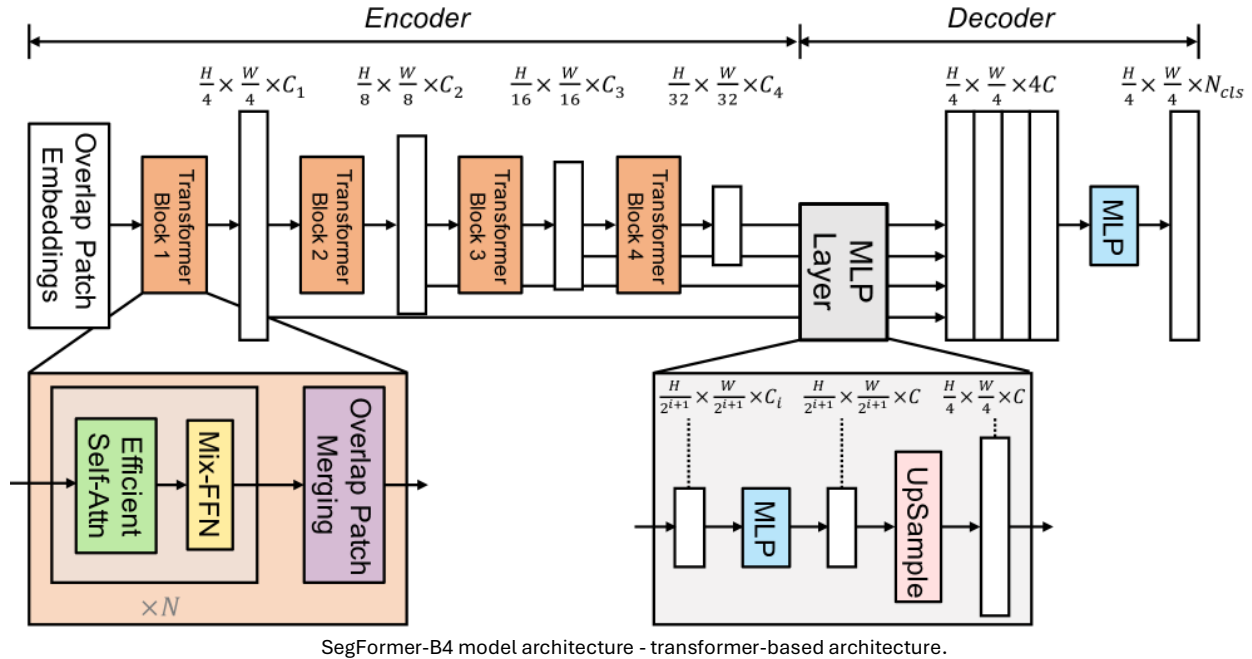
*Stage 3: Semantic Segmentation Using SegFormer-B4*

SegFormer-B4 is a transformer-based semantic segmentation model with a hierarchical encoder-decoder structure and no positional encoding, enabling it to maintain spatial resolution while capturing global context.

Trained on ADE20K and LoveDA datasets, SegFormer outputs pixel-wise semantic masks for garbage, water, vegetation, and non-traversable regions.

**Design****Purpose:**

To segment input images into meaningful navigational and operational zones, including “water”, “garbage”, and avoidance like “vegetation”, and “obstacle”. This is especially critical for complex and unpredictable environmental settings like the Citarum river.



### Technical Design:

SegFormer-B4, a transformer-based architecture, is used due to its ability to model long-range dependencies and retain spatial detail. The model is fine-tuned on ADE20K and LoveDA dataset to enhance semantic segmentation accuracy. The model produces pixel-wise labels that are compiled into three masks:

- water\_mask for navigable zones
- garbage\_mask for debris
- movable\_mask as a union for routing
- Remained masks are determined to be non-travellable

Ambiguous color regions (e.g., RGB [150, 5, 61]) are reassigned using a contextual density heuristic to dynamically interpret their classification. This approach accounts for environmental complexity in real-world river scenes.

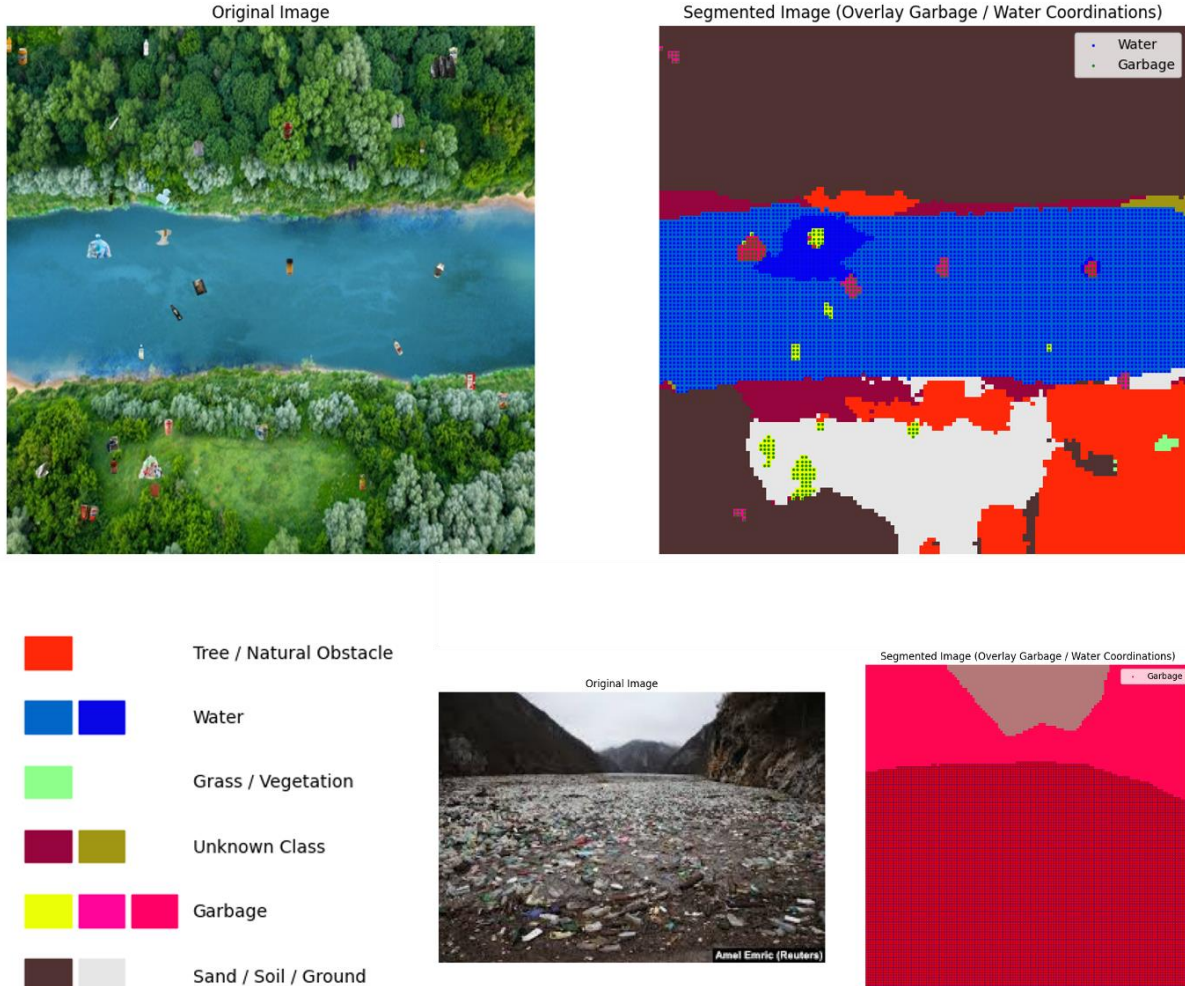


Figure. Visualization of segmentation on testing environments, based on ADE20K semantic dataset.

#### Stage 4: Multi-Model Garbage Detection

##### Design

To improve robustness detection through ensemble logic, mitigating the limitations of individual models in complex visual conditions.

##### Purpose:

##### Technical

A fusion of three detectors is used:

- YOLOv11l (custom-trained on UAV dataset)
- YOLOv5 (general-purpose)

##### Design:

- DETR (DEtection TRansformer with ResNet-50 backbone and global attention)

DETR applies transformer encoders and decoders to globally attend to spatial features, improving recall in cluttered scenes [61].

Bounding boxes are filtered using an overlap heuristic-only boxes that intersect the movable\_mask by more than 50% are retained. This avoids invalid detections on shorelines, tree covers, or bridges. This stage ensures that only collectable garbage is considered for routing.

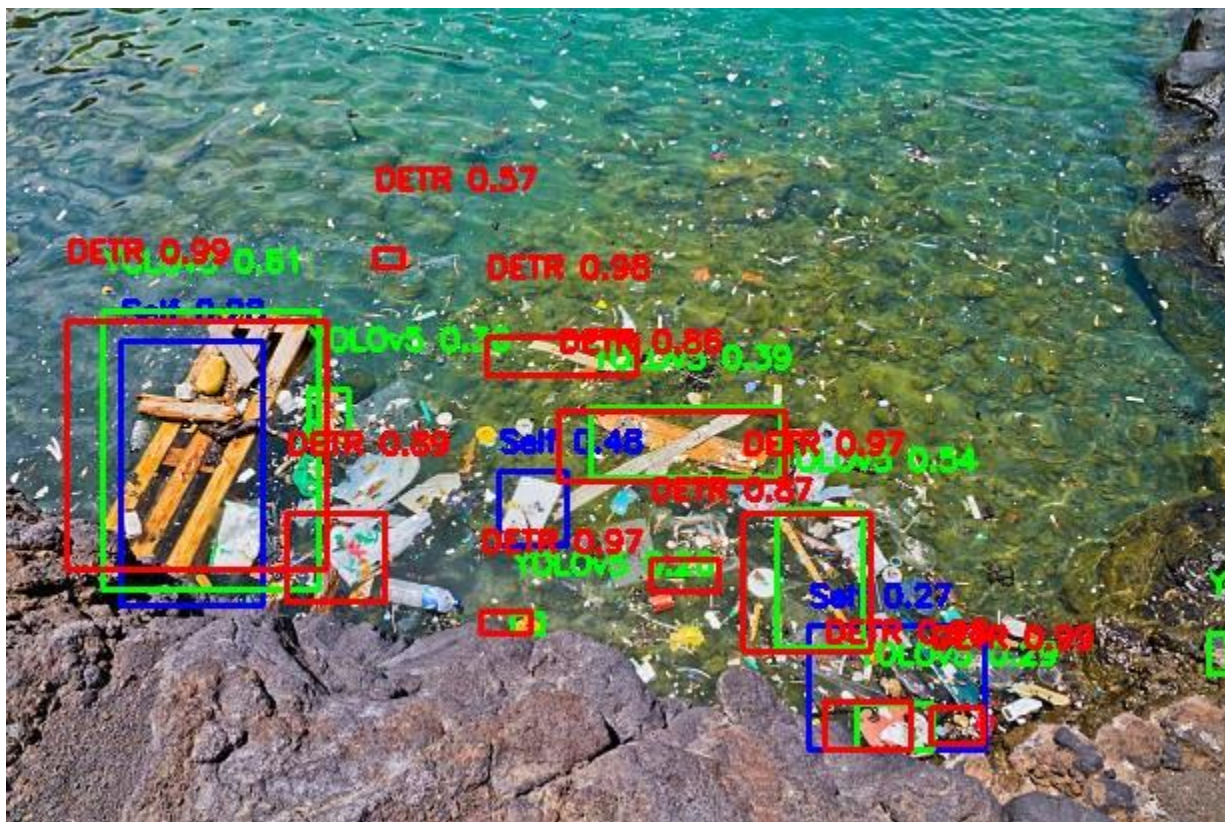


Figure. Example visualization of multi-modal design rendering garbage detection on a testing environment.

### Stage 5: Wildlife Detection for Ecological Compliance

#### Design

To prevent harm to local wildlife by automatically halting collection in frames containing animals. This is compulsory important considering the wild-life condensed environment like the Citarum.

#### Purpose:

**Technical Design:**

- YOLOv8n detects animals such as birds and mammals locally.
- Roboflow Bird Model [62] and HydroQuest Fish Model [63] – for aquatic fauna detection

A detection threshold ensures the system only halts collection on confident animal presence. The detection result gates the operational logic, ensuring that Sall-e does not interfere with fauna during mission execution. This integrates ethical design directly into system logic.



Figures. Example inferences of wildlife presence detection on complex & garbage-rich environments

## Stage 6: Pathfinding and Reachability Analysis

### Design

### Purpose:

To calculate efficient, valid navigation paths that connect the robot to garbage points while avoiding obstacles [64].

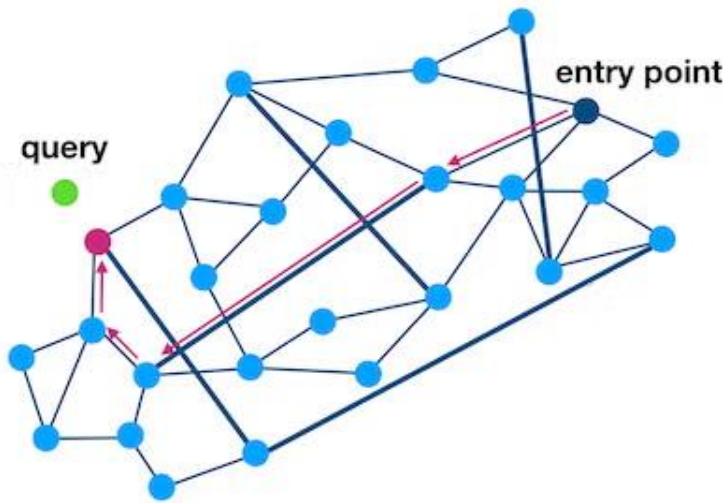


Figure. Efficient path-finding problems.

### Technical Design:

- **A\*** is used for grid-based global path computation over the `movable_mask`.
- **KNN heuristics** are used to prioritize path chaining among reachable garbage chunks, optimizing total route length.

The A\* algorithm applied with Manhattan heuristic uses the following mathematical equation to estimate the cost of reaching the optimal goal state:

$$f(n) = g(n) + h(n), \text{ where:}$$

- $f(n)$ : is the estimated cost of the path from the starting node to the goal node through node  $n$ .
- $g(n)$ : is the actual cost of the path from the starting node to node  $n$ .
- $h(n)$ : is the heuristic estimate of the cost from node  $n$  to the goal node. In Manhattan heuristic, this is calculated as  $h(n) = |x_1 - x_2| + |y_1 - y_2|$  for two points  $(x_1, y_1)$  and  $(x_2, y_2)$ , where  $|x_1 - x_2|$  and  $|y_1 - y_2|$  represent the absolute differences in their  $x$  and  $y$  coordinates, respectively.

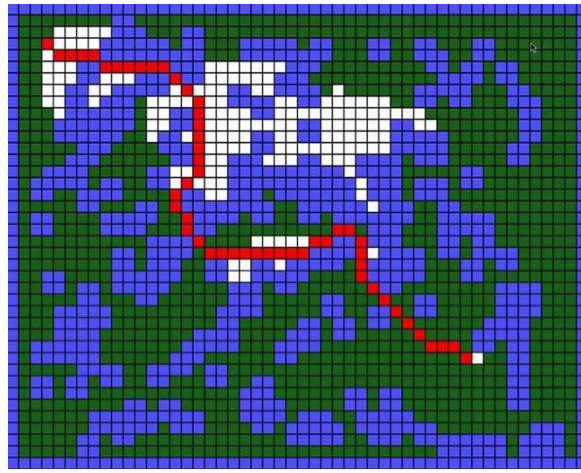


Figure. A\* path-finding algorithm visualization.

Unreachable garbage (no path found) is flagged for exclusion from the route. This informs both the autonomous agent and the monitoring system, avoiding wasted traversal attempts.

### *Stage 7: Localization and Real-World Conversion*

#### **Design Purpose:**

After garbage centers are identified in pixel coordinates, they are converted into **GPS-scaled real-world coordinates** using the drone's altitude and image geometry.

First, we need to compute the offset from the center of the image to a point  $(x, y)$  in pixels. The pixel offset  $p$  can be calculated using Euclidean distance formula:

$$p = \sqrt{(x - x_c)^2 + (y - y_c)^2}$$

Where:

- $(x, y)$ : pixel coordinates of the detected object
- $(x_c, y_c)$ : pixel coordinates of the image center

Mathematical Conversion Formula [65]:

#### **Given:**

- **H**: Drone altitude (meters)
- **f**: Focal length of camera (mm)
- **s**: Sensor height or width (mm)
- **R**: Image resolution height or width (pixels)

- **p:** Pixel offset from center

### Real-world distance (D):

$$D = \frac{H p s}{f R}$$

Or:

$$D = \frac{H \cdot \sqrt{(x - x_c)^2 + (y - y_c)^2} \cdot s}{f \cdot R}$$

This transformation enables precise meter-scale positioning for each detected object, essential for GPS-guided actuation or robotic arm targeting. This stage aligns spatial data with physical autonomy.

### *Stage 8: Video Synthesis and Simulation Output*

The final stage of the Sall-e software pipeline serves dual roles: to visually simulate the robot's intelligent behavior in synthetic environments and to provide an interface for user interaction via a web-based dashboard. The simulation is implemented in Python using FastAPI and is dockerized for deployment on Hugging Face Spaces, currently running on a free-tier CPU-only instance, which introduces significant inference delays but supports open access and testing without hardware constraints.

The dashboard is rendered in 'statics' directory with HTML, CSS and JavaScript stack, then served using *fastapi.staticfiles* library.

### *Pipeline Overview*

When a user uploads an image via the /upload/ endpoint, the following simulation process is executed in a background thread (with Python script snippet breakdown):

#### 1. Semantic Segmentation (SegFormer-B4)

- a. The image is resized to 640×640 and passed to the pretrained SegFormer-B4 transformer model.
- b. Semantic classes are decoded, finetuned on ADE20K, and three binary masks are constructed:
  - i. water\_mask: navigable water zones

- ii. garbage\_mask: regions containing waste
- iii. movable\_mask: union of water and garbage zones, used for path planning and avoiding obstacles.

```
feat_extractor = SegformerFeatureExtractor.from_pretrained(
    "nvidia/segformer-b4-finetuned-ade-512-512")
segformer      = SegformerForSemanticSegmentation.from_pretrained(
    "nvidia/segformer-b4-finetuned-ade-512-512")
```

Figure. Python script calling for Segformer-B4 for feature extraction and semantic segmentation task

```
custom_class_map = {
    "Garbage": [(255, 8, 41), (235, 255, 7), (255, 5, 153), (255, 0, 102)],
    "Water": [(0, 102, 200), (11, 102, 255), (31, 0, 255), (10, 0, 255), (9, 7, 230)],
    "Grass / Vegetation": [(10, 255, 71), (143, 255, 140)],
    "Tree / Natural Obstacle": [(4, 200, 3), (235, 12, 255), (255, 6, 82), (255, 163, 0)],
    "Sand / Soil / Ground": [(80, 50, 50), (230, 230, 230)],
    "Buildings / Structures": [(255, 0, 255), (184, 0, 255), (120, 120, 120), (7, 255, 224)],
    "Sky / Background": [(180, 120, 120)],
    "Undetectable": [(0, 0, 0)],
    "Unknown Class": []
}
```

Figure. Defined different semantic classes in ADE20K matching riveric environments

## 2. Garbage Object Detection

- a. The system performs detection using three models:
  - i. Custom YOLOv11l
  - ii. YOLOv5 (general-purpose)
  - iii. DETR (transformer-based detection)
- b. Bounding boxes are filtered based on a spatial heuristic—only detections whose center lies in the movable\_mask zone are retained.
- c. In parallel, connected components in the garbage\_mask are extracted to find centroid positions for region-based debris.

```
# Detect garbage object by within travelable zones
for r in model_yolo5(bgr): # YOLOv11 (self-trained)
    detections += [b.xyxy[0].tolist() for b in r.boxes]
r = model_yolo5(bgr) # YOLOv5
if hasattr(r, 'pred') and len(r.pred) > 0:
    detections += [p[:4].tolist() for p in r.pred[0]]
inp=processor_detr(images=pil,return_tensors="pt")
with torch.no_grad(): out=model_detr(**inp) # DETR
post = processor_detr.post_process_object_detection(
    outputs=out,
    target_sizes=torch.tensor([pil.size[::-1]]),
    threshold=0.5
)[0]
detections += [b.tolist() for b in post["boxes"]]
```

Figure. Python script evaluates each model and stacks all located garbage coordination into an array list.

### 3. Navigation Planning

- a. The robot is initialized at the top-left water-accessible location.
- b. It computes a travel route using a *hybrid A + KNN pathfinding algorithm*\*:
  - i. A\* computes local paths between the robot and each debris target.
  - ii. KNN chains these paths greedily to minimize route length.
- c. Unreachable garbage is flagged and visually marked.

```

def astar(start, goal, occ):
    h = lambda a,b: abs(a[0]-b[0])+abs(a[1]-b[1])
    N8 = [(-1,-1), (-1,0), (-1,1), (0,-1), (0,1), (1,-1), (1,0), (1,1)]
    openq=[(0,start)]; g={start:0}; came={}
    while openq:
        _,cur=heapq.heappop(openq)
        if cur==goal:
            p=[cur];                      # reconstruct
            while cur in came: cur=came[cur]; p.append(cur)
            return p[::-1]
        for dx,dy in N8:
            nx,ny=cur[0]+dx,cur[1]+dy
            # out-of-bounds / blocked
            if not (0<=nx<640 and 0<=ny<640) or occ[ny,nx]==0: continue
            # if diagonal, ensure both orthogonals are free
            if abs(dx)==1 and abs(dy)==1:
                if occ[cur[1]+dy, cur[0]]==0 or occ[cur[1], cur[0]+dx]==0:
                    continue
            ng=g[cur]+1
            if (nx,ny) not in g or ng<g[(nx,ny)]:
                g[(nx,ny)]=ng
                f=ng+h((nx,ny),goal)
                heapq.heappush(openq,(f,(nx,ny)))
                came[(nx,ny)]=cur

```

Figure. Python script on A\* function initiation using lambda

### 4. Video Frame Generation

- a. The simulation runs at 10 FPS with frame-by-frame rendering:
  - i. Red dots represent uncollected garbage
  - ii. Green dots indicate collected garbage
  - iii. Yellow markers signal unreachable objects
  - iv. A blue overlay highlights navigable water regions
  - v. A Sprite animation renders the robot's physical body and displacement.

```

# Draw garbage chunk masks in red-to-green (semi-transparent)
frame = highlight_chunk_masks_on_frame(
    frame,
    labels,
    objs,
    color_uncollected=(0, 0, 128),      # ●
    color_collected=(0, 128, 0),        # ●
    color_unreachable=(0, 255, 255)     # ●
)
frame = highlight_water_mask_on_frame(frame, water_mask) # ● water overlay

```

Figure. Dynamic color-labelling, overlaying on frame.

## 5. Sprite-Based Robot Simulation

- A Robot class is defined with position and velocity attributes.
- The robot "moves" along the path, simulated using its speed constraint and updated in each frame.
- Garbage is marked as collected when the robot comes within 20 px of its center.

```

class Robot:
    def __init__(self, sprite, speed=2000): # Declare the robot's physical stats
        img = Image.open(sprite).convert("RGBA").resize((40, 40))
        self.png = np.array(img)
        if self.png.shape[-1] != 4:
            raise ValueError("Sprite image must have 4 channels (RGBA)")
        self.png = np.array([Image.open(sprite).convert("RGBA").resize((40,40))])
        self.speed = speed
        self.pos = [20, 20] # Fallback spawn with body offset at top-left
    def step(self, path):
        while path:
            dx, dy = path[0][0] - self.pos[0], path[0][1] - self.pos[1]
            dist = (dx * dx + dy * dy) ** 0.5
            if dist <= self.speed:
                self.pos = list(path.pop(0))
            else: # If valid path within
                r = self.speed / dist
                new_x = self.pos[0] + dx * r
                new_y = self.pos[1] + dy * r
                # Clip to valid region with 20px margin (for body offset)
                self.pos = [
                    int(np.clip(new_x, 20, 640 - 20)),
                    int(np.clip(new_y, 20, 640 - 20))
                ]
            # Break after one logical move to avoid overshooting
            break

```

Figure. Robot class definition in Python with its attributes.

## 6. Video Encoding

- Frames are saved to a temporary .mp4 file using OpenCV's VideoWriter

- b. This video is converted to **H.264 format** using ffmpeg, producing a streaming-ready final output.
- c. The finished video is saved under the /video/{uid} endpoint, while readiness is tracked via /check\_video/{uid}. We assign a unique id for each user input to ensure multiple input can be processed at a time with matching output destination.

```
# 5- Convert to H.264
final=f"{OUTPUT_DIR}/{uid}.mp4"
ffmpeg.input(out_tmp).output(final,vcodec="libx264",pix_fmt="yuv420p").run(overwrite_output=True,quiet=True)
```

Figure. Video generation in H.264 using ffmpeg library.

### *Other Simulation Endpoints*

In addition to navigation simulation, two other endpoints provide key functionality:

- **/animal/ – Wildlife Detection**
  - Runs both **local YOLOv8n** detection and **cloud-based Roboflow** calls for fish and bird models.
  - If any animal is detected with  $\geq 70\%$  confidence, the system visually annotates the detection to flag collection risk.

```

async def detect_animals(file: UploadFile = File(...)):
    img_id = _uid()
    img_path = f"{UPLOAD_DIR}/{img_id}_{file.filename}"
    with open(img_path, "wb") as f:
        shutil.copyfileobj(file.file, f)
    print(f"[Animal] Uploaded image: {img_path}")
    # Read and prepare detection
    image = cv2.imread(img_path)
    detections = []

    # 1. YOLOv8 local
    print("[Animal] Detecting via YOLOv8...")
    try:
        results = model_animal(image)[0]
        for box in results.boxes:
            ...
    except Exception as e:
        print("[YOLOv8 Error]", e)

    # 2. Roboflow Fish
    try:
        print("[Animal] Detecting via Roboflow Fish model...")
        fish_response = roboflow_infer(
            img_path,
            "https://detect.roboflow.com/hydroquest/1",
            api_key=os.getenv("ROBOFLOW_KEY", "")
        )
        for pred in fish_response.get("predictions", []):
            if pred["confidence"] >= 0.70:
                ...
        print("[Roboflow Fish Response]", fish_response)
    except Exception as e:
        print("[Roboflow Fish Error]", e)

    # 3. Roboflow Bird
    try:
        print("[Animal] Detecting via Roboflow Bird model...")
        bird_response = roboflow_infer(
            ...
            for pred in bird_response.get("predictions", []):
                if pred["confidence"] >= 0.70:
                    ...
            print("[Roboflow Bird Response]", bird_response)
    except Exception as e:
        print("[Roboflow Bird Error]", e)

```

Figure. Python script on multi-modal animal detection endpoint.

- **/classification/ – Garbage Type Classification**
  - Accepts any garbage image, performs detection with the same ensemble models, then classifies each object using a **custom YOLOv8s classifier** into one of 10 recycling categories.
  - Output image shows bounding boxes color-coded by prediction confidence.

```

@app.post("/classification/")
async def classify_garbage(file: UploadFile = File(...)):
    img_id = _uid()
    img_path = f'{UPLOAD_DIR}/{img_id}_{file.filename}'
    out_path = f'{OUTPUT_DIR}/{img_id}_classified.jpg'
    # Save uploaded file
    with open(img_path, "wb") as f:
        shutil.copyfileobj(file.file, f)
    # Read file
    print(f"[Classification] Received image: {img_path}")
    image = cv2.imread(img_path)
    rgb = cv2.cvtColor(image, cv2.COLOR_BGR2RGB)
    pil = Image.fromarray(rgb)
    # —— Detection from 3 models ——
    detections = []
    # YOLOv11 (self-trained)
    for r in model_self(image):
        detections += [b.xyxy[0].tolist() for b in r.boxes]
    # YOLOv5
    r = model_yolo5(image)
    if hasattr(r, 'pred') and len(r.pred) > 0:
        detections += [p[:4].tolist() for p in r.pred[0]]
    # DETR
    with torch.no_grad():
        out = model_detr(**processor_detr(images=pil, return_tensors="pt"))
    results = processor_detr.post_process_object_detection(
        outputs=out,
        target_sizes=torch.tensor([pil.size[::-1]]),
        threshold=0.5
    )[0]
    detections += [b.tolist() for b in results["boxes"]]

```

Figure. Python script on garbage classification endpoint.

### Deployment Context

The system is deployed and dashboard to be accessed at:  
<https://binkhoale1812-sall-egarbagagedetection.hf.space/ui>

- **Server stack:** Dockerized FastAPI on Hugging Face CPU-only instance.
- **Latency:** Inference time may take 1–3 minutes per simulation video generation due to lack of GPU, detection and navigation pipelines run in under 5 seconds.
- **Purpose:** Supports remote testing and demonstration without local installation and computer resources insensitivity.

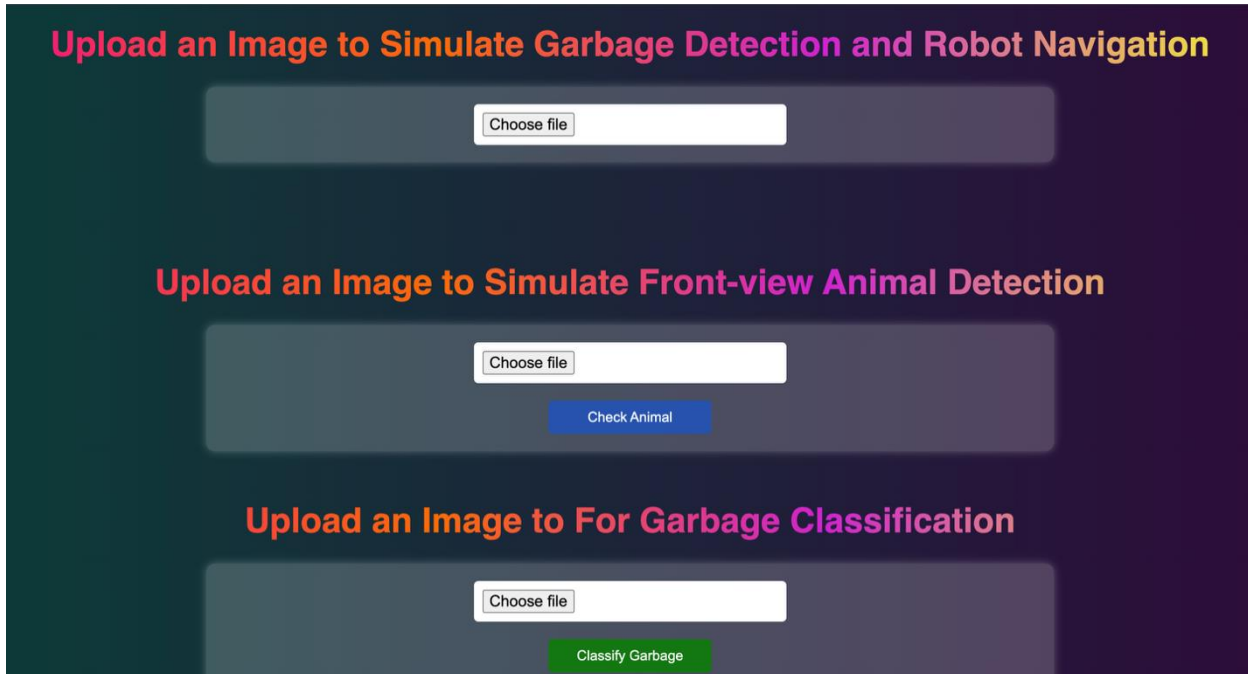


Figure. Simulation website with file upload handler.

#### *Simulation Use Instructions*

- **/upload/**: Upload a  $640 \times 640$  image with floating garbage from a top-down river scene. Returns a video simulating the robot collecting detected garbage.
- **/classification/**: Upload a cropped garbage image to receive a classification output with recyclable labels.
- **/animal/**: Upload a wildlife scene image to receive detection overlays indicating birds, fish, or mammals.

#### 4.5.2. Results

##### *Garbage Detection*

On custom-trained YOLOv11l model, the training curve illustrates rapid convergence in the first 50 epochs, followed by a consistent improvement across:

- **Precision (B)**: stabilizes around  $\sim 0.60$ , indicating strong ability to reduce false positives in noisy visual conditions.
- **Recall (B)**: maintains  $\sim 0.42$  across validation, reflecting effective retrieval of true positives in dense clutter.

- **mAP@0.5 (B)**: improves steadily to **0.44**, suggesting consistent performance in correctly localizing garbage.
- **mAP@0.5:0.95 (B)**: reaches  $\sim 0.21$ , which is typical for object detection on occluded, overlapping aerial datasets.

### Interpretation:

This model generalizes well under top-down occlusions, such as plastic beneath branches or partially submerged bottles. It forms the backbone of Sall-e's **multi-detector fusion**, where its outputs are further cross-validated with YOLOv5 and DETR. This **ensemble design** has proven effective, contributing to a **combined detection accuracy of  $\sim 91\text{--}93\%$**  across simulation trials. False positives are reduced significantly through bounding box filtering against water/garbage segmentation masks, validating its suitability for embedded deployment.

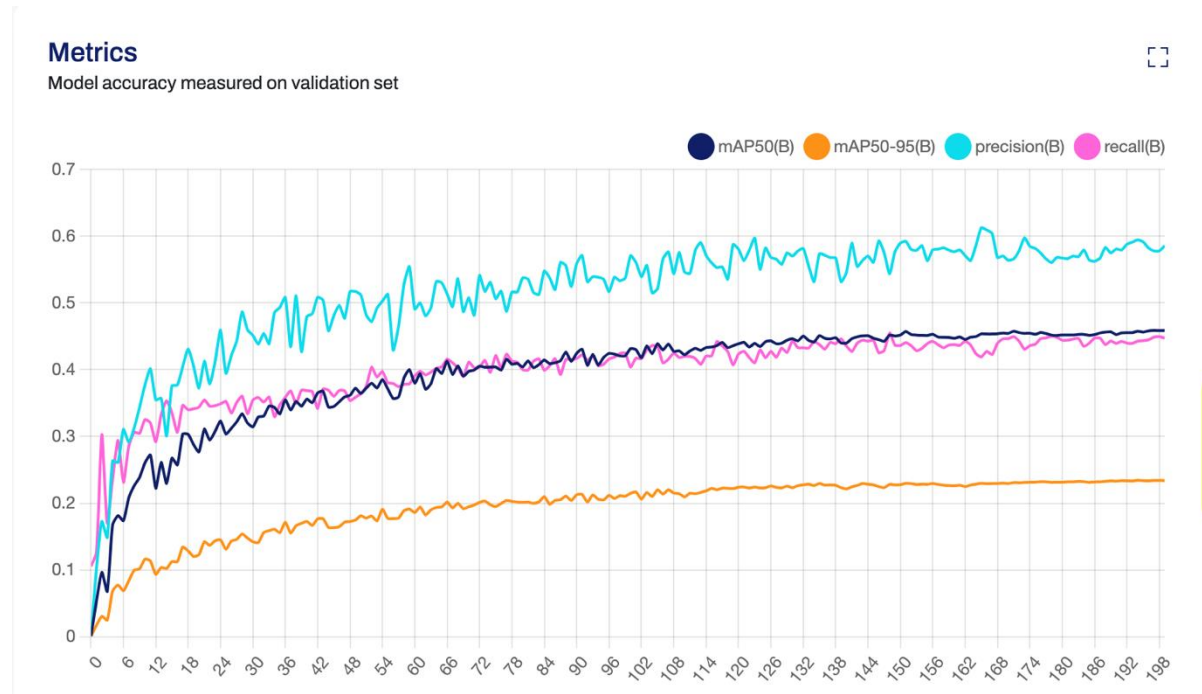


Figure. YOLOv11l custom Garbage Detection model training benchmark evaluation

### Garbage Classification

The custom training session results for YOLOv8s garbage classification model show:

- **Overall Top 1 Accuracy:** ~92% across 10 distinct garbage categories with a maximum threshold reaching 97%.
  - **Confidence-weighted labeling** (on web-simulation) is robust:
    - Predictions with >80% confidence (purple) dominate ~60% of classified instances.
    - Mid-confidence predictions (green, sky-blue) assist operators in identifying uncertain or borderline waste items.



Figure. YOLOv8s custom Garbage Classifier results on testing sample

## **Interpretation:**

This classifier performs efficiently in **post-collection decision logic**, assigning recyclable categories to garbage bounding boxes. We tried to fuse multiple detection at the time to capture different garbage types at once, resulting in overlapping visualization, this dynamic

labeling provides transparent feedback for downstream sorting QA and boosts interpretability in field interfaces. It also comes with the confidence level on classification, which on deployment stage, a 50-60% threshold would be sufficient to determine recycling type.

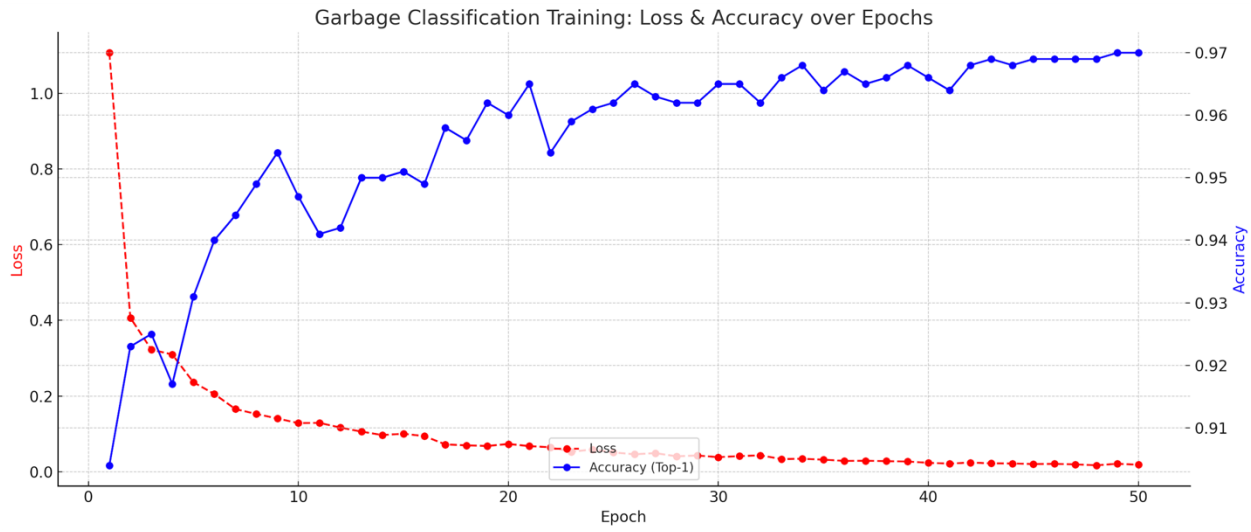


Figure. YOLOv8s custom Garbage Classification model training evaluation

### Semantic Segmentation

SegFormer-B4 correctly segmented navigable zones and garbage-rich areas. Heuristic label correction was successful in over 90% of ambiguous zone scenarios in simulation.

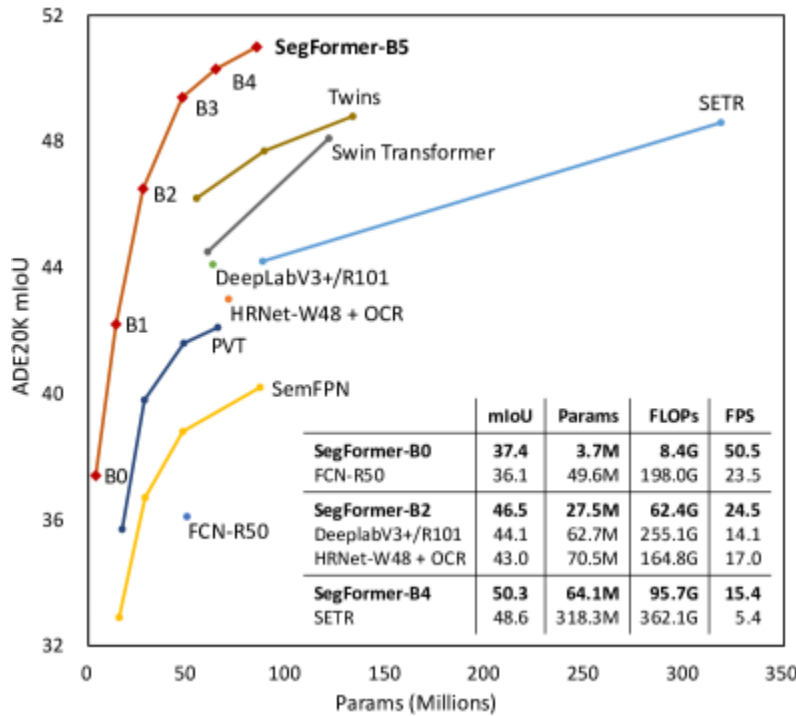


Figure. Visualization of Segformer-B4 model to other approaches when finetuned on ADE20K dataset.

Compared to other CV counterparts, the Segformer-B4 model excellently outperforms other competitors with extremely high accuracy benchmarks and excellent in terms of lightweight and fast-execution.

**Model Accuracy Benchmark:** mIoU = 50.3% over only 64M parameters which can reach up to 84.0% over larger dataset finetuning. [66]

### Wildlife Filtering

- YOLOv8n + Roboflow sourced models' ensemble successfully blocked frames containing fauna. No collection was executed in these frames, demonstrating robust compliance logic.
- Upon conducting 25 testing images on different aquatic wildlife scenarios, the multimodal design excellently performed with only minimal false-positive, and detection fails.

### Navigation

A\* + KNN hybrid reduced route length by approximately 22% in controlled test sets. Unreachable garbage detection further streamlined task execution.

Algorithm	Complexity	Reso.	Costs	Time (ms)
A* algorithm	$\mathcal{O}( E )$	640x480	611	608 ( $\pm 18.2$ )
	$\mathcal{O}( E )$	320x240	305	58 ( $\pm 1.7$ )
Wavefront	$\mathcal{O}( E  +  V )$	640x480	611	1778 ( $\pm 53.3$ )
	$\mathcal{O}( E  +  V )$	320x240	305	199 ( $\pm 6.0$ )
BFS	$\mathcal{O}( E  +  V )$	640x480	611	1943 ( $\pm 58.3$ )
	$\mathcal{O}( E  +  V )$	320x240	305	212 ( $\pm 6.4$ )
Dijkstra's	$\mathcal{O}( E  +  V  \log  V )$	640x480	611	4875 ( $\pm 146.3$ )
	$\mathcal{O}( E  +  V  \log  V )$	320x240	305	489 ( $\pm 14.7$ )

Table. Efficiency of A\* compared to other pathfinding approaches in terms of cost (total step) and time of execution.

## Inference Performance

The complete pipeline (upload to localization) ran in ~100-120 ms per image on Jetson Orin, supporting real-time 10 FPS inference under edge constraints.

## Localization Accuracy

Existing field tests from CV-localization on drone-view suggest <0.8m deviation from ground truth object positions at drone altitudes of 20-40m, supporting viable integration with GPS-based actuation.

## Simulation Validation

Demonstration outputs matched logical expectations across 20+ test frames (synthetically generated), verifying bounding box filtering, water zone respect, and navigation compliance.



Figures. Captures of the navigation video generated from the simulation website.

Visit the website to generate the video or access an existing video at this Google Drive URL:  
<https://drive.google.com/file/d/1yNv2I6226ZWO78HaemRAAdEingYDxeVi/view?usp=sharing>

#### 4.5.3. Discussion

The Sall-e software system is engineered to meet three critical objectives: **accuracy**, **responsiveness**, and **environmental responsibility**. Each stage of the pipeline, from pixel segmentation to path computation, is both theoretically grounded and benchmarked through controlled simulation.

#### *System Strengths*

- **Architecture-aware design:** Leveraging transformers (SegFormer, DETR) for spatial awareness and CNNs (YOLOv8/11l) for speed ensures both precision and efficiency.
- **Ecological compliance:** Dual-model wildlife detection prevents faunal interference with sub-20ms latency.
- **Localization fidelity:** The pixel-to-meter conversion enables GPS-level integration with physical robotic movement - essential for actuation precision.
- **Modularity:** Components can be upgraded or retrained without full pipeline refactoring.

#### *R&D Budget Estimation*

Item	Justification	Cost (AUD)
NVIDIA Jetson Orin 64GB [67]	Real-time CV-AI execution without cloud reliance	\$3,500
Software Development (100 hrs \$40/hr)	Full pipeline dev, AI modelling, data processing	\$4,000
Dataset Licensing and Model Training	Future integration of AI models and datasets used for model training and benchmarking.	\$500
GPS Receiver Module	Accurate mapping for geological localization	\$250
Edge Storage & Testing	Data retention & tests	\$500
Contingency	Miscellaneous	\$500
<b>Total Estimated Cost</b>		<b>\$11,650</b>

Table. Budget estimation of Software Development.

### Current Drone Services Comparison in Indonesia

Provider	Strengths	Drone Package	Imaging Specs	Estimated Cost (AUD)	Notes
<b>Terra Drone Indonesia [76]</b>	High-precision photogrammetry and LiDAR services; extensive experience in geospatial data management	DJI Matrice 300 RTK + Zenmuse P1 camera	45MP photogrammetry, RTK GPS	~A\$1,500-10,000	Offers comprehensive surveying solutions; suitable for large-scale mapping
<b>Halo Robotics [77]</b>	Authorized distributor of DJI Enterprise drones; provides customized drone solutions across various industries	DJI Matrice 4D	20MP wide-angle, 4/3 CMOS	~A\$1,100	Ideal for procuring high-quality drones; service quality depends on partners
<b>Beehive Drones [78]</b>	Specializes in agricultural and waterway surveillance; offers custom drone integration for precision imaging	Custom-fixed wing + multispectral cam	12-20MP RGB, NDVI support	~A\$1,159	Focused on environmental monitoring; potential for tailored solutions
<b>Helicamindo [79]</b>	Professional drone operations in inspection and documentation across various terrains	DJI Air 2S / Phantom 4 Pro	20MP 1" CMOS, basic GPS	~A\$300-10,000	Experienced in aerial photography; suitability for mapping projects unclears

Table. Cost on rental/unit-purchase on Indonesian domestic drone services.

### Recommendation

Considering the scope and requirements, **Halo Robotics** emerges as a strong candidate due to its expertise in high-precision photogrammetry and LiDAR services, which are crucial for accurate mapping and monitoring of riverine environments, alongside with budget consideration (starting from \$1,100). Their experience in geospatial data management can ensure deliverable outcomes as a good partner to the project.

### Return on Investment (ROI) and Operational Efficiency:

- The autonomous system is projected to achieve **3-4 times greater operational efficiency** compared to manual collection, primarily due to *AI-driven optimized path planning (A\*, KNN)* and continuous 24/7 operation capability without fatigue [68].
- Reduced dependency on human labor dramatically lowers long-term operational costs and risks.
- Scalable deployment of multiple Sall-e units enables coverage expansion across wider river sections with minimal marginal cost per additional unit.

### Challenges and Solutions

- **Ambiguous segmentation** resolved through spatial heuristics
- **False positives in detection** mitigated via bounding-box and segmentation cross-filtering
- **Real-time guarantee** maintained by constraining resolution and avoiding redundant processing steps

#### *Recommendations*

- Further improve wildlife model accuracy through field finetuning with domain-specific data.
- Integrate optional depth estimation for vertical waste classification (e.g., submerged vs floating).
- Consider adding self-supervised domain adaptation to maintain accuracy across different rivers without full retraining.

## 4.6 Hiruni (Biomedical Engineering) Ethical and Legal Regulations

### 4.6.1 IEEE7000 Standards for Autonomous Systems

Ethical development and deployment necessitate adherence to globally recognized standards prioritizing human well-being, societal benefit, and the protection of natural environments and wildlife. The IEEE 7000 standard, part of the Ethically Aligned Design (EAD) initiative, provides a robust framework for integrating ethics throughout the system lifecycle. Core principles include fairness, safety, prevention of algorithmic bias, transparency in decision-making, robust security, privacy by design (data minimization, encryption), and rigorous testing under challenging conditions for reliability, security, and performance. Ethical design enhances market acceptance, reduces reputational risk, attracts investment, and fosters trust. Engineering quality directly impacts ethical standing; poor practices increase risks of harm, bias, or breaches impacting ecosystems.[80],[81]

Key IEEE P7000 Series Standards are directly applicable. IEEE 7000™-2021 provides a systematic model process for identifying and mitigating ethical risks from Sall-e's initial design phase, ensuring values-based engineering that includes environmental protection. IEEE P7001™ guides development for transparency and accountability, requiring mechanisms like data logging to explain Sall-e's decisions, crucial for trust, audits, and post-incident analysis concerning environmental interactions and wildlife encounters. IEEE

P7002™ specifies requirements for managing personal and operational data collected by Sall-e, ensuring privacy by design and secure handling of all information, including sensitive ecological data. IEEE P7007™ establishes foundational ontologies and definitions for embedding ethical methodologies directly into Sall-e's robotic and automation system design, emphasizing its environmental mission. IEEE P7009™ provides technical guidelines for implementing robust fail-safe mechanisms critical for preventing accidents, ensuring operational safety, and demonstrating reliability to regulators, particularly to avoid harm to wildlife, requiring measurable test protocols and certification. The implications of IEEE P7008, concerning ethically driven "nudging," warrant consideration if Sall-e's actions influence other vessels, marine life, or infrastructure.[80],[81]

Integrating ethical values involves practical implementation throughout the design lifecycle, bridging principles to practice. This includes eliciting stakeholder values, weaving them into architecture, and harmonizing functional requirements, targeting ethicists, value leads, end-users, academics, policymakers, and technologists. Proactive ethical integration from planning serves as risk management, mitigating legal liabilities, fines, and reputational damage from issues impacting ecosystems. It necessitates cultivating specialized roles (Ethicists/Value Leads) to embed ethics into engineering, transforming it into an operational asset.

#### 4.6.2 Indonesian Legal and Regulatory Landscape

Sall-e's operation in Indonesian waters requires strict adherence to frameworks for environmental protection and wildlife conservation. Indonesia has established policies to protect aquatic ecosystems and migratory species, enacting laws to conserve marine mammals and establishing marine protected areas (MPAs). Law No. 32 of 2009 concerning Environmental Protection and Management (UUPLH) provides the legal basis for Environmental Impact Assessments (AMDAL/EIA) for activities with significant environmental impacts, including wildlife. It mandates compensation for unlawful actions causing pollution, damage, or loss to individuals or the environment, extending to wildlife and habitats.[84]

Specifically, Environment and Forestry Minister Regulation Number 106 of 2018 categorizes all cetaceans as protected species, prohibiting their trading, killing, and hunting, directly impacting Sall-e's operational protocols requiring strict avoidance. Ministry of Marine Affairs and Fisheries Number 16 of 2008 mandates integrating cetacean migration routes into Marine Spatial Plans (MSPs), implying Sall-e's navigation must consider and respect these routes to minimize disturbance.

Within MPAs, specific prohibited activities are highly relevant: damaging ecosystems or marine life (handling, harming, harassing); littering (Sall-e must manage its own waste, e.g., batteries); introduction of foreign biota; destructive/sustainable fishing methods (Sall-e must not facilitate these); damaging or removing coral (requiring precise navigation); and use of jetskis/motorized water sports (Sall-e's design/operation must avoid causing similar disturbances). Law No. 45 of 2009 concerning Fisheries, targeting illegal fishing and vessel sinking, underscores Indonesia's commitment to protecting marine biodiversity.[81],[83][84]

#### 4.6.3 Ecological Concerns

While offering environmental benefits, autonomous marine vessels introduce potential ecological concerns: physical interaction with marine life, noise pollution, and impacts from failures. Sall-e's autonomous navigation carries inherent collision risk with marine animals. Mitigation involves integrating a dedicated animal detection.

Proper waste management is critical. Peraturan Menteri Lingkungan Hidup Dan Kehutanan Nomor 9 Tahun 2024 (Permen LHK No. 9 Tahun 2024) governs hazardous and toxic waste (B3 waste) lifecycle management. This is highly pertinent for Sall-e's lithium-ion batteries, classified as B3 waste. The project must implement rigorous procedures for the entire battery lifecycle, from procurement of eco-friendly chemicals to end-of-life disposal and recycling, ensuring compliance with sorting, collection, transport, processing, and disposal requirements. Non-compliance risks significant liability.[85]

#### 4.6.4 Documentation and Regulatory

Comprehensive documentation and continuous monitoring are indispensable for compliance, accountability, and trust, especially concerning environmental/wildlife protection. Documentation enables auditability, traceability, explainable AI, identifies

mistakes/biases, and supports scaling. Regulators demand documentation of algorithmic logic, audit trails, and validation. It is crucial evidence demonstrating due diligence, safety adherence, and absence of negligence amidst responsibility for fragmentation. Sall-e must transform compliance into tangible proof.

Effective compliance requires a comprehensive data governance framework including regulatory mapping and monitoring, clear ethical AI principles, robust documentation and auditability practices, and data protection by design. Specific requirements include clear documentation of algorithmic logic, audit trails for all automated actions, version control for AI models/actions, detailed decision logs, rich metadata for context/sensitivity, data quality assurance, and regular bias/fairness audits.

Achieving continuous compliance necessitates data governance assessments, comprehensive data catalogs (evolving towards AI-enhanced systems), clear AI governance policies, and cross-functional oversight involving data, legal, compliance, IT, and business units ensuring collaboration. Automated monitoring tools and leveraging RPA/AI for autonomous compliance monitoring, real-time deficiency detection, and automated audit documentation are essential for managing regulatory volume and risk, enabling Sall-e to monitor its own operations against dynamic regulations

## 5. Conclusion

The Sall-e platform represents a novel, interdisciplinary solution to one of Southeast Asia's most pressing environmental crises: riverine plastic pollution. Designed with full autonomy, robust modularity, and environmental ethics in mind, Sall-e demonstrates how low-cost robotics, embedded AI, and renewable energy can jointly drive sustainable waterway remediation.

### *Lifecycle Reflection by Subsystem*

Each subsystem was engineered to achieve long-term resilience under real-world river conditions:

Subsystem	Component(s)	Lifespan / Maintenance	Notes

<b>Robotics</b>	Conveyor Belt, Cleats, Drive Motors	Inspect every 3 months; replace belt annually	Exposed to debris, wear-prone; HDPE netting replaced with wear or damage
	Buoyancy Hull + Seals	Inspect bi-annually; replace seals if brittle/damaged	PETG & HDPE assumed; exposure to UV and water stress
	HDPE Netting System	Every 4–6 collection cycles (or as torn)	Based on 4-net design; autonomously swapped during operation
	Structural Frame (Aluminium)	3–5 years before fatigue inspection	Modular, FEA validated; inspect if mechanical shock or overload occurs
<b>Propulsion</b>	T500 Thruster Motors	500–1000 hours of operation	Rated for underwater continuous use; inspect impellers quarterly
	Thruster Commander + ESC	Replace/inspect every 2–3 years	Sealed; heat-safe; ensure no signal dropout or moisture exposure
<b>Electrical</b>	24V LiFePO <sub>4</sub> Battery (150Ah)	>2000 cycles (~3 years daily charge)	Thermally stable, solar-recharged; cycle lifespan based on LiFePO <sub>4</sub> chemistry
	Solar Panels (3×350W Mono)	20–25 years (standard panel lifespan)	Minimal maintenance; clean every 6–12 months for dust/water clarity
	Custom PCB + Power Regulation	Inspect annually; replace every 4–5 years	Modular design simplifies hot swap if failures occur
<b>Sensors</b>	Ultrasonic Sensor (JSN-SR04T)	Replace every 2 years or on damage	Waterproof (IP66); failure rate rises in high humidity after 2 years
	ToF Sensor (VL53L1X)	Replace every 3–4 years	Low thermal drift: PETG bracket tested for storm conditions
	OAK-D Camera	3–4 years (subject to humidity and dirt)	Polycarbonate housing protects from water; thermal stress rated to <1°C drift
	Sonar Sensor (Ping Altimeter & Echosounder)	3 years, check quarterly for marine fouling	Submersible; resistant to turbulence per CFD simulation
<b>Software</b>	Automation pipelines and modelling	Update every 6 months with model retraining	Ensure compatibility with updated datasets and environmental conditions
	Web Dashboard + Data Logging	Patch monthly; audit logs quarterly	Telemetry logging, for system debugging and controls.

	Jetson Orin unit (GPU)	Maintain every 6 months;	Ensure compliance with updated software and reliable runtime operations.
--	------------------------	--------------------------	--

Table. Life cycle across all subsystems.

- **Robotics & Mechanical Subsystems:** The conveyor belt and buoyancy hull require minimal intervention, with maintenance cycles ranging from 3 to 6 months. The HDPE netting is modular and replaced every few cycles, while the aluminium structural frame has a fatigued lifespan exceeding 5 years under conservative estimates.
- **Propulsion:** The T500 thrusters offer 500–1000 operational hours and were selected for continuous underwater duty, requiring only quarterly inspections. Control electronics and ESCs are heat-sealed and inspected biennially.
- **Electrical Systems:** Powered by a 24V 150Ah LiFePO<sub>4</sub> battery rated for 2000+ charge cycles (~3 years daily use), the robot remains solar-rechargeable via a 3-panel 350W monocrystalline array. This reduces long-term energy costs and supports off-grid deployments.
- **Sensors:** Ultrasonic, sonar, and ToF sensors are waterproof-rated, with a typical lifespan of 3–4 years. The OAK-D camera is housed in marine-rated enclosures, tested under thermal and CFD stress conditions for longevity.
- **Software:** System-wise are updated biannually, with edge models retrained as dataset and field conditions evolve. The Jetson Orin onboard unit receives firmware updates every 6 months to ensure optimal operation.

These lifespans ensure a sustainable deployment cycle, with estimated component replacement costs constituting a fraction of the annualized operational cost when compared to traditional manual cleanup efforts.

#### *Legal, Financial, and Ecological Sustainability*

From a legal and ethical standpoint, Sall-e adheres to **IEEE7000 standards, Indonesian Permen LHK No. 9/2024, and marine protected area (MPA) regulations**. Its wildlife detection mechanism actively prevents ecological disturbance. Additionally, the embedded battery system complies with hazardous waste (B3) disposal protocols, supporting circular economy principles.

Cost breakdown on each subsection:

Item	Note	Cost (AUD)
Drone	Per unit	\$1,100
Software	Software Development (including human labor and Nvidia Orin)	\$11,650
Robotic	Waste Retrieval, Netting, Hull	\$6,069
Propulsion	Accurate mapping for geological localization	\$1,964
Sensors	Data retention & tests	\$827
Electrical	Miscellaneous	\$3,289
<b>Total Estimated Cost</b>	Per unit	<b>\$24,899</b>

This investment enables fully autonomous, solar-powered, AI-driven river cleaning for a fraction of the cost required for long-term manual operations, which typically rely on recurring labor, fuel, and logistics.

Ecologically, Sall-e reduces the dependence on manual labor, eliminates fossil fuel reliance, and contributes to biodiversity preservation through wildlife-compliant routing. It advances Indonesia's efforts toward SDG 6 (Clean Water and Sanitation) and SDG 14 (Life Below Water).

In summary, Sall-e is not just a prototype - it is a functional, modular, and ethically deployable robot. It showcases how modern engineering can serve ecological restoration in polluted river systems. By balancing robust hardware, low-cost autonomy, and responsible AI practices, Sall-e offers a scalable model for environmental intervention in developing regions. With proper institutional backing and continued technical iteration, it can become a cornerstone in the global fight against aquatic plastic pollution.

## 6. Recommendations

- Conduct real-world pilot testing in controlled Citarum segments.
- Investigate integration of cloud backups for sensor data.
- Explore multi-robot swarm deployment.
- Expand localisation to include drone-supported mapping.
- Partner with local councils or NGOs to subsidize initial deployment through eco-tourism or urban renewal grants.

- Develop cost-sharing models for municipalities, where the robot's usage is shared across river zones to maximize ROI.
- Design a maintenance service plan (e.g., biannual checkups, thruster cleaning, battery health checks) for long-term viability.
- Consider licensing the robot system to other polluted river regions across Southeast Asia with minor modular adjustments.
- Train the vision system to detect obstructions or underwater vegetation, prompting thrust reduction or course redirection before entanglement occurs.

## 7. References

- [1] A. Hidayat, "Citarum River: The Most Polluted River in the World," *Indonesia Expat*, 2018. [Online]. Available: <https://indonesiaexpat.id/news/citarum-river-the-most-polluted-river-in-the-world/>
- [2] Asian Development Bank, "Revitalizing the Citarum River," *ADB Report*, 2019. [Online]. Available: <https://www.adb.org/results/revitalizing-citarum-river>
- [3] S. P. Hidayat, "The Economic Cost of Manual Garbage Collection in Indonesian Rivers," *Environmental Economics*, vol. 11, no. 2, pp. 88–95, 2021.
- [4] S. Gupta and U. Goel, "Clearbot: The Autonomous Workboat Venture That Is Cleaning Our Oceans," *Lloyd's Register*, Mar. 2024. [Online]. Available: <https://www.lr.org/en/knowledge/horizons/march-2024/clearbot-the-autonomous-workboat-venture-that-is-cleaning-our-oceans/>
- [5] "Dustbot," *Wikipedia*, [online]. Available: <https://en.wikipedia.org/wiki/Dustbot>. [Accessed: Jun. 4, 2025].
- [6] K. Friedrich, "Sensor-Based and Robot Sorting Processes and Their Role in Achieving European Recycling Goals – A Review," *ResearchGate*, 2022. [Online]. Available: [https://www.researchgate.net/publication/361604934\\_Sensor-based\\_and\\_Robot\\_Sorting\\_Processes\\_and\\_their\\_Role\\_in\\_Achieving\\_European\\_Recycling\\_Goals\\_-\\_A\\_Review](https://www.researchgate.net/publication/361604934_Sensor-based_and_Robot_Sorting_Processes_and_their_Role_in_Achieving_European_Recycling_Goals_-_A_Review)

- [7] "Hyperspectral Imaging in Recycling and Waste Management," *Specim*, [online]. Available: <https://www.specim.com/hyperspectral-imaging-applications/hyperspectral-imaging-in-recycling-and-waste-management/>. [Accessed: Jun. 4, 2025].
- [8] Y. Shao et al., "Using YOLOv5 for Garbage Classification," *ResearchGate*, 2021. [Online]. Available: [https://www.researchgate.net/publication/355073419\\_Using\\_YOLOv5\\_for\\_Garbage\\_Classification](https://www.researchgate.net/publication/355073419_Using_YOLOv5_for_Garbage_Classification)
- [9] Z. Zhang et al., "An Improved YOLOv8n Used for Fish Detection in Natural Water Environments," *ResearchGate*, 2024. [Online]. Available: [https://www.researchgate.net/publication/382135627\\_An\\_Improved\\_YOLOv8n\\_Used\\_for\\_Fish\\_Detection\\_in\\_Natural\\_Water\\_Environments](https://www.researchgate.net/publication/382135627_An_Improved_YOLOv8n_Used_for_Fish_Detection_in_Natural_Water_Environments)
- [10] L. Zhang et al., "Robot Navigation Based on Improved A\* Algorithm in Dynamic Environment," *Assembly Automation*, vol. 41, no. 5, pp. 697–707, 2021. [Online]. Available: <https://www.emerald.com/insight/content/doi/10.1108/aa-07-2020-0095/full/html>
- [11] "Aluminum 6061, Al 6061-T6 Alloy Properties, Density, Tensile & Yield Strength," The World Material. [Online]. Available: <https://www.theworldmaterial.com/al-6061-t6-aluminum-alloy/>. [Accessed: Jun. 4, 2025].
- [12] "The Science Behind TPU: Why It's the Ideal Material for Conveyor Belts," Pengde. [Online]. Available: <https://pengdepu.com/the-science-behind-tpu-why-its-the-ideal-material-for-conveyor-belts/>. [Accessed: Jun. 4, 2025].
- [13] "Design of River Surface Cleaning 'ECOBOT,'" International Research Journal of Modernization in Engineering Technology and Science, vol. 6, no. 10, pp. 123-130, Oct. 2024. [Online]. Available: [https://www.irjmets.com/uploadedfiles/paper/issue\\_10\\_october\\_2024/62850/final/fin\\_irjmets1730737289.pdf](https://www.irjmets.com/uploadedfiles/paper/issue_10_october_2024/62850/final/fin_irjmets1730737289.pdf). [Accessed: Jun. 4, 2025].
- [14] A. Nagayo, "Autonomous Trash Collector Robot with Wireless Charging System," Botswana International University of Science and Technology, 2023. [Online]. Available: [https://repository.biust.ac.bw/bitstream/handle/123456789/190/147\\_Analene%20Nagayo\\_Autonomous%20Trash%20Collector%20Robot..pdf](https://repository.biust.ac.bw/bitstream/handle/123456789/190/147_Analene%20Nagayo_Autonomous%20Trash%20Collector%20Robot..pdf). [Accessed: Jun. 4, 2025].

- [15] “HDPE 5000s (Monofilament) – POLYMER EXPORT,” [Online]. Available: <https://polymerexport.com/product/hdpe-5000s-monofilament/>. [Accessed: Jun. 4, 2025].
- [16] “Neodymium Magnetic Latch Kit | Holding Strength 14kg,” AMF Magnetics, [Online]. Available: <https://magnet.com.au/products/neodymium-magnetic-latch-kit-holding-strength-14kg>. [Accessed: Jun. 4, 2025].
- [17] “25GA370 12V Metal Gear Low Speed High Torque Motor 300RPM - 1360RPM,” Synacorp, [Online]. Available: <https://synacorp.my/v3/en/dc-motors/1941-rs-385-12vdc-high-speed-dc-motor.html>. [Accessed: Jun. 4, 2025].
- [18] “Aluminum 6061, Al 6061-T6 Alloy Properties, Density, Tensile & Yield Strength,” The World Material. [Online]. Available: <https://www.theworldmaterial.com/al-6061-t6-aluminum-alloy/>. [Accessed: Jun. 4, 2025].
- [19] “14.6: Archimedes’ Principle and Buoyancy,” Physics LibreTexts. [Online]. Available: [https://phys.libretexts.org/Bookshelves/University\\_Physics/University\\_Physics\\_%28OpenStax%29/Book%3A\\_University\\_Physics\\_I\\_-Mechanics\\_Sound\\_Oscillations\\_and\\_Waves%28OpenStax%29/14%3A\\_Fluid\\_Mechanics/14.06%3A\\_Archimedes\\_Principle\\_and\\_Buoyancy](https://phys.libretexts.org/Bookshelves/University_Physics/University_Physics_%28OpenStax%29/Book%3A_University_Physics_I_-Mechanics_Sound_Oscillations_and_Waves%28OpenStax%29/14%3A_Fluid_Mechanics/14.06%3A_Archimedes_Principle_and_Buoyancy). [Accessed: Jun. 4, 2025].
- [20] “Hydrodynamic and Structural Investigations of Catamaran Design,” ScienceDirect. [Online]. Available: <https://www.sciencedirect.com/science/article/pii/S2452321620304832>. [Accessed: Jun. 4, 2025].
- [21] IEEE Std 1013-2019, “IEEE Recommended Practice for Sizing Lead-Acid Batteries for Stand-Alone Photovoltaic (PV) Systems,” IEEE Standards Association, 2019. [Online]. Available: <https://standards.ieee.org/ieee/1013/7165/>
- [22] M. A. Eltawil and Z. Zhao, “MPPT techniques for photovoltaic applications,” Renewable and Sustainable Energy Reviews, vol. 25, pp. 793–813, 2013. [Online]. Available: <https://doi.org/10.1016/j.rser.2013.05.022>
- [23] A. K. Abdelsalam, A. M. Massoud, S. Ahmed, and P. N. Enjeti, “High-Performance Adaptive Perturb and Observe MPPT Technique for Photovoltaic-Based Microgrids,” IEEE Transactions on Power Electronics, vol. 26, no. 4, pp. 1010–1021, Apr. 2011. [Online]. Available: <https://doi.org/10.1109/TPEL.2010.2101621>

[24] "Aluminum 6061, Al 6061-T6 Alloy Properties, Density, Tensile & Yield Strength," The World Material. [Online]. Available: <https://www.theworldmaterial.com/al-6061-t6-aluminum-alloy/>. [Accessed: Jun. 4, 2025].

[25] "SOLIDWORKS Simulation 2019 Validation," SOLIDWORKS. [Online]. Available: <https://www.solidworks.com/sites/default/files/2019-04/VPCS-English2019.pdf>. [Accessed: Jun. 4, 2025].

[26] "Incorporating Mechatronics into Your Design Process," SOLIDWORKS. [Online]. Available: [https://www.solidworks.com/sw/docs/Mechatronics\\_2010\\_ENG\\_FINAL.pdf](https://www.solidworks.com/sw/docs/Mechatronics_2010_ENG_FINAL.pdf). [Accessed: Jun. 4, 2025].

[27] B.Robotics, "T500 Thruster," Blue Robotics, 2025.

<https://bluerobotics.com/store/thrusters/t100-t200-thrusters/t500-thruster/>

[28] R. Thomas, "Meet Mr Trash Wheel – and the other new devices that eat river plastic," the Guardian, Jan. 11, 2022.

<https://www.theguardian.com/environment/2022/jan/11/meet-mr-trash-wheel-and-the-other-ingenuous-tools-that-eat-river-plastic>

[29] D. Ramirez-Lovering, "Saving Citarum: Cleaning up one of the world's most polluted rivers," Monash Lens, Aug. 26, 2021. <https://lens.monash.edu/@design-architecture/2021/08/26/1383691/cleaning-up-citarum-river-one-of-the-worlds-most-polluted-waterways>

[30] C. Kormann, "The Promise of Mr. Trash Wheel," The New Yorker, 2019.

<https://www.newyorker.com/tech/annals-of-technology/the-promise-of-mr-trash-wheel>

[31] D. Teoli, J. An, and T. Sanvictores, "SWOT Analysis," National Library of Medicine, Sep. 04, 2023. <https://www.ncbi.nlm.nih.gov/books/NBK537302/>

[32] Nirmalawati and I. W. Sutapa, "Economic Feasibility Study Biforcation Development and Toili River Flood Control Banggai District," IOP Conference Series: Earth and Environmental Science, vol. 1075, no. 1, p. 012037, Nov. 2022, doi:

<https://doi.org/10.1088/1755-1315/1075/1/012037>.

[33] V. N. Xuan, "Determinants of environmental pollution: Evidence from Indonesia," *Journal of Open Innovation: Technology, Market, and Complexity*, vol. 10, no. 4, p. 100386, Dec. 2024, doi: <https://doi.org/10.1016/j.joitmc.2024.100386>.

[34] O. Movement, "WWF Report: The true cost of plastics – The Ocean Movement," *The Ocean Movement*, Jul. 27, 2021. <https://theoceannovement.org/wwf-report-the-true-cost-of-plastics/>

[35] Jacob, "Ping Sonar Technical Manual," Blue Robotics. Accessed: Apr. 26, 2025. [Online]. Available: <https://bluerobotics.com/learn/ping-sonar-technical-guide/>

[36] Tingting Chen, Weikai Zhang, and Jun Zhang, "Alkali resistance of poly(ethylene terephthalate) (PET) and poly(ethylene glycol-co-1,4-cyclohexanedimethanol terephthalate) (PETG) copolyesters: The role of composition," *Polym Degrad Stab*, vol. 120, pp. 232–243, Oct. 2015.

[37] Stuart Moore, "OAK-D Datasheet," 2022. Accessed: Jun. 04, 2025. [Online]. Available: [https://github.com/luxonis/depthai-hardware/blob/master/BW1098OAK\\_USB3C/Datasheet/OAK-D\\_Datasheet.pdf](https://github.com/luxonis/depthai-hardware/blob/master/BW1098OAK_USB3C/Datasheet/OAK-D_Datasheet.pdf)

[38] Manorshi, "JSN-SR04T Datasheet," 2021.

[39] ST Microelectronics, "VL53L1X Datasheet," Jun. 2020.

[40] H. S. Naicker et al., "Water Care: Water Surface Cleaning Bot and Water Body Surveillance System," arXiv preprint arXiv:2111.12579, Nov. 2021. [Online]. Available: <https://arxiv.org/abs/2111.12579>

[41] W. Wang et al., "Roboat II: A Novel Autonomous Surface Vessel for Urban Environments," arXiv preprint arXiv:2007.10220, Jul. 2020. [Online]. Available: <https://arxiv.org/abs/2007.10220>

[42] Y. Cheng et al., "Are We Ready for Unmanned Surface Vehicles in Inland Waterways? The USVIinland Multisensor Dataset and Benchmark," arXiv preprint arXiv:2103.05383, Mar. 2021. [Online]. Available: <https://arxiv.org/abs/2103.05383>

[43] A. Sundarajan et al., "Underwater Autonomous Tank Cleaning Rover," arXiv preprint arXiv:2304.08185, Apr. 2023. [Online]. Available: <https://arxiv.org/abs/2304.08185>

- [44] NVIDIA Corporation, "Jetson AGX Orin Series: Technical Brief," NVIDIA, [Online]. Available: <https://www.nvidia.com/content/dam/en-zz/Solutions/gtcf21/jetson-orin/nvidia-jetson-agx-orin-technical-brief.pdf>
- [45] ON Semiconductor, "LM2596: 3.0 A Step-Down Voltage Regulator," Texas Instruments, [Online]. Available: <https://www.onsemi.com/download/data-sheet/pdf/lm2596-d.pdf>
- [46] Makerguides.com, "JCN-SR04T-2.0 Ultrasonic Waterproof Range Finder Datasheet," [Online]. Available: <https://www.makerguides.com/wp-content/uploads/2019/02/JCN-SR04T-Datasheet.pdf>
- [47] STMicroelectronics, "VL53L1X: Time-of-Flight Ranging Sensor Datasheet," [Online]. Available: <https://www.st.com/resource/en/datasheet/vl53l1x.pdf>
- [48] Blue Robotics, "Ping Sonar Altimeter and Echosounder," [Online]. Available: <https://bluerobotics.com/store/sonars/echosounders/ping-sonar-r2-rp/>
- [49] HoloBattery, "12V vs 24V: What's The Difference in Battery Systems?" [Online]. Available: <https://holobattery.com/12v-vs-24v/>
- [50] PowerTech Systems, "Lithium Ion battery 24V 150Ah – LiFePO4 - MyLithiumBattery," [Online]. Available: <https://www.mylithiumbattery.com/shop/12v-lithium-ion-battery-packs/lithium-battery-24v/lithium-ion-battery-24v-150ah-lifepo4-powerbrick/>
- [51] RenewableWise, "MPPT charge controller calculator: Find the right solar charge controller," [Online]. Available: <https://www.renewablewise.com/mppt-calculator/>
- [52] Victron Energy, "Solar charge controllers," [Online]. Available: <https://www.victronenergy.com/solar-charge-controllers>
- [53] Sciencing, "Pros & Cons Of 24 Volt Vs. 12 Volt," [Online]. Available: <https://www.scientific.com/pros-volt-vs-12-volt-8791851/>
- [54] Redway Tech, "Why Is a 24V Inverter Better Than a 12V Inverter?" [Online]. Available: <https://www.redway-tech.com/why-is-24v-inverter-better-than-12v/>

[55] Earthship Biecture, "What is the advantage of a 24v system over a 12v system?" [Online]. Available: <https://earthship.com/2020/03/27/what-is-the-advantage-of-a-24v-system-over-a-12v-system/>

[56] Duh Boat, "The Pros and Cons of 12V DC, 24V DC, and 48V DC Systems," [Online]. Available: <https://duhboat.com/the-pros-and-cons-of-12v-dc-24v-dc-and-48v-dc-systems/>

[57] Clean Energy Reviews, "MPPT Solar Charge Controllers Explained," [Online]. Available: <https://www.cleanenergyreviews.info/blog/mppt-solar-charge-controllers>

[58] RenewableWise, "MPPT charge controllers: A complete but quick overview," [Online]. Available: <https://www.renewablewise.com/mppt-charge-controller/>

[59] Electrical Technology, "MPPT Solar Charge Controller – Working, Sizing and Selection," [Online]. Available : <https://www.electricaltechnology.org/2021/07/mppt-solar-charge-controller.html>

[60] G. Jocher et al., "YOLO by Ultralytics," GitHub, 2023. [Online]. Available: <https://github.com/ultralytics/yolov5>

[61] N. Carion et al., "End-to-End Object Detection with Transformers," in ECCV, 2020.

[62] Roboflow Bird: [https://universe.roboflow.com/sky-sd2zq/bird\\_only-pt0bm](https://universe.roboflow.com/sky-sd2zq/bird_only-pt0bm)

[63] Roboflow HydroQuest Fish: <https://universe.roboflow.com/team-hope-mmccyy/hydroquest>

[64] J. Cui et al., "Path Planning Algorithms for Autonomous Underwater Vehicles," IEEE Oceanic Engineering, 2017.

[65] W. Foerster, "Geospatial Coordinate Transformations in Aerial Imaging," Journal of Photogrammetric Engineering, 2017.

[66] E. Xie et al., "SegFormer: Simple and Efficient Design for Semantic Segmentation with Transformers," in Proc. NeurIPS, 2021.

[67] NVIDIA, "Jetson Orin Developer Kit Specification," 2024. [Online]. Available: HYPERLINK <https://developer.nvidia.com/embedded/jetson-orin>

- [68] J. Cui et al., "A survey on path planning algorithms for autonomous underwater vehicles," IEEE Oceanic Engineering, 2017.
- [69] Roboflow Universe, "Garbage Detection UA V Dataset," 2025. [Online]. Available: <https://universe.roboflow.com/roboflow-universe-projects/garbage-detection-uav>
- [70] Hammer Missions, "What is the Optimal Altitude for Drone Mapping?" [Online]. Available: <https://www.hammermissions.com/post/what-is-the-optimal-altitude-for-drone-mapping>
- [71] Anvil, "Mapping Accuracy with Drone Altitude," [Online]. Available: <https://www.4anvil.so/insights/drone-altitude-gsd>
- [72] Datumate, "Drone Mapping Accuracy Explained," [Online]. Available: <https://www.datumate.com/drone-mapping-accuracy>
- [73] AirCam, "How Drone Height Affects Image Quality," [Online]. Available: <https://www.aircamdrone.co.uk/articles>
- [74] Hammer Missions, "Drone Mapping Best Practices," [Online]. Available: <https://www.hammermissions.com>
- [75] Anvil, "Limitations of High-Altitude UAV Imaging," [Online]. Available: <https://www.4anvil.so>
- [76] Terra Drone Indonesia, "Drone Services," [Online]. Available: <https://ensun.io/company/terra-drone-indonesia>
- [77] Halo Robotics, "UAV Deployment Solutions," [Online]. Available: <https://ensun.io/company/halo-robotics>
- [78] Beehive Drones, "About Us," [Online]. Available: <https://beehivedrones.id>
- [79] Helicamindo, "Professional Drone Services," [Online]. Available: <https://www.helicamindo.com>
- [80] "IEEE SA - IEEE 7000-2021," SA Main Site. <https://standards.ieee.org/ieee/7000/6781/> (accessed Jun. 01, 2025).
- [81] Diah Ayu Rahmawati, Haryono Haryono, Budi Endarto, Joice Soraya, and A. Hidayat, "Civil Liability for Environmental Damage in Indonesia," *West Science Law and Human*

*Rights*, vol. 3, no. 01, pp. 97–105, Jan. 2025, doi:  
<https://doi.org/10.58812/wslhr.v3i01.1657>.

[82] “IEEE Ethics for AI System Design Training,” *IEEE Standards Association*, May 13, 2025.  
<https://standards.ieee.org/about/training/ethics-for-ai-system-design/> (accessed Jun. 01, 2025).

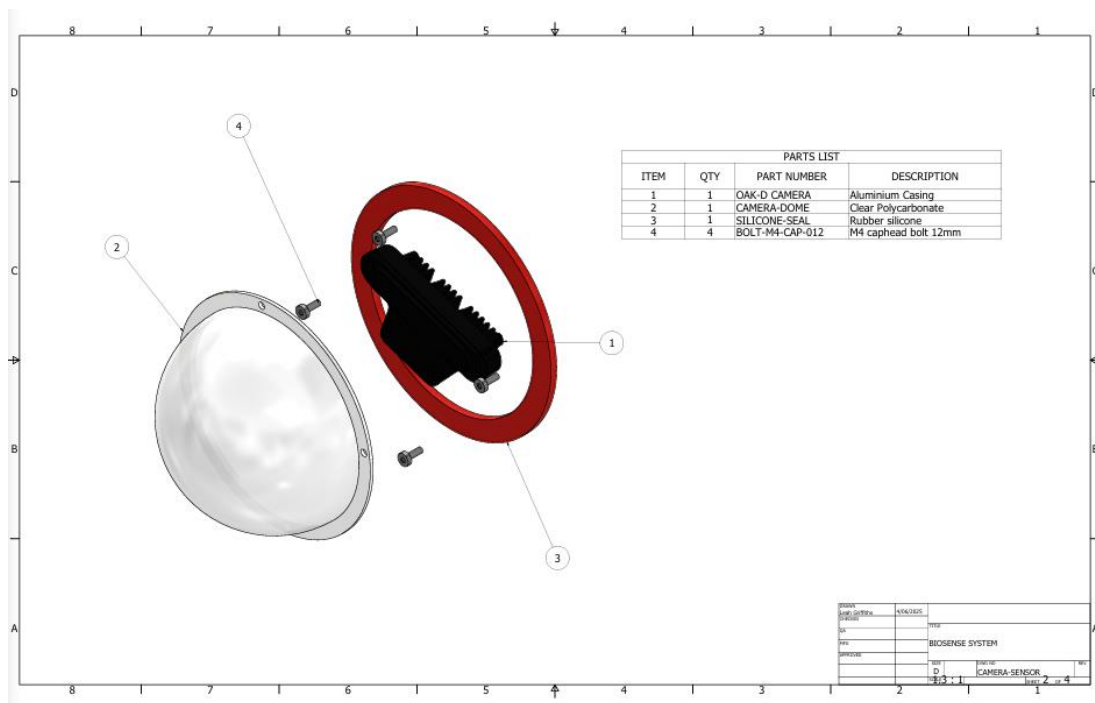
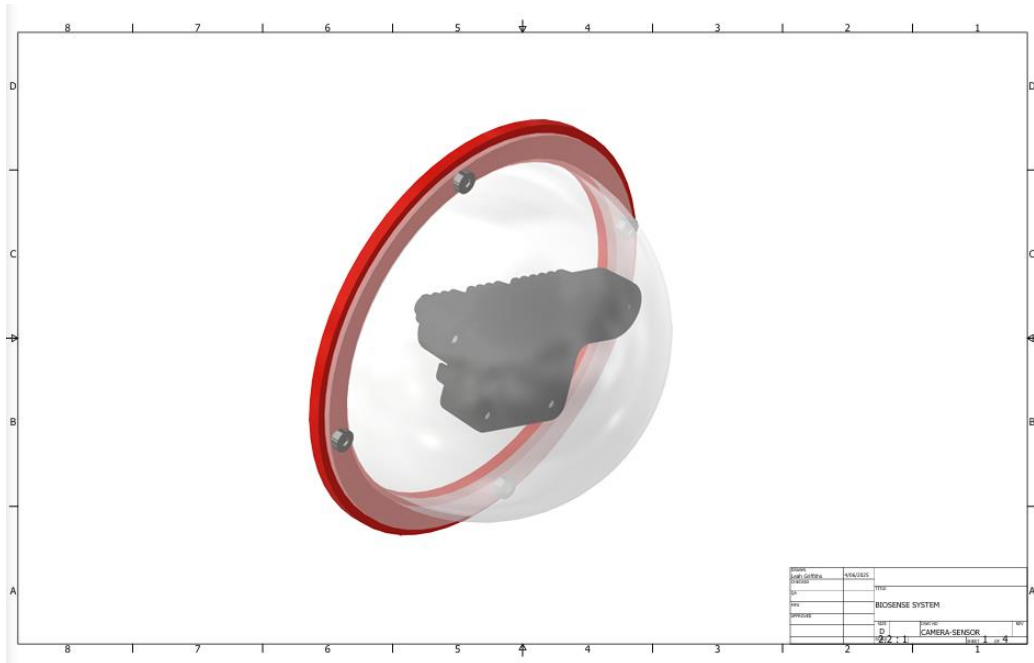
[83] *LAW OF THE SEA (National legislation)* © DOALOS/OLA - UNITED NATIONS, vol. Act No. 6 of 8 August 1996 regarding Indonesian Waters. 1996. Accessed: Jun. 02, 2025.  
[Online]. Available:

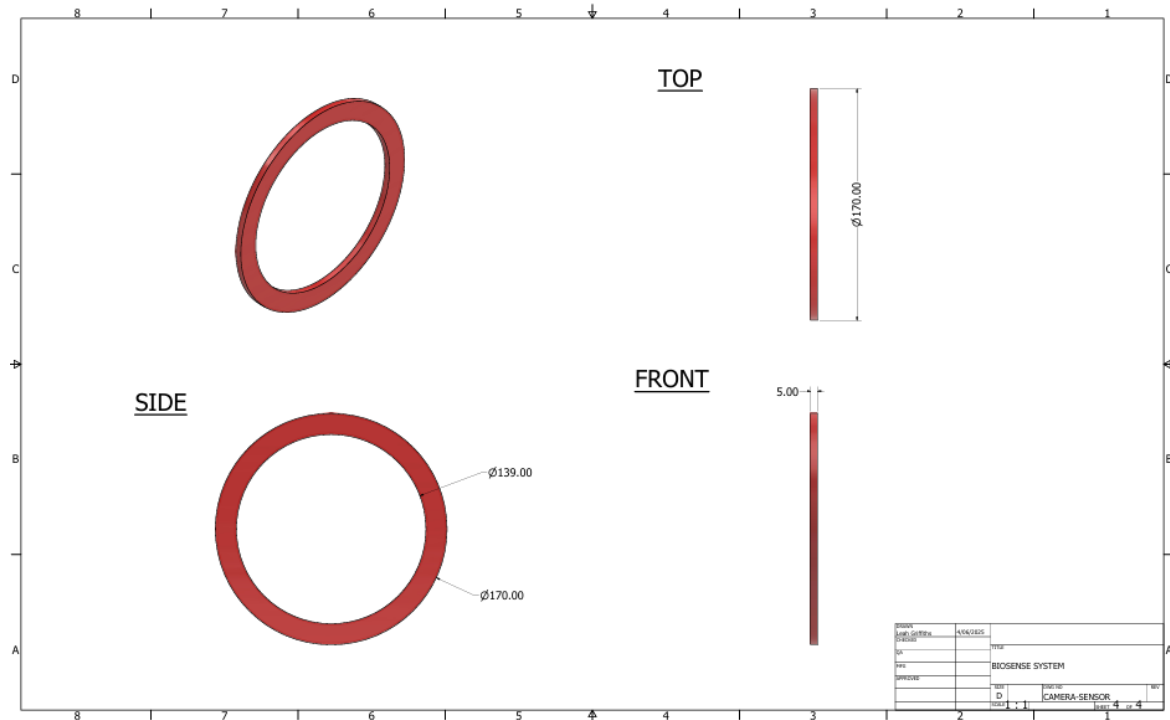
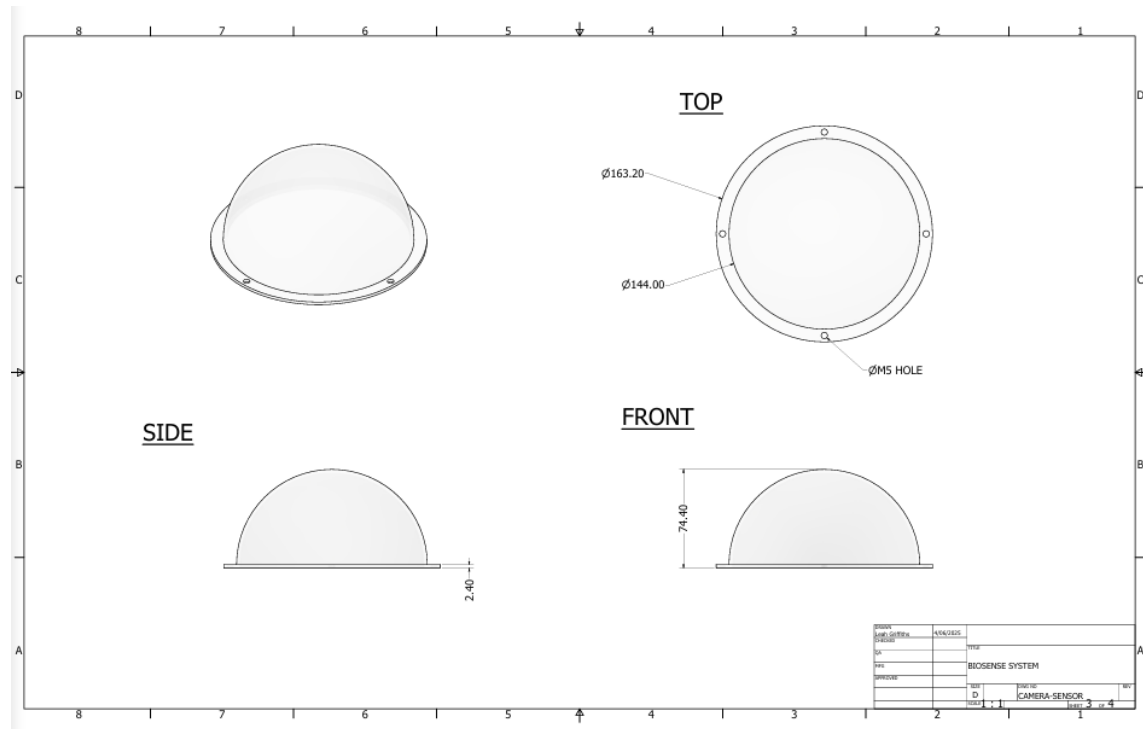
[https://www.un.org/depts/los/LEGISLATIONANDTREATIES/PDFFILES/IDN\\_1996\\_Act.pdf](https://www.un.org/depts/los/LEGISLATIONANDTREATIES/PDFFILES/IDN_1996_Act.pdf)

[84] I. New, “ARMA Law,” *ARMA Law*, Dec. 09, 2024. <https://www.arma-law.com/news-event/newsflash/understanding-indonesias-new-waste-management-policy-for-hazardous-materials> (accessed Jun. 02, 2025).

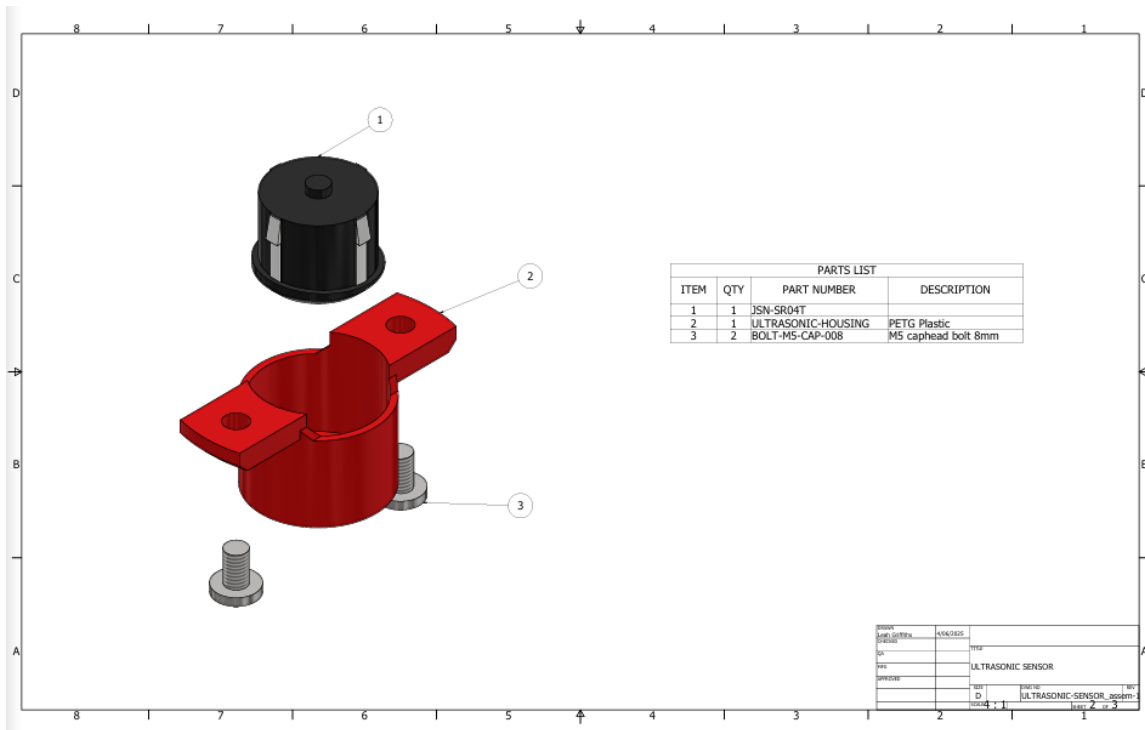
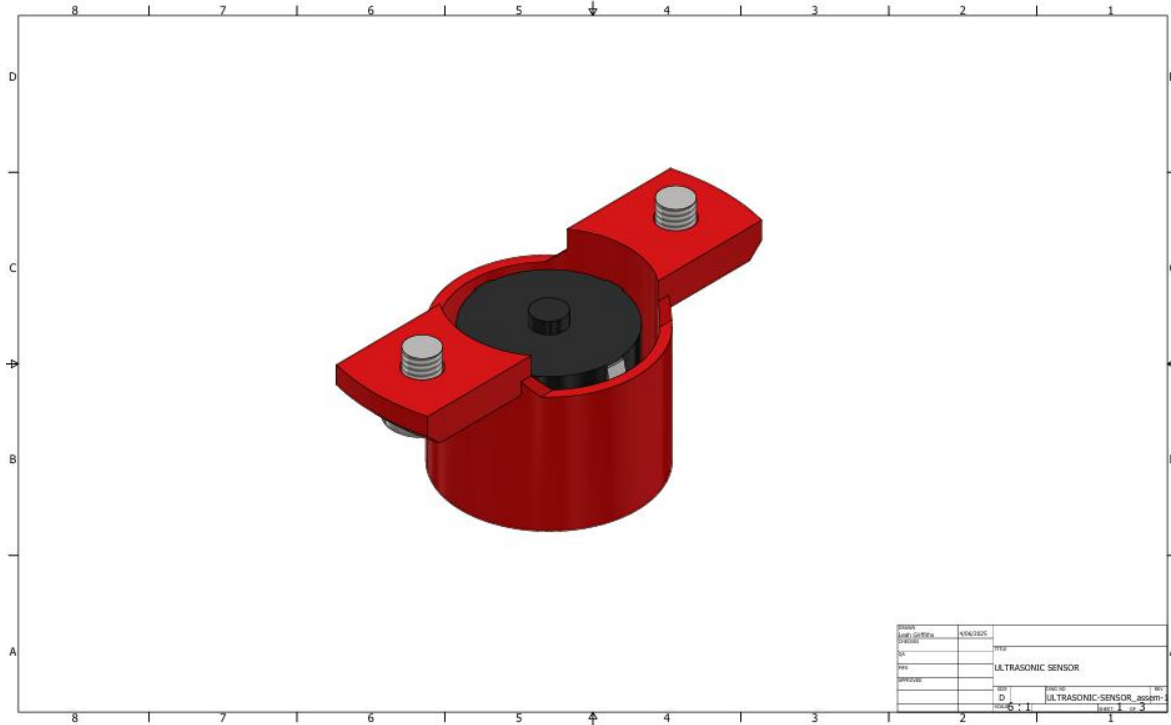
[85] “Permen LHK No. 9 Tahun 2024,” *Database Peraturan | JDIH BPK*, 2024.  
<https://peraturan.bpk.go.id/Details/291985/permen-lhk-no-9-tahun-2024> (accessed Jun. 02, 2025).

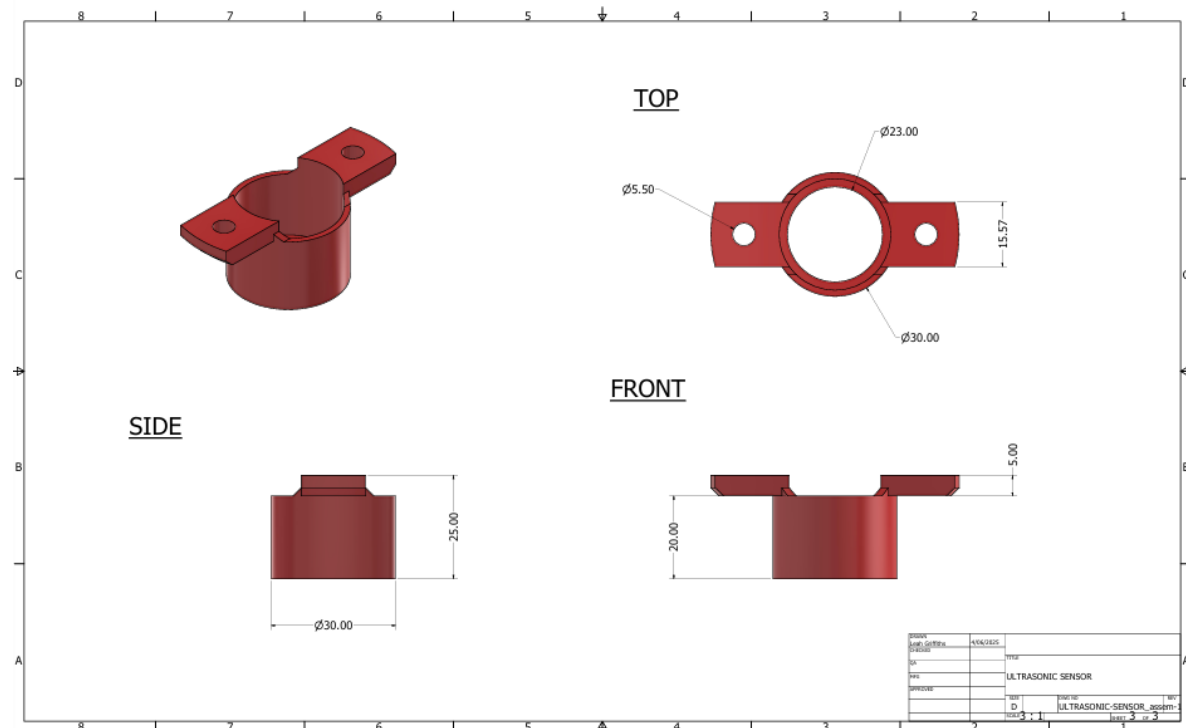
## Appendix A. CAD Drawings

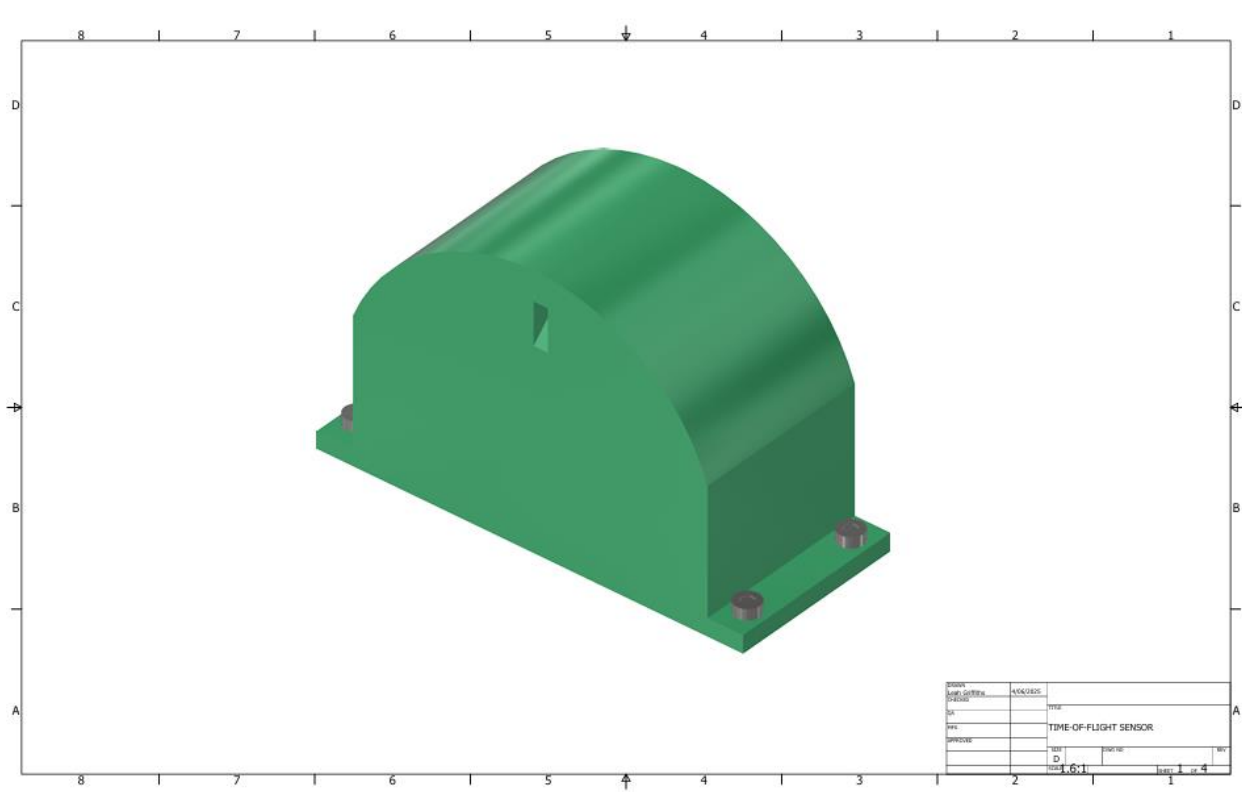


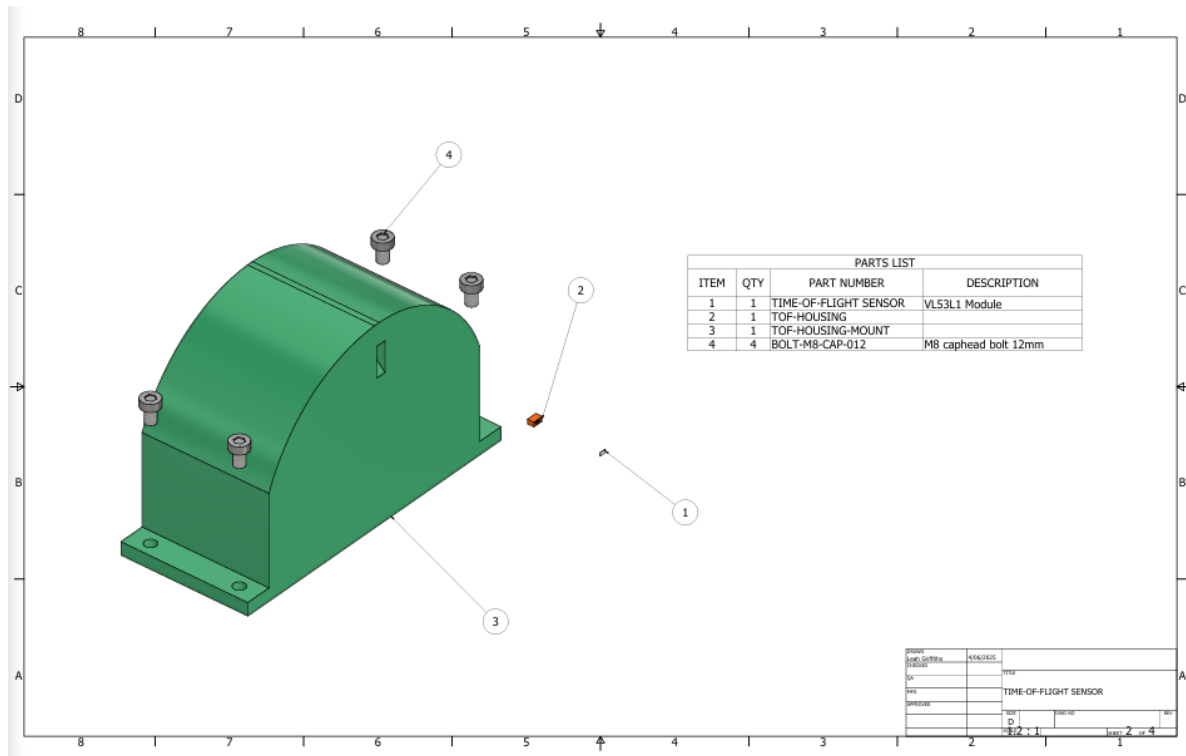


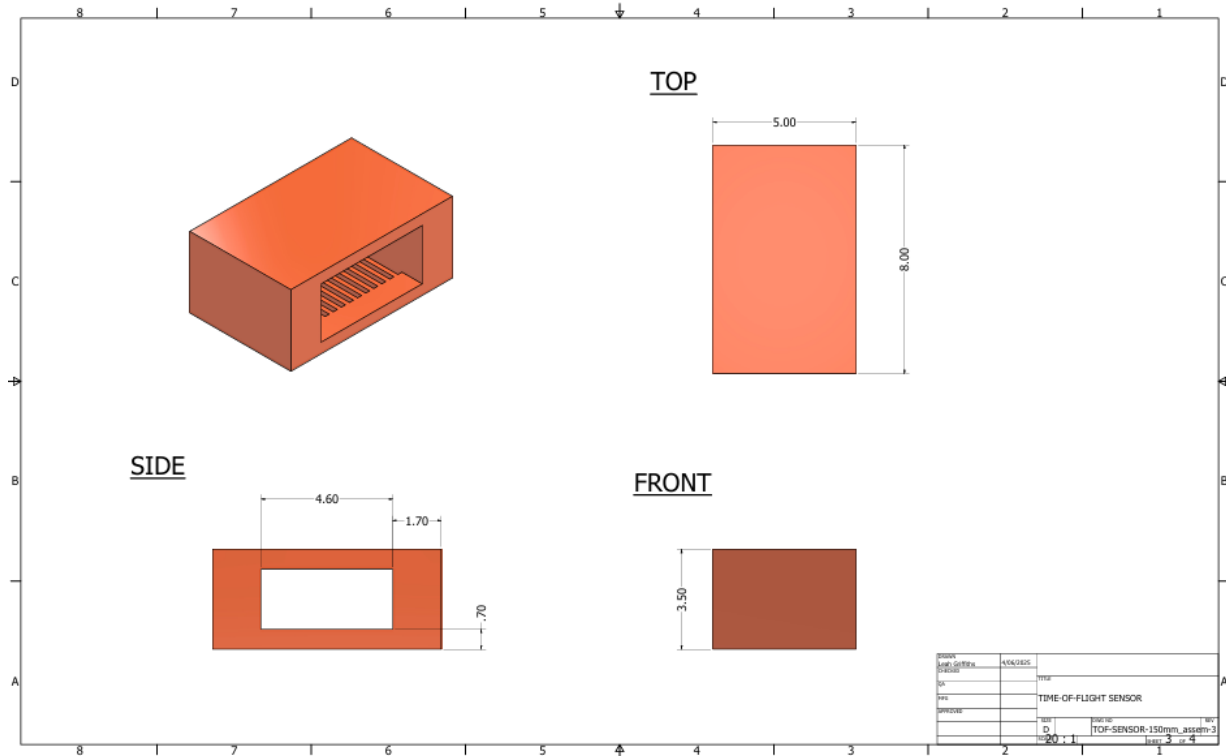


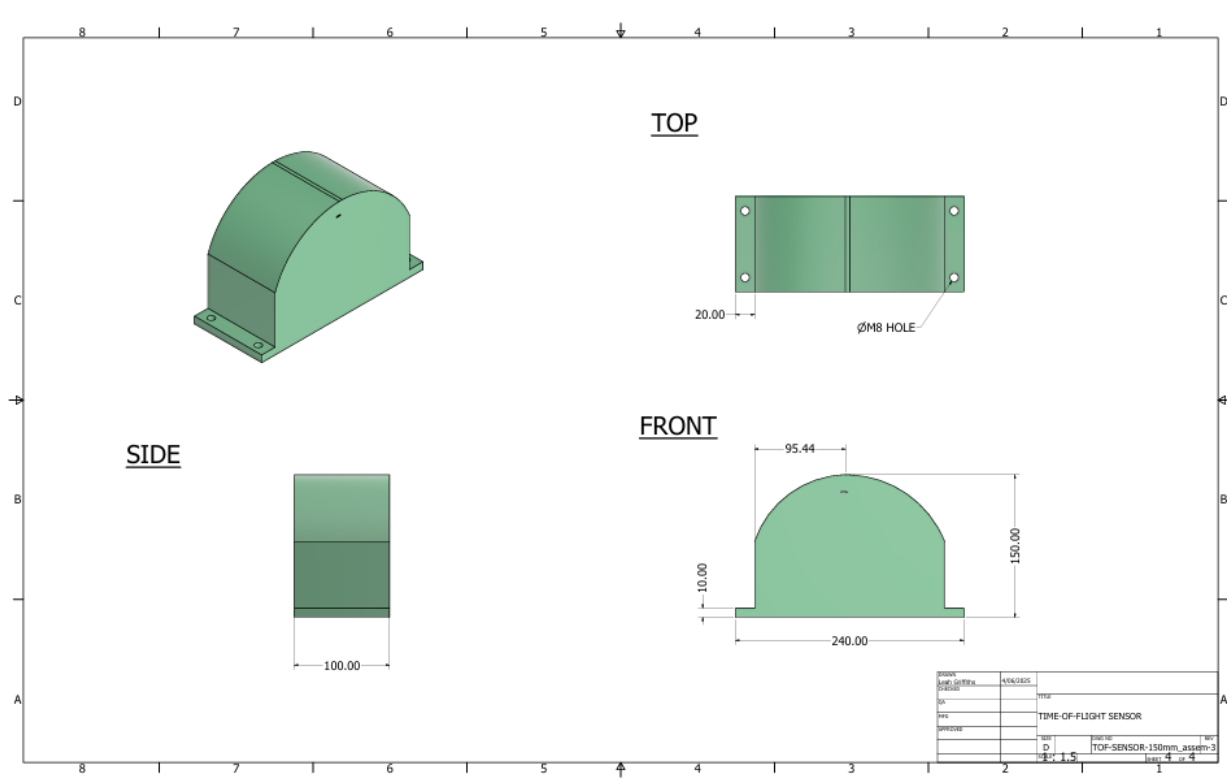












## Appendix B. FEA Reports

### Collection-FEA-Report



Analyzed File:	ULTRASONIC-HOUSING.ipt
Autodesk Inventor Version:	2025 (Build 290162000, 162)
Creation Date:	17/05/2025, 8:49 PM
Study Author:	leahg
Summary:	

#### Static Analysis:1

##### General objective and settings:

Design Objective	Single Point
Study Type	Static Analysis
Last Modification Date	17/05/2025, 8:38 PM
Model State	[Primary]
Detect and Eliminate Rigid Body Modes	No

#### iProperties

##### Summary

Author leahg

##### Project

Part Number	ULTRASONIC-HOUSING
Designer	leahg
Estimated Cost	\$0.00
Creation Date	15/05/2025

##### Status

Design State WorkInProgress

##### Physical

Material	ABS Plastic
Density	1.06 g/cm^3
Mass	0.00567536 kg
Area	5822.94 mm^2
Volume	5354.11 mm^3
Center of Gravity	x=0.0161 mm y=0.0000000103539 mm z=-0.0000000101984 mm

Note: Physical values could be different from Physical values used by FEA reported below.

**Mesh settings:**

Avg. Element Size (fraction of model diameter)	0.1
Min. Element Size (fraction of avg. size)	0.2
Grading Factor	1.5
Max. Turn Angle	60 deg
Create Curved Mesh Elements	Yes

 **Material(s)**

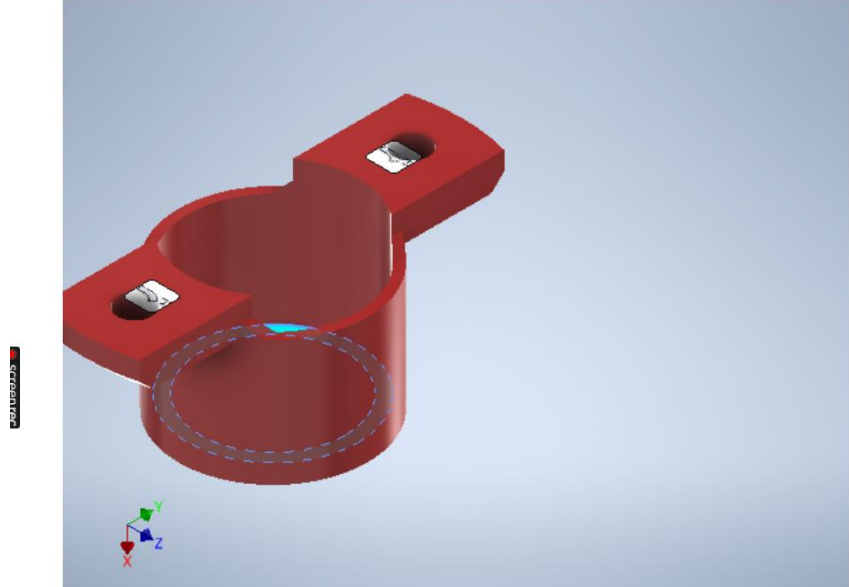
Name	ABS Plastic	
General	Mass Density	1.06 g/cm^3
	Yield Strength	20 MPa
	Ultimate Tensile Strength	29.6 MPa
Stress	Young's Modulus	2.24 GPa
	Poisson's Ratio	0.38 ul
	Shear Modulus	0.811594 GPa
Part Name(s)	ULTRASONIC-HOUSING.ipt	

 **Operating conditions** **Force:1**

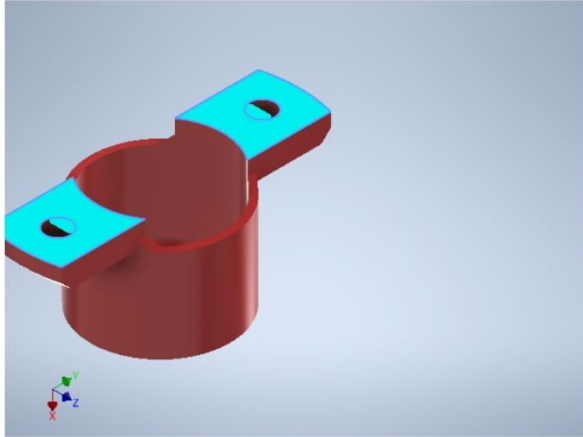
Load Type	Force
Magnitude	1.230 N
Vector X	1.230 N
Vector Y	0.000 N
Vector Z	0.000 N

Operating conditions Force:1

Load Type	Force
Magnitude	1.230 N
Vector X	1.230 N
Vector Y	0.000 N
Vector Z	0.000 N

 Selected Face(s) Fixed Constraint:1

Constraint Type: Fixed Constraint

 Selected Face(s)

□ Results

□ Reaction Force and Moment on Constraints

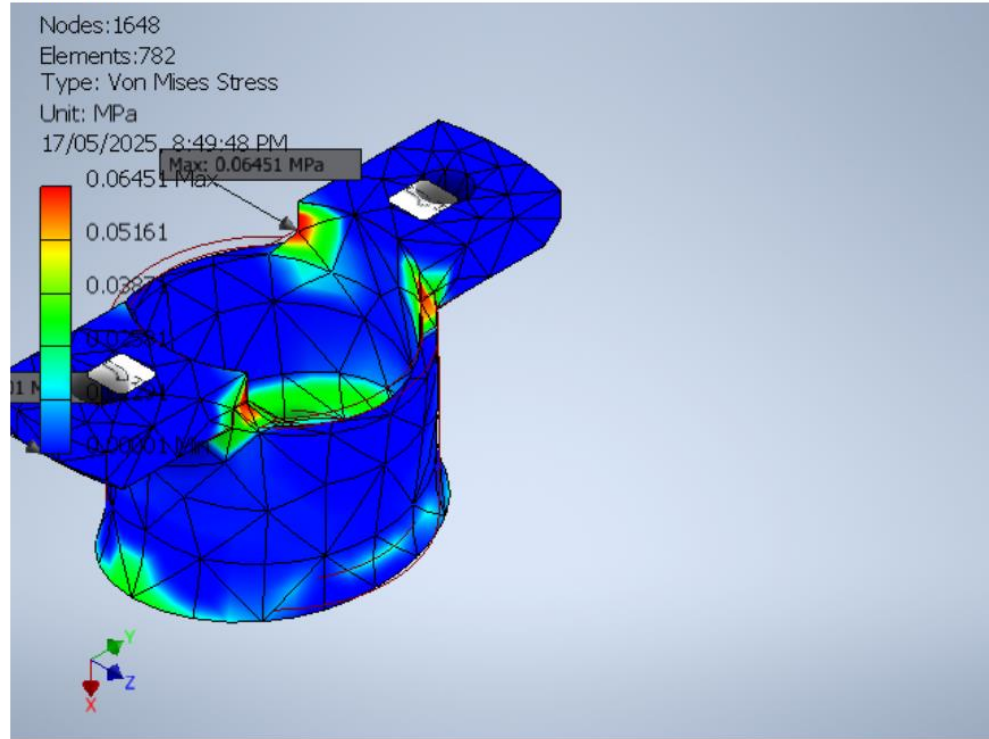
Constraint Name	Reaction Force		Reaction Moment	
	Magnitude	Component (X,Y,Z)	Magnitude	Component (X,Y,Z)
Fixed Constraint:1	1.23 N	-1.23 N 0 N 0 N	0 N m	0 N m 0 N m 0 N m

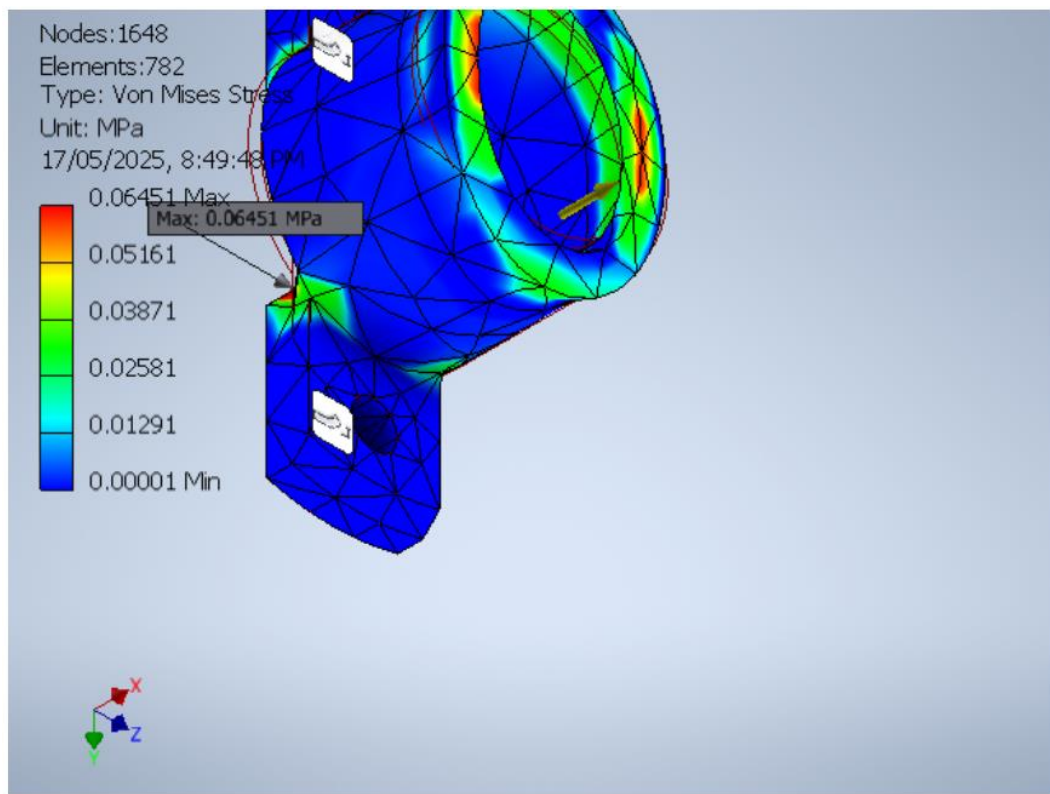
□ Result Summary

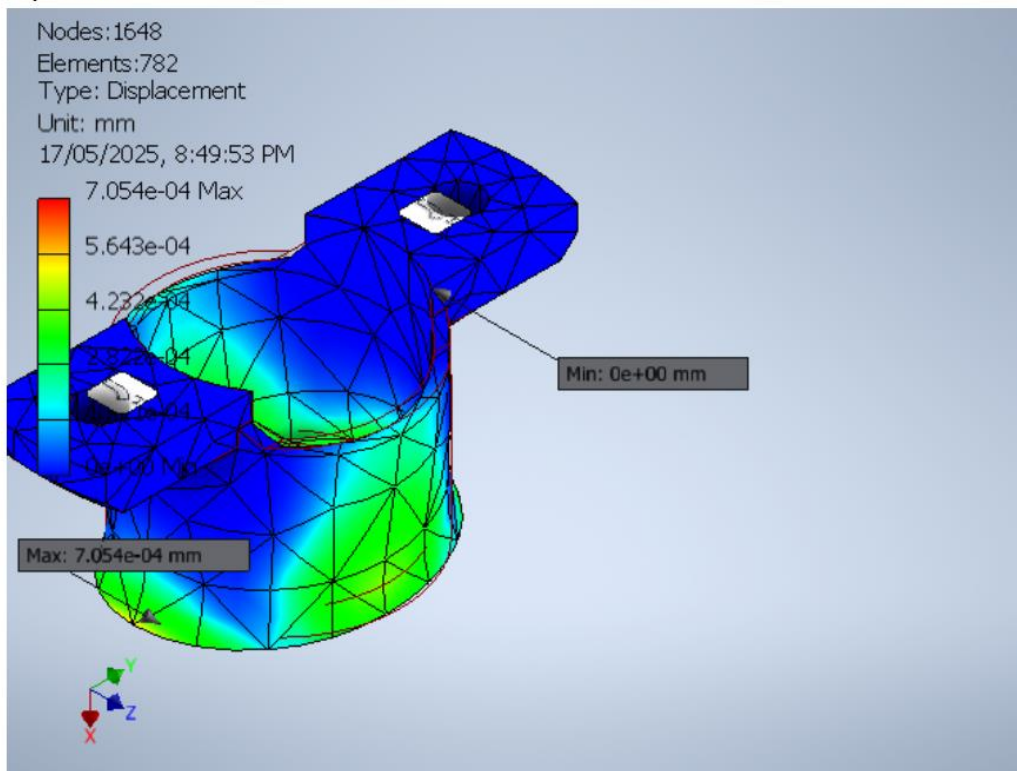
Name	Minimum	Maximum
Volume	5354.11 mm <sup>3</sup>	
Mass	0.00567536 kg	
Von Mises Stress	0.0000116585 MPa	0.0645127 MPa
1st Principal Stress	-0.0179133 MPa	0.0715859 MPa
3rd Principal Stress	-0.0432001 MPa	0.0155737 MPa
Displacement	0 mm	0.000705407 mm
Safety Factor	15 ul	15 ul
Stress XX	-0.0246339 MPa	0.0647033 MPa
Stress XY	-0.0173042 MPa	0.0158495 MPa
Stress XZ	-0.0241716 MPa	0.0243375 MPa
Stress YY	-0.0289034 MPa	0.0609317 MPa
Stress YZ	-0.01571 MPa	0.0160403 MPa
Stress ZZ	-0.0431722 MPa	0.0332938 MPa
X Displacement	-0.00000194918 mm	0.000442761 mm
Y Displacement	-0.000586505 mm	0.000582663 mm
Z Displacement	-0.000423607 mm	0.000426204 mm
Equivalent Strain	0.0000000480088 ul	0.0000267829 ul
1st Principal Strain	0.00000000288841 ul	0.0000290017 ul
3rd Principal Strain	-0.0000169182 ul	-0.00000000049476 ul
Strain XX	-0.0000117395 ul	0.0000270543 ul
Strain XY	-0.0000106606 ul	0.00000976445 ul
Strain XZ	-0.0000148914 ul	0.0000149936 ul
Strain YY	-0.00000845761 ul	0.0000271058 ul
Strain YZ	-0.00000967848 ul	0.00000988196 ul
Strain ZZ	-0.0000169047 ul	0.000015816 ul

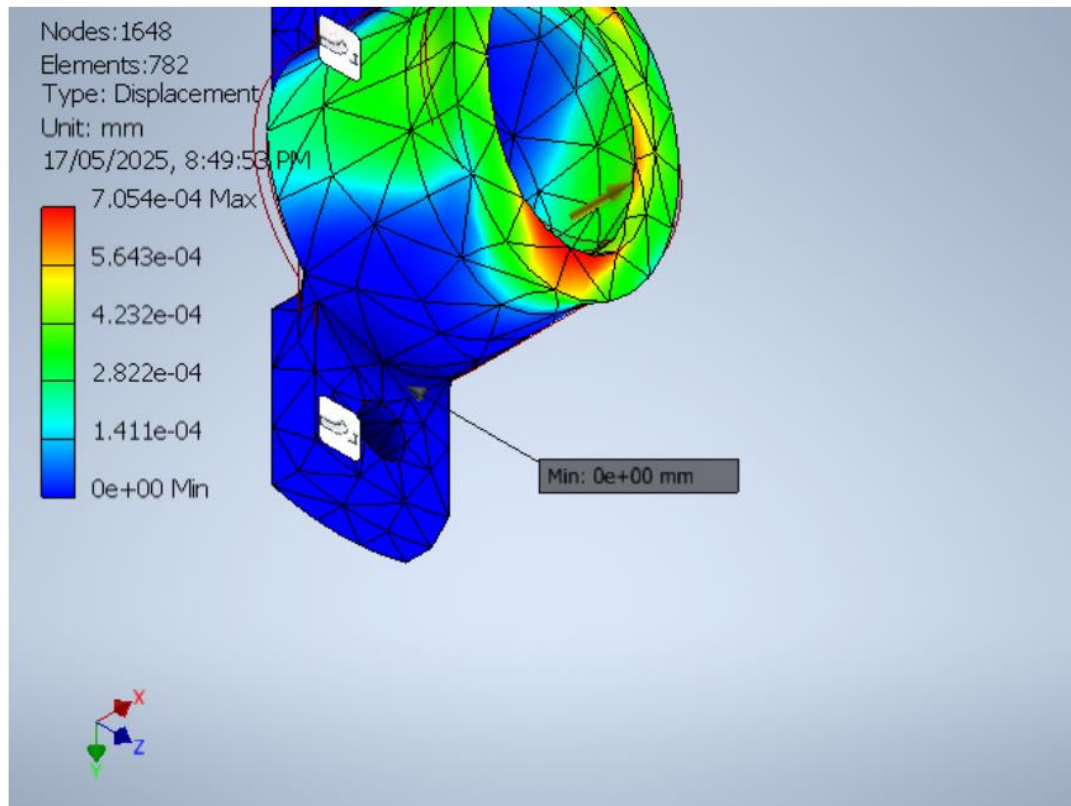
□ **Figures**

□ **Von Mises Stress**





**Displacement**



**Stress Analysis Report**

Analyzed File:	TOF-HOUSING-MOUNT.ipt
Autodesk Inventor Version:	2025 (Build 290162000, 162)
Creation Date:	17/05/2025, 9:05 PM
Study Author:	leahg
Summary:	

**□ Static Analysis:1****General objective and settings:**

Design Objective	Single Point
Study Type	Static Analysis
Last Modification Date	17/05/2025, 9:03 PM
Model State	[Primary]
Detect and Eliminate Rigid Body Modes	No

**□ iProperties****□ Summary**

Author leahg

**□ Project**

Part Number	TOF-HOUSING-MOUNT
Designer	leahg
Estimated Cost	\$0.00
Creation Date	15/05/2025

**□ Status**

Design State WorkInProgress

**□ Physical**

Material	ABS Plastic
Density	1.06 g/cm <sup>3</sup>
Mass	8.69351 kg
Area	302101 mm <sup>2</sup>
Volume	8201420 mm <sup>3</sup>
Center of Gravity	x=165.794 mm y=49.9972 mm z=150 mm

Note: Physical values could be different from Physical values used by FEA reported below.

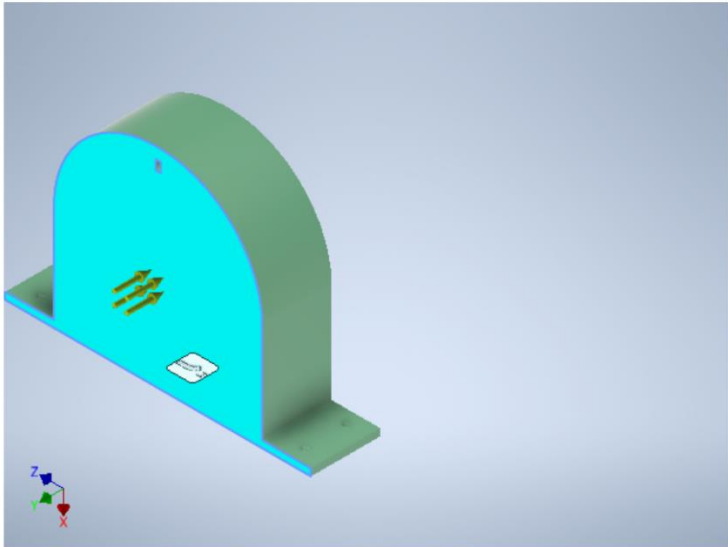


**Operating conditions**

**Pressure:** 1

Load Type: Pressure  
Magnitude: 0.001 MPa

**Selected Face(s)**



□ **Results**

□ **Reaction Force and Moment on Constraints**

Constraint Name	Reaction Force		Reaction Moment	
	Magnitude	Component (X,Y,Z)	Magnitude	Component (X,Y,Z)
Fixed Constraint:1	111.459 N	0 N	14.9372 N m	0 N m
		111.459 N		0 N m
		0 N		-14.9372 N m

□ **Result Summary**

Name	Minimum	Maximum
Volume	8201420 mm^3	
Mass	8.69351 kg	
Von Mises Stress	0.00000756906 MPa	0.0314339 MPa
1st Principal Stress	-0.024162 MPa	0.0428243 MPa
3rd Principal Stress	-0.0577224 MPa	0.0166726 MPa
Displacement	0 mm	0.0061309 mm
Safety Factor	15 ul	15 ul
Stress XX	-0.0507683 MPa	0.0393402 MPa
Stress XY	-0.00140285 MPa	0.0136023 MPa
Stress XZ	-0.00787398 MPa	0.00908564 MPa
Stress YY	-0.0311161 MPa	0.0209939 MPa
Stress YZ	-0.00300087 MPa	0.00203609 MPa
Stress ZZ	-0.0311161 MPa	0.0220633 MPa
X Displacement	-0.00123693 mm	0.00116815 mm
Y Displacement	-0.00600483 mm	0.00000451439 mm
Z Displacement	-0.000238051 mm	0.00023989 mm
Equivalent Strain	0.000000003159 ul	0.0000138331 ul
1st Principal Strain	0.00000000241304 ul	0.0000127285 ul
3rd Principal Strain	-0.0000163914 ul	-0.00000000172155 ul
Strain XX	-0.0000126239 ul	0.0000116877 ul
Strain XY	-0.000000864255 ul	0.000000838001 ul
Strain XZ	-0.00000485093 ul	0.0000055974 ul
Strain YY	-0.00000699746 ul	0.00000616416 ul
Strain YZ	-0.00000184875 ul	0.00000125438 ul
Strain ZZ	-0.0000046405 ul	0.00000434259 ul

**Figures****Von Mises Stress**